Standard Model of Electromagnetism and Chirality in Crystals

R. Winkler[1,2] and U. Zülicke[3]

[1]*Department of Physics, Northern Illinois University, DeKalb, Illinois 60115, USA*
[2]*Materials Science Division, Argonne National Laboratory, Lemont, Illinois 60439, USA*
[3]*MacDiarmid Institute, School of Chemical and Physical Sciences, Victoria University of Wellington, P.O. Box 600, Wellington 6140, New Zealand*

(Received 8 January 2026; revised 26 April 2026; accepted 29 May 2026; published 17 August 2026)

We present a general, systematic, and quantitative theory of electromagnetism and chirality in crystalline solids. Symmetry is its basic guiding principle, enabling us to consider macroscopic multipole densities without reference to any specific microscopic configurations. We use a formal analogy between space inversion i and time inversion θ to identify two complementary, comprehensive classifications of crystals, based on five categories of electric and magnetic multipole order—called polarizations—and five categories of chirality. The five categories of polarizations (parapolar, electropolar, magnetopolar, antimagnetopolar, and multipolar) embody the variety of ways in which electromagnetic multipole order can be realized in solids, thus expanding the familiar notion of electric dipolarization in ferroelectrics and magnetization in ferromagnets to higher-rank multipole densities characterizing, e.g., altermagnets and alterelectrics. Group theory also permits the absolute, gauge-invariant quantification of these multipole densities. The five categories of chirality (parachiral, electrochiral, magnetochiral, antimagnetochiral, and multichiral) extend the notion of enantiomorphism—conventionally associated with the lack of spatial mirror symmetries—to include all possibilities for creating nonsuperposable images by applying the inversions i, θ, and $i\theta$. In particular, multichiral systems lack all inversion symmetries and therefore have four different enantiomorphs. Each category of chirality is shown to arise from particular superpositions of electric and magnetic multipole densities. Our theory has great predictive power by relating electric and magnetic multipolar order with, e.g., distinctive features in the crystal structure, the electronic band structure, property tensors, and response tensors of quantum materials. These findings are critical for a large community working on fundamental and applied aspects of novel quantum materials.

DOI: 10.1103/jvv7-z2fq

Subject Areas: Condensed Matter Physics

I. INTRODUCTION

Recent work has identified a multitude of new forms of electric and magnetic order in quantum materials that transcends the traditional understanding of crystalline solids. Beyond the textbook examples of ferroelectrics and ferromagnets, these new forms include, for example, multiferroics [1], unconventional hidden-order phases [2], altermagnets [3–5], and chirality in novel domains [6,7]. The richness of materials and phenomena is reminiscent of particle physics when, mid-20th century, more and more "elementary" particles were discovered until the standard model of particle physics was worked out, which could organize and interpret these findings systematically. Then, as now, symmetry plays a crucial role for obtaining a deeper understanding of how seemingly disparate phenomena are connected [8]. Here, we use symmetry as the guiding concept to develop a standard model of electromagnetism and chirality in crystalline solids that provides a physically transparent, unified predictive framework for the fascinating world of quantum materials.

Symmetry is the most fundamental organizing principle in solid-state physics, linking the periodic crystal structure of solids with physical properties. Translational symmetry is usually the starting point for a discussion of crystal symmetries; it yields the well-known 14 Bravais lattices [9]. These lattices are complemented by point-group symmetries, including space inversion i, to obtain the 230 crystallographic space groups [10]. In a last step, to account for magnetic phenomena, one may incorporate time inversion θ to construct the 1651 magnetic space groups (MSGs) [11].

Important progress in our understanding of the physical properties of crystalline solids was made early on based on Neumann's principle [12,13], stating that macroscopic properties of a crystal structure do not require knowledge of the space group characterizing a crystal structure.

Published by the American Physical Society under the terms of the Creative Commons Attribution 4.0 International license. Further distribution of this work must maintain attribution to the author(s) and the published article's title, journal citation, and DOI.

TABLE I. Inversion groups that can be formed from space inversion i, time inversion θ, and the combined inversion $i\theta$. The quantity e denotes the unit element.

$C_1 = \{e\}$	Trivial inversion group
$C_i = \{e, i\}$	Space inversion group
$C_\theta = \{e, \theta\}$	Time inversion group
$C_{i\theta} = \{e, i\theta\}$	Combined inversion group
$C_{i\times\theta} = \{e, i, \theta, i\theta\}$	Full inversion group

Instead, these properties are already determined by the simpler crystallographic point groups (also called crystal classes [14]) that include proper and improper rotations as their group elements but no translations [10,11,14–16].

In the present work, we follow Neumann's principle by not considering translational symmetries, but we go one step further by taking space inversion symmetry (SIS) and time inversion symmetry (TIS) as the starting point. SIS and TIS are among the most fundamental symmetries describing the Universe. Both SIS and TIS are so-called black-white symmetries; they are represented by two-element groups, $C_i = \{e, i\}$ and $C_\theta = \{e, \theta\}$, that are obviously isomorphic [17]. (Here, e denotes the unit element.) We interpret the isomorphism as *SIS-TIS duality*.

Space inversion i and time inversion θ can be combined in the full inversion group $C_{i\times\theta} = \{e, i, \theta, i\theta\}$ that treats the three elements i (SIS), θ (TIS), and $i\theta$ (combined inversion symmetry, CIS) on an equal footing. This allows us to define two complementary, comprehensive classifications of crystals, using five categories of polarizations and five categories of chirality. In each scheme, the five categories are related to the five subgroups of the group $C_{i\times\theta}$ (see Table I). Jointly, the five categories of polarizations and the five categories of chirality yield the succinct and comprehensive description illustrated in Fig. 1 that we call the *standard model* of electromagnetism and chirality in crystals.

In the following, we briefly summarize the essence of the standard model and the obtained results. We are particularly interested in electric and magnetic multipole order as an organizing principle for characterizing different phases of crystalline matter. Such phases are associated with spontaneously formed rank-ℓ multipole densities, which we call *polarizations*. Following Ref. [18], we identify four types of polarizations—electric, magnetic, electrotoroidal, and magnetotoroidal (see Table II). The *signature* ss' indicates how a polarization behaves under space inversion (even/odd if $s = +/-$) and time inversion (even/odd if $s' = +/-$).

Examples of polarizations include the electric dipolarization in ferroelectrics ($\ell = 1$ and signature $-+$) and the magnetization in ferromagnets ($\ell = 1$, $+-$). Early studies identified the crystal classes permitting a bulk electric dipolarization [12,13] or a bulk magnetization [19–21]. More recent work focused on higher-rank multipolar order

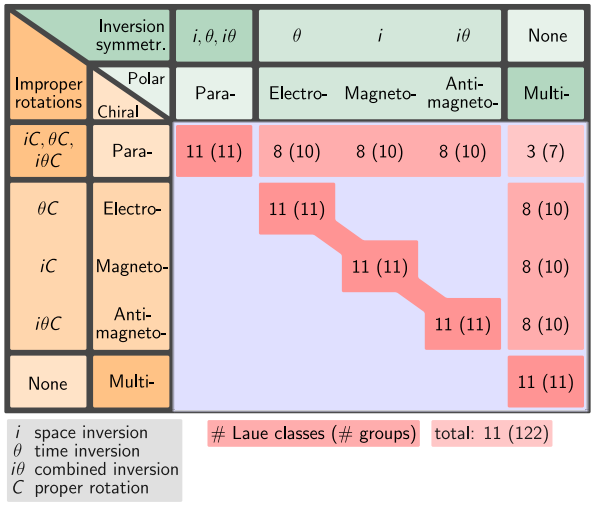


FIG. 1. Standard model of broken crystal symmetries. Crystal structures of materials fall into 12 types classified by the allowed polarizations and chirality. The presence of inversion symmetries i, θ, and $i\theta$ defines five categories of polarizations, while symmetry under improper rotations iC, θC, and $i\theta C$ defines five categories of chirality. Triadic relations among the categories and types are highlighted by conjoint tiles. For each type, the number of Laue classes and magnetic point groups (crystal classes) realizing it are indicated.

[18,22–26]. Some work also studied electrotoroidal [27,28] and magnetotoroidal [29] multipoles, though their physical significance has remained unclear [30]. We clarify how toroidal multipole densities emerge in crystals and manifest in physical properties.

The treatment of multipole densities as strictly macroscopic quantities distinguishes our theory from other work [23–26]. Group theory expanding on Neumann's principle provides a precise formalism for discussing electric and magnetic multipole order in solids and avoids all difficulties that have been identified with previous extrapolations of classical electromagnetism from finite systems to crystalline solids [31–35]. We have recently applied this method to obtain a systematic, universally applicable absolute, gauge-invariant *quantification* of electric and magnetic multipole densities in crystals [36]. These multipole densities represent natural order parameters for electric and magnetic phase transitions in crystals [37,38]. Our approach is also complementary to numerical procedures proposed to extract bulk polarizations from first-principles

TABLE II. Signature ss' of multipoles of order ℓ. Respective columns define the electric, magnetic, and toroidal multipoles represented via irreducible spherical tensors $T^{ss'}_\ell$ of the full rotation group $R_{i\times\theta}$.

	Electric	Magnetic	Electrotoroidal	Magnetotoroidal
ℓ even	$++$	$--$	$-+$	$+-$
ℓ odd	$-+$	$+-$	$++$	$--$

calculations of atomic-site multipoles [39,40]. Previous work assumed that multipole order beyond dipolar order $\ell = 1$ is an exotic, rare phenomenon [40–42]. We show that multipolar order $\ell > 1$ is actually common among crystalline materials.

In the standard model, both the five categories of polarizations and the five categories of chirality classify the electric and magnetic order in crystal structures based on the presence or absence of the inversion symmetries i, θ, and $i\theta$ but from rather different perspectives.

The five categories of polarizations reflect the presence or absence of the inversion symmetries i, θ, and $i\theta$ as *independent* elements in the symmetry group G of a physical system [18]. See the first two rows in Fig. 1. In the *parapolar* category, all three inversion symmetries i, θ, and $i\theta$ represent good symmetries, so only even-ℓ electric multipole densities called *parapolarizations* are allowed (see Table II). These even-ℓ multipole densities are also allowed in all other categories. For the three *unipolar* categories, only one among the inversions i, θ, or $i\theta$ represents a good symmetry. In the *electropolar* category, TIS is a good symmetry that permits odd-ℓ electric multipole densities called *electropolarizations*. In the *magnetopolar* category, SIS is a good symmetry that permits odd-ℓ magnetic multipole densities called *magnetopolarizations*. In the *antimagnetopolar* category, CIS is a good symmetry that permits even-ℓ magnetic multipole densities called *antimagnetopolarizations*. Finally, in the *multipolar* category, all three symmetries i, θ, and $i\theta$ are broken, so all four types of polarizations may coexist.

Each category of polarizations gives rise to distinctive features in the electronic band structure [18], as illustrated in the upper part of Fig. 2. The lower part in the figure summarizes materials classes belonging to the five categories of polarizations. The $\ell = 1$ multipole density within each category corresponds to a ferroic order parameter

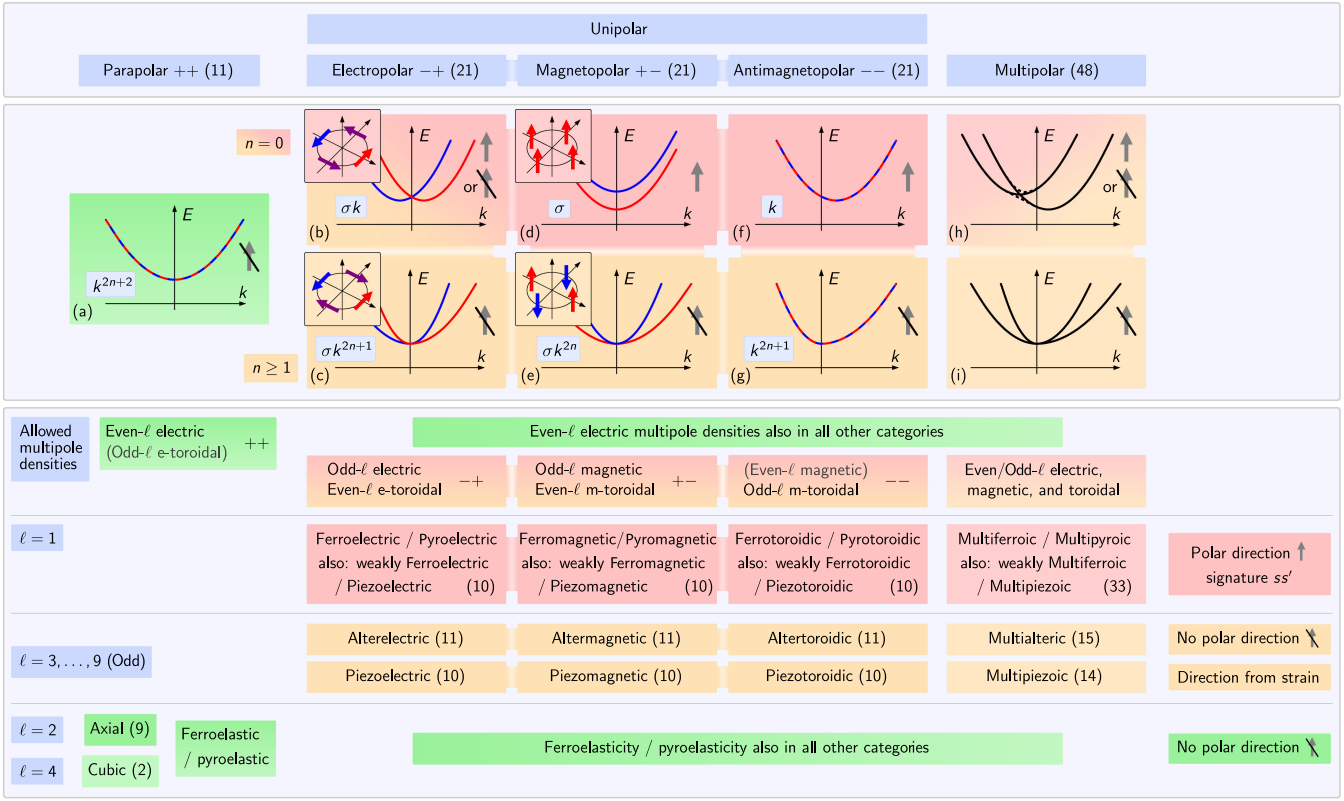


FIG. 2. Categories of polarizations. The upper part with panels (a)–(i) shows characteristic electron-band dispersions $E_\sigma(\mathbf{k})$. The symbol k represents a generic wave-vector component, red and blue curves are associated with the two values of the spin quantum number σ, and n is a non-negative integer. Panels (b), (d), (f), and (h) visualize the case $n = 0$ when a polar direction with signature ss' (i.e., a dipolarization $T_1^{ss'}$) is symmetry allowed, as indicated by the gray arrows. Panels (c), (e), (g), and (i) correspond to $n \geq 1$, when polar directions are forbidden (strikethrough gray arrows). Realizations of the electropolar and multipolar cases with $n = 0$ [panels (b) and (h)] without a symmetry-allowed polar direction are also possible. In the parapolar case [panel (a)], polar directions are always forbidden (for any $n \geq 0$). The lower part summarizes how magnetic crystal classes belonging to different categories of polarizations permit different electric and magnetic multipole densities (rank ℓ) that manifest themselves via characteristic physical properties. The features listed in the lower part are directly linked with the characteristic electron-band dispersions shown in the upper part (see text). Numbers in braces indicate the number of crystal classes that realize each case. More details on all 122 crystal classes are provided in Table XIX.

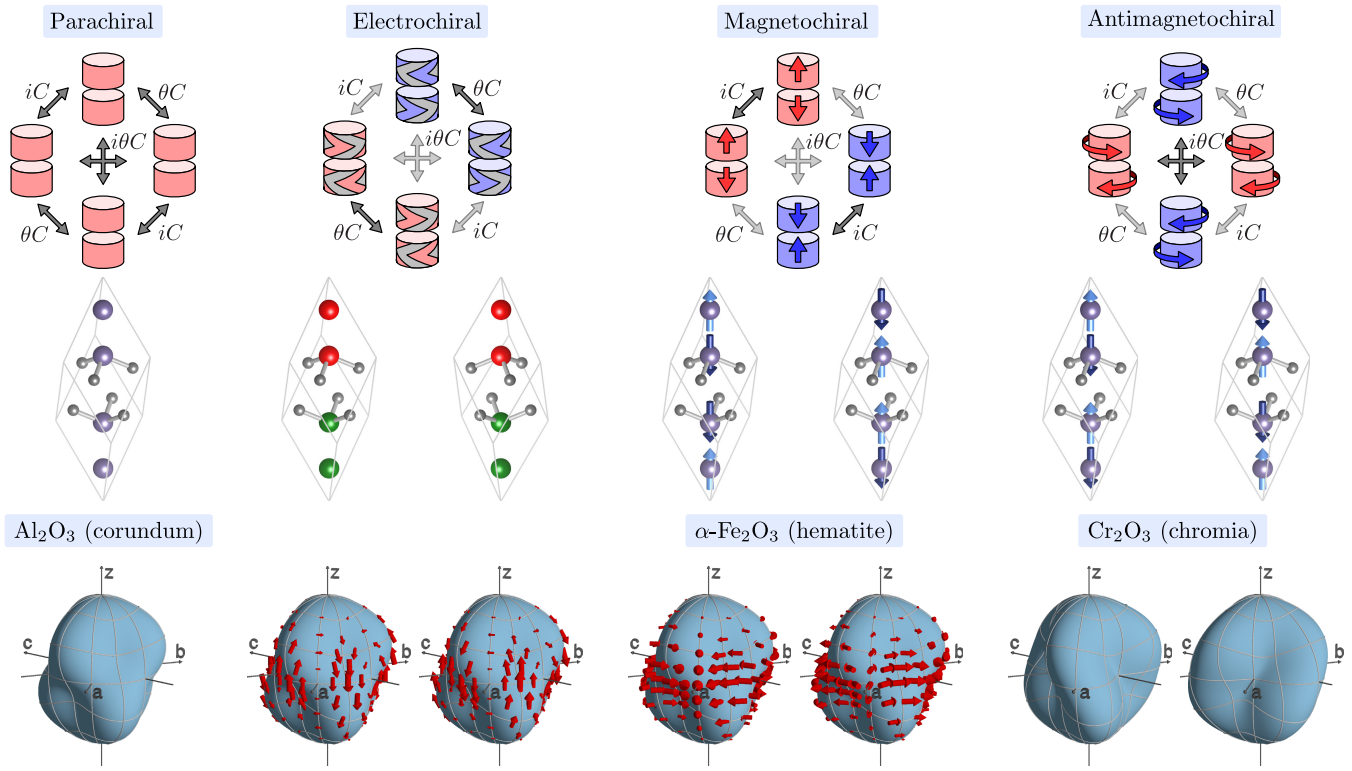


FIG. 3. Examples of parachiral and unichiral systems. Straight (curved) colored arrows in the upper-row panels indicate translational (rotational) motion of the shown object. The middle-row panels display the parachiral corundum structure and its unichiral derivatives. The bottom-row panels show energy surfaces with associated spin textures for crystal structures from the middle row. The two enantiomorphs shown for each unichiral case are transformed into each other by two generalized improper rotations (indicated in the upper row by light-gray double arrows) but are invariant under the third (dark-gray double arrow).

exhibiting a polar direction, while multipole densities with rank $\ell > 1$ have no such directionality. All these cases can be clearly distinguished in the band structure, and they are characterized by distinct, observable (macroscopic) physical effects.

Very generally, one speaks of chirality when a system exists in, at least, two versions called enantiomorphs that cannot be superposed upon each other by proper (pure) rotations C [43–50]. Ordinarily, this is tantamount to the case in which the enantiomorphs are mapped onto each other by improper rotations iC. By treating the inversion symmetries i, θ, and $i\theta$ on the same footing, we identify five categories of chirality that reflect the presence or absence in G of any *composite* symmetry elements γC with $\gamma \in \{i, \theta, i\theta\}$, i.e., the presence or absence of γ-improper rotations. See the first two columns in Fig. 1. Systems whose symmetries include i-improper and θ-improper (and thus also $i\theta$-improper) rotations are *parachiral* and show no enantiomorphism. See the left column in Fig. 3 for an illustration. In contrast, each of the three *unichiral* categories includes γ-improper rotations for only one inversion symmetry $\gamma = i$, θ, or $i\theta$. Systems with only θ-improper rotations among its symmetries are *electrochiral* and exist in two enantiomorphic versions that are transformed into each other by i-improper and $i\theta$-improper rotations. In addition to this conventional case, we identify the categories of *magnetochiral* systems (having only i-improper rotations) and *antimagnetochiral* systems (having only $i\theta$-improper rotations). Each of these categories permits two enantiomorphs. The two enantiomorphs of magnetochiral systems are superposed by θ-improper and $i\theta$-improper rotations, whereas θ-improper and i-improper rotations transform between the two enantiomorphs of antimagnetochiral systems. In addition, systems whose only symmetries are proper rotations (none of them combined with i, θ, or $i\theta$) are *multichiral* and exist in four distinct enantiomorphs.

Examples of chiral media based on variations of the corundum structure of Al_2O_3 are shown in Fig. 3. The new forms of chirality identified here require magnetic order; they are realized in magnetic crystals. More specifically, we show that it is the *interplay* of different electric and magnetic multipole densities that gives rise to the different categories of chirality. Very generally, the enantiomorphism realized in unichiral and multichiral media can be identified via observable effects such as optical activity [51] and nonreciprocal directional dichroism [52], which have opposite signs for the different enantiomorphs. Multichiral systems require multiple such probes to distinguish all four enantiomorphs. The enantiomorphism is

also expressed in the electronic band structure, as demonstrated in the bottom row of Fig. 3.

Studying the morphology of the 122 magnetic point groups has been essential for gaining a basic understanding of general materials properties [53–62]. Our systematic approach reveals fundamental patterns in the structure of magnetic point groups and the composition of Laue classes assembled by them. We identify 12 group types, where each type is characterized by a distinct combination of a category of polarizations and a category of chirality that act jointly like a unique identifier for each group type (see Fig. 1). These group types provide a comprehensive, fine-grained classification of all 122 magnetic crystallographic point groups and of the physical properties the groups imply. Figure 1 also indicates how many Laue classes contain groups of each type and how many crystallographic magnetic point groups in total realize each type. Quantification of multipole densities [36] gives practical measures of polarizations and chiralities that will be studied in a future publication.

Group theory provides yet deeper insights. For example, the group morphology becomes remarkably similar for each of the three unipolar categories (electropolar, magnetopolar, and antimagnetopolar) and for each of the three unichiral categories (electrochiral, magnetochiral, and antimagnetochiral), which reflects the isomorphisms relating the two-element groups C_i, C_θ, and $C_{i\theta}$ (see Table I). The groups in these categories can thus be combined in *triadic relations* that imply striking correspondences between apparently dissimilar systems and their physical properties. We illustrate this point by tabulating the form of material tensors for all magnetic point groups. Triadic sets of group types are highlighted in Fig. 1 by conjoint tiles.

The standard model simplifies and greatly extends earlier studies [3,4,54–62]. It has great predictive power by relating electric and magnetic multipolar order with, e.g., distinctive features in the crystal structure, the electronic band structure, property tensors, and response tensors of quantum materials. It elucidates hidden orders in solids [2]; the exhaustive classification covers the full spectrum of conventional and unconventional electric and magnetic order, including altermagnetism [3,4] and piezomagnetism [63], which are currently attracting great interest. The standard model is equally applicable to insulators and metals. It is a strong base to inspire the design of new experimental probes and techniques [64].

The remainder of this article is organized as follows. Section II focuses on the description of electric and magnetic multipole order in solids. Here, we explain the emergence of the five categories of polarizations and their associated physical properties. Our theory of chirality in solids is developed in Sec. III. We discuss our results and their physical implications, as well as future research directions building on them, in Sec. IV alongside our conclusions. Technical details are provided in the appendixes, which establish the mathematical backbone for the standard-model classification illustrated in Fig. 1. Appendix A elucidates the general composition of magnetic point groups. The classification of continuous and discrete magnetic point groups is discussed in Appendix B. Appendix C outlines the theoretical basis for defining compound multipoles. Appendix D includes a tabulation of spherical tensors and multipole order permitted by the 122 crystallographic magnetic point groups. The commonalities regarding the shape of material tensors implied by symmetry is elucidated in Appendix E. Finally, Appendix F tabulates materials candidates for the different categories of chirality introduced in Sec. III.

Throughout this work, we adhere to the Schönflies notation to denote symmetry elements and symmetry groups [65]. We use the concept of Laue classes [66] as a basic organizational principle for magnetic point groups: A Laue class $L(G_{\rm p})$ combines the point groups G that represent the same set of proper (pure) rotations C, when the inversion symmetries $\gamma = i$, θ, and $i\theta$ are stripped off from improper rotations γC in G. The group $G_{\rm p}$ formed by the proper rotations C is called the *class root* of $L(G_{\rm p})$. A thorough introduction to the structure of magnetic point groups and their Laue classes is provided in Appendix A.

II. MULTIPOLE ORDER IN SOLIDS

Tensors denote quantities that transform in a well-defined way under the symmetry group G of a physical system. Commonly, discussions of tensors focus on the rotational symmetries of these quantities [67,68]. In this work, we are particularly interested in the effect of the inversion symmetries i, θ, and $i\theta$. In Sec. II A, we thus extend the classification of tensors to also account for inversion symmetries.

Very generally, physical quantities may be nonzero in a system with symmetry group G if these quantities are invariant under the symmetry elements in G. According to Neumann's principle, the pattern of invariant tensors characterizing the macroscopic properties of a crystal structure is determined by the crystallographic point group G defining the crystal class of the crystal structure [12–14]. An important example of such tensors are electric and magnetic multipole densities that represent electromagnetic order in solids (Sec. II B). By focusing on how these multipoles transform under the inversion symmetries i, θ, and $i\theta$, we identify five categories of multipole order, as illustrated in Fig. 1.

To describe the full range of possible electric and magnetic orders that can arise in crystals, the formation of compound tensors needs to be discussed (Sec. II C). The construction of irreducible tensors representing multipole densities is explained in Sec. II D. In Sec. II E, we briefly review the theory developed in Ref. [36] for an absolute quantification of electric and magnetic multipole densities in crystals.

In a microscopic analysis, the concept of invariant tensors also allows one to classify the terms that may exist in the Hamiltonian of a physical system and to discuss under what circumstances these terms may be nonzero. In the context of crystalline solids, this is known as the theory of invariants [14]. It allows one to derive, in a systematic way, the different terms that arise in a Taylor expansion of the spin-dependent electronic band structure. These terms can be classified according to the same categories in Fig. 1 so that we establish a one-to-one correspondence between the categories of multipole order and distinctive features of the band structure (Fig. 2 and Sec. II F).

Insights gained from the standard model are used in Sec. II G to relate the band-structure features elucidated in Sec. II F to specific materials classes. We introduce the term *alteric* as a unifying concept referring to multipole order with rank $\ell > 1$. For magnetopolar systems, this term refers to the celebrated altermagnets [4], but alterelectric and altertoroidic media also exist. We discuss weak ferroicity in Sec. II H. We briefly comment on the general mechanisms for TIS breaking in magnetic systems and associated physical phenomena in Sec. II J.

A. Irreducible tensors

An irreducible tensor T_Γ associated with a group G represents a physical quantity that transforms according to the irreducible representation (IR) Γ of G. If G is a crystallographic point group, we call T_Γ an irreducible crystallographic tensor. An irreducible spherical tensor

$$T_\ell^{ss'} \equiv \{T_{\ell m}^{ss'}\colon\ m = -\ell, -\ell+1, \ldots, \ell-1, \ell\} \qquad (1)$$

represents a physical quantity that transforms according to the IR $D_\ell^{ss'}$ of the full rotation group $R_{i\times\theta} \equiv R \times C_{i\times\theta}$ with $R \equiv SO(3)$ [67,68]. (Detailed information about $R_{i\times\theta}$ is provided in Appendix B 1.) Here, $\ell = 0, 1, 2, \ldots$ denotes the tensor's rank, and m distinguishes its $2\ell+1$ independent components. The signature ss' [69] indicates how a tensor transforms under SIS (even/odd if $s = +/-$) and TIS (even/odd if $s' = +/-$).

Spherical tensors $T_\ell^{ss'}$ transforming irreducibly under $R_{i\times\theta}$ are generally reducible under crystallographic point groups G; i.e., such tensors are not adapted to discuss crystal properties. Tensors $T_\ell^{ss'}$ can be decomposed into crystallographic tensors T_Γ transforming irreducibly under subgroups G of $R_{i\times\theta}$ by projecting the tensor $T_\ell^{ss'}$ onto the IRs Γ of G. This decomposition follows the compatibility relations tabulated in Ref. [16], as discussed in Ref. [18]. Equivalently, a crystallographic tensor T_Γ transforming according to an IR Γ of a subgroup G of $R_{i\times\theta}$ can be projected onto the IRs $D_\ell^{ss'}$ of $R_{i\times\theta}$ [11]. The latter approach of associating a crystallographic tensor T_Γ with an IR $D_\ell^{ss'}$ of $R_{i\times\theta}$ can be viewed as the inverse of using compatibility relations to decompose a spherical tensor $T_\ell^{ss'}$ into components T_Γ that transform irreducibly under a crystallographic point group G. While the compatibility relations connect infinitely many IRs $D_\ell^{ss'}$ of $R_{i\times\theta}$ with a finite number of IRs Γ of each crystallographic point group, the correspondence between spherical tensors $T_\ell^{ss'}$ and crystallographic tensors T_Γ can be made unique. Crystallographic tensors T_Γ transforming according to an IR Γ of G can be rearranged into linear combinations $\tilde{T}_\Gamma$, each again transforming according to the IR Γ of G, such that under $R_{i\times\theta}$ each $\tilde{T}_\Gamma$ transforms according to exactly one IR $D_\ell^{ss'}$ of $R_{i\times\theta}$. The above analysis clarifies the relation between the spherical tensors frequently used in other work to discuss crystal properties and symmetry-adapted crystallographic tensors. Examples will be discussed below.

A physical quantity Q is allowed under a symmetry group G if Q is invariant under G, i.e., Q transforms according to the identity representation Γ_1 of G. Note that, according to Neumann's principle [12,13], the symmetry group relevant for macroscopic properties such as material tensors is the crystallographic point group G defining the crystal class of a crystal structure; i.e., space groups are not needed to discuss such macroscopic properties. We call the largest symmetry group that leaves Q invariant the *maximal group* of Q. According to Neumann's principle, the maximal group of material tensors is always a subgroup of $R_{i\times\theta}$.

More specifically, a physical quantity represented by a spherical tensor $T_\ell^{ss'}$ becomes allowed if the symmetry is reduced from $R_{i\times\theta}$ to a subgroup G of $R_{i\times\theta}$ such that a linear combination of components $T_{\ell m}^{ss'}$ of $T_\ell^{ss'}$ transforms according to the identity representation of G. This is equivalent to the condition that mapping the IR $D_\ell^{ss'}$ of $R_{i\times\theta}$ onto the IRs of G includes the identity representation Γ_1 of G. All continuous and discrete groups discussed in this work are subgroups of $R_{i\times\theta}$. Therefore, we use the complete set of irreducible tensors $T_\ell^{ss'}$ of $R_{i\times\theta}$ as a convenient reference to discuss functions transforming according to IRs of subgroups of $R_{i\times\theta}$. Note, however, that any linear combination of tensors transforming according to the same IR Γ of G yields a tensor that likewise transforms according to the IR Γ of G. In that sense, it is generally not possible, given a system with crystallographic point group G, to associate distinct observable physics with crystallographic tensors transforming according to the same IR of G while transforming according to different IRs of $R_{i\times\theta}$.

Irreducible rank-0 tensors $T_0^{ss'} = \{T_{00}^{ss'}\}$ of $R_{i\times\theta}$ are called scalars. Tensors T_0^{++} are already invariant under $R_{i\times\theta}$ and thus also invariant under all subgroups of $R_{i\times\theta}$. The maximal groups of the remaining tensors $T_0^{ss'}$ are the spherical subgroups $G_{\rm sp}$ with $R \subsetneq G_{\rm sp} \subsetneq R_{i\times\theta}$ for which $T_0^{ss'}$ is odd under those symmetry elements of $R_{i\times\theta}$ that are not contained in $G_{\rm sp}$ (i.e., the tensors $T_0^{ss'}$ are odd under the symmetry elements labeled "∘" in Table XI of

TABLE III. Physical quantities transforming like irreducible tensor components $T^{ss'}_{\ell 0}$ of $R_{i\times\theta}$. The symbol $\mathscr{E}$ ($\mathscr{B}$) denotes a homogeneous electric (magnetic) field, and $\mathbf{v}$ is a velocity field. An electric dipolarization $\mathscr{P}$ (magnetization $\mathscr{M}$) transforms in all respects like an electric field $\mathscr{E}$ (magnetic field $\mathscr{B}$). The product $\star$ is a generic placeholder for mixed terms regarding the respective quantities.

		$(\mathscr{E},\mathscr{P}),(\mathscr{B},\mathscr{M})$	$(\mathscr{E},\mathscr{P})\star(\mathscr{B},\mathscr{M})$	$\mathbf{v}$	$\mathbf{v}\star(\mathscr{E},\mathscr{B},\mathscr{P},\mathscr{M})$	Maximal group
T^{++}_{00}	Electric	$\mathscr{E}\cdot\mathscr{P},\mathscr{B}\cdot\mathscr{M}$				$R\times C_{i\times\theta}=R_{i\times\theta}$
T^{-+}_{00}	Electrotoroidal				$\mathbf{v}\cdot\mathscr{B},\mathbf{v}\cdot\mathscr{M}$	$R\times C_{\theta}=R_{\theta}$
T^{+-}_{00}	Magnetotoroidal				$\mathbf{v}\cdot\mathscr{E},\mathbf{v}\cdot\mathscr{P}$	$R\times C_{i}=R_{i}$
T^{--}_{00}	Magnetic		$\mathscr{E}\cdot\mathscr{B},\mathscr{P}\cdot\mathscr{M}$			$R\times C_{i\theta}=R_{i\theta}$
T^{++}_{u0}	Electrotoroidal					$C_{\infty}\times C_{i\times\theta}=C_{\infty h}\times C_{\theta}$
T^{-+}_{u0}	Electric	$\mathscr{E},\mathscr{P}$			$\mathbf{v}\times\mathscr{B},\mathbf{v}\times\mathscr{M}$	$D_{\infty}[C_{\infty}]\times C_{\theta}=C_{\infty v}\times C_{\theta}$
T^{+-}_{u0}	Magnetic	$\mathscr{B},\mathscr{M}$			$\mathbf{v}\times\mathscr{E},\mathbf{v}\times\mathscr{P}$	$D_{\infty}(C_{\infty})\times C_{i}=D_{\infty h}(C_{\infty h})$
T^{--}_{u0}	Magnetotoroidal		$\mathscr{E}\times\mathscr{B}$	$\mathbf{v}$		$D_{\infty}(C_{\infty})\times C_{i\theta}=D_{\infty h}(C_{\infty v})$

Appendix B 1). Examples of physical quantities transforming like tensors $T^{ss'}_{0}$ include the four types of charges (electric, magnetic, electrotoroidal, and magnetotoroidal).

Irreducible rank-1 tensors $T^{ss'}_{1}$ of $R_{i\times\theta}$ represent spherical vectors; they are equivalent to Cartesian vectors. The component $m=0$ of rank-1 tensors $T^{ss'}_{1}$, and more generally the component $m=0$ of any rank-ℓ tensor $T^{ss'}_{\ell}$ with $\ell>0$, becomes allowed under the continuous cyclic groups $G_{c\infty}$ and the continuous dihedral groups $G_{d\infty}$. These groups, including their IRs and basis functions, are discussed in more detail in Appendix B 2. The maximal groups of tensor components $T^{ss'}_{\ell 0}$ are generally the dihedral groups $G_{d\infty}$. More specifically, the maximal groups for the $m=0$ tensor components depend on the parity of the index ℓ [70]; i.e., we must distinguish between ℓ even ("g") and ℓ odd ("u"). Beyond that, the index ℓ is not relevant; i.e., for any even or odd $\ell\geq 0$, tensor components $T^{ss'}_{\ell 0}$ transform the same under the continuous axial groups, and for any $\ell>0$, they have the same maximal axial groups. The cyclic groups $G_{c\infty}$ are subgroups of the dihedral groups $G_{d\infty}$. Therefore, the tensor components $T^{ss'}_{\ell 0}$ are likewise invariant under the cyclic groups $G_{c\infty}$, but the distinction based on the parity of ℓ is lost.

Interestingly, the maximal groups of tensor components T^{-+}_{u0}, T^{+-}_{u0}, and T^{--}_{u0} are the dihedral groups $D_{\infty}[C_{\infty}]\times C_{\theta}$, $D_{\infty}(C_{\infty})\times C_{i}$, and $D_{\infty}(C_{\infty})\times C_{i\theta}$, respectively. However, a tensor component T^{++}_{u0} is not invariant under any of the continuous dihedral groups. It is only invariant under continuous cyclic groups $G_{c\infty}$, including $C_{\infty}\times C_{i\times\theta}$. This is shown explicitly in Table XIV in Appendix B 2.

Examples of physical quantities transforming like tensor components $T^{ss'}_{u0}$ are given in Table III. For instance, $D_{\infty}[C_{\infty}]\times C_{\theta}=C_{\infty v}\times C_{\theta}$ represents the maximal group of a physical system in the presence of a homogeneous electric field $\mathscr{E}$. Similarly, the dual group $D_{\infty}(C_{\infty})\times C_{i}=D_{\infty h}(C_{\infty h})$ is the maximal group of a physical system in the presence of a homogeneous magnetic field $\mathscr{B}$. Scalar products of spherical vectors yield scalars [67]; see examples in Table III. Note that the maximal group of a tensor component $T^{ss'}_{\ell m}$ may be larger than the symmetry group permitting a physical realization of $T^{ss'}_{\ell m}$. For example, a scalar $\mathscr{B}^2$ is clearly even under TIS. Nonetheless, it will arise only if a magnetic field $\mathscr{B}$ has broken TIS.

B. Categories of multipole order in crystals

Beyond Table III, examples of spherical tensors include the electric and magnetic multipoles [71,72] as well as their toroidal complements [73,74], where the tensor rank ℓ represents the multipole order. Specifically, $\ell=0$ corresponds to the monopole, $\ell=1$ to the dipole, $\ell=2$ to the quadrupole, etc. Therefore, spherical tensors are directly related to multipole order in solids. The distinct behavior of different multipoles under inversion symmetries is summarized in Table II, which gives the signatures ss' for electric, magnetic, and toroidal multipoles. Here, we follow the common convention that electric charges have the signature $++$, which implies that magnetic charges have the opposite signature $--$ [71]. The transformational behavior of electric, magnetic, and toroidal multipoles is given in Table IV.

The columns of Table II define the electric, magnetic, and toroidal IRs $D^{ss'}_{\ell}$ of the full rotation group $R_{i\times\theta}$. The IRs $D^{ss'}_{\ell}$ and associated irreducible spherical tensors $T^{ss'}_{\ell}$ fall into eight fundamentally distinct *families* that are defined via three parities associated with s, s', and ℓ [70].

As discussed above, a physical quantity transforming according to an IR $D^{ss'}_{\ell}$ of $R_{i\times\theta}$ becomes permitted by symmetry in a system with symmetry group $G\subset R_{i\times\theta}$ if mapping $D^{ss'}_{\ell}$ onto the IRs of G includes the identity representation Γ_1 of G. Following Refs. [12,13,18] and exploiting the general correspondence discussed above between irreducible spherical tensors $T^{ss'}_{\ell}$ under $R_{i\times\theta}$ and crystallographic tensors T_{Γ} under crystallographic point groups G, we *define* electric, magnetic, and toroidal order via Table II; i.e., the presence of multipole order is characterized by the condition

TABLE IV. Categories of polarizations and chirality in crystalline solids. Based on the decomposition (2) of magnetic point groups in terms of the five inversion groups C_ζ, categories of polarizations characterizing multipole order are defined in the upper part of the table. Symmetry operations present (absent) in a given inversion group are indicated by "•" ("∘"). Electric, magnetic, and toroidal multipole densities with even/odd order ℓ and given signature ss' that are allowed (forbidden) under an inversion group are also labeled by "•" ("∘"). The lower part of the table defines categories of chirality. Here, "•" ("∘") indicates that symmetry elements γC are present (absent) in a point group belonging to a category. The number n of distinct system realizations (enantiomorphs) for each chirality is given, and the scalars $T_0^{ss'}$ that are allowed (forbidden) under a chirality are indicated by "•" ("∘").

							Electric		Magnetic		Electrotoroidal		Magnetotoroidal	
Polarization		e	i	θ	$i\theta$	C_ζ	Even $++$	Odd $-+$	Even $--$	Odd $+-$	Even $-+$	Odd $++$	Even $+-$	Odd $--$
Parapolar	(PP)	•	•	•	•	$C_{i\times\theta}$	•	∘	∘	∘	∘	•	∘	∘
Electropolar	(EP)	•	∘	•	∘	C_θ	•	•	∘	∘	•	•	∘	∘
Magnetopolar	(MP)	•	•	∘	∘	C_i	•	∘	∘	•	∘	•	•	∘
Antimagnetopolar	(AMP)	•	∘	∘	•	$C_{i\theta}$	•	∘	•	∘	∘	•	∘	•
Multipolar	(MuP)	•	∘	∘	∘	C_1	•	•	•	•	•	•	•	•
Chirality		C	iC	θC	$i\theta C$	n	T_0^{++}		T_0^{--}		T_0^{-+}		T_0^{+-}	
Parachiral	(PC)	•	•	•	•	1	•		∘		∘		∘	
Electrochiral	(EC)	•	∘	•	∘	2	•		∘		•		∘	
Magnetochiral	(MC)	•	•	∘	∘	2	•		∘		∘		•	
Antimagnetochiral	(AMC)	•	∘	∘	•	2	•		•		∘		∘	
Multichiral	(MuC)	•	∘	∘	∘	4	•		•		•		•	

that mapping $D_\ell^{ss'}$ onto the IRs of G includes the identity representation Γ_1 of G. This generalized definition of multipole order based on the transformation properties of the rotation group [18,67,75] is independent of a microscopic model for multipole order. It embraces how electric and magnetic multipoles are introduced by electrodynamics for finite systems [71,72]. Yet it applies equally to finite and infinite systems. Also, it applies equally to insulators and metals. The quantitative theory of multipole order developed in Ref. [36] and reviewed in Sec. II E conforms with the generalized definition of multipole order.

We note that, in electrostatics, a finite charge distribution ρ inside a sphere may be replaced by a suitable collection of point electric multipoles located at the center of the sphere; these multipoles yield the same potential distribution and thus observable properties outside the sphere as ρ itself [76,77]. Similarly, in magnetostatics, a finite equilibrium current distribution may be replaced by a collection of point magnetic multipoles. The point electric and magnetic multipoles omit those "degrees of freedom" of the charge or current distribution that do not give rise to any potential outside the sphere [76,77]. This applies, in particular, to static toroidal moments that do not contribute to measurable fields $\mathscr{E}$ or $\mathscr{B}$ outside the sphere (nor do these moments interact with external fields $\mathscr{E}$ or $\mathscr{B}$) [73,78], which is the reason why toroidal moments have been associated with "hidden order." In the following, we will not pursue such considerations of multipole order based on electrostatics and magnetostatics. We find below that electric, magnetic, and toroidal moments arise routinely, e.g., in the context of the electronic band structure.

In crystalline solids, multipole order is represented by macroscopic multipole *densities*. Examples include the electric dipolarization and the magnetization. Whereas multipole densities in crystals defy a simplistic definition using classical electromagnetism (as explained in Refs. [31–35], see also Sec. II E), group theory provides a precise formalism for discussing electric and magnetic multipole order in solids [12,13,18,36]. Analogous to the multipoles in finite systems, the multipole densities transform as spherical tensors $T_\ell^{ss'}$. According to Neumann's principle, the relevant symmetry group governing the appearance of these multipole densities is the crystallographic point group associated with the space group of a crystal structure [12,13].

The basic classification of electromagnetic multipole densities permitted by different magnetic point groups derives from the possibility to decompose each group G as

$$G = \tilde{G} \times C_\zeta, \tag{2}$$

where C_ζ is the inversion group that can be formed from inversion symmetries γ that are contained as group elements in G (see Table I), and $\tilde{G}$ is the subgroup of G that contains none of the inversion symmetries as an individual group element [79]. The five different inversion groups C_ζ that may appear in Eq. (2) define five categories of multipole order [18] (see the upper part of Table IV for the association between categories and their corresponding inversion groups). Groups G whose decompositions (2) contain the same inversion group C_ζ belong to the same category of multipole order. As shown in Table IV, the five categories are each characterized by a certain pattern of

allowed and forbidden electric, magnetic, electrotoroidal, and magnetotoroidal multipole densities. More specifically, Tables XXI and XXII in Appendix D list the lowest order of multipole densities permitted by each crystallographic magnetic point group G.

The parapolar category subsumes crystal structures that have both SIS and TIS, which therefore permit only even-ℓ electric multipole densities [16] (also called parapolarizations [18]). Even-ℓ electric multipole densities are also allowed in all other categories discussed below. Media that are both paraelectric and paramagnetic fall into this category.

Electropolar crystals have only TIS; thus, odd-ℓ electric multipole densities (electropolarizations [18]) are allowed, in addition. Pyroelectric and ferroelectric media with their bulk electric dipolarization ($\ell = 1$) [12,13] are familiar examples from the electropolar category, as are the zinc-blende materials with their bulk electric octupolarization ($\ell = 3$) [18]. A macroscopic electropolarization can also emerge from microscopic magnetic order. For example, odd-parity magnets [80,81] fall into the electropolar category (see Sec. II I).

Having only SIS, the magnetopolar category permits odd-ℓ magnetic multipole densities (magnetopolarizations [18]) and therefore includes both ferromagnets ($\ell = 1$) [19–21] and altermagnets ($\ell \geq 3$) [3,4,18,82] (see Sec. II G). The antimagnetopolar category is characterized by SIS and TIS both being broken but CIS still being a good symmetry, which allows even-ℓ magnetic multipole densities (antimagnetopolarizations [18]) to exist. The $i\theta$-symmetric antiferromagnets [83–86] belong to the antimagnetopolar category.

Crystal structures without SIS, TIS, and CIS are in the multipolar category. The low symmetry of these systems allows electropolarizations, magnetopolarizations, and antimagnetopolarizations to coexist. Figure 2 summarizes the five categories of polarizations and the multipole densities permitted for each category.

A more thorough discussion of the five categories will be given in Secs. II F–II J, when we elaborate on how the categories of multipole order are linked to distinct features in the electronic band structure and related observable effects.

C. Compound tensors

In physical systems, quantities behaving like higher-rank irreducible tensors often arise as products or polynomials of quantities transforming like lower-rank irreducible tensors. Before discussing important examples, we briefly review how such higher-rank tensors can be formed.

Two irreducible tensors $T^{s_1 s_1'}_{\ell_1}$ and $T^{s_2 s_2'}_{\ell_2}$ can be combined to form compound tensors [87]. Such compound tensors are generally reducible; i.e., they can be decomposed into irreducible compound tensors. This conforms to the multiplication rules for the IRs of $R_{i\times\theta}$. The product $D^{s_1 s_1'}_{\ell_1} \times D^{s_2 s_2'}_{\ell_2}$ of two IRs $D^{s_1 s_1'}_{\ell_1}$ and $D^{s_2 s_2'}_{\ell_2}$ of $R_{i\times\theta}$ can be decomposed into IRs $D^{(s_1 s_2)(s_1' s_2')}_{\ell}$. Given the ranks ℓ_1 and ℓ_2 of $D^{s_1 s_1'}_{\ell_1}$ and $D^{s_2 s_2'}_{\ell_2}$, the range of ranks ℓ of $D^{(s_1 s_2)(s_1' s_2')}_{\ell}$ obeys the relation [67]

$$|\ell_1 - \ell_2| \leq \ell \leq \ell_1 + \ell_2, \tag{3}$$

and the signature $(s_1 s_2)(s_1' s_2')$ of the IRs $D^{(s_1 s_2)(s_1' s_2')}_{\ell}$ is the product of the signatures $s_1 s_1'$ and $s_2 s_2'$ of the IRs it is derived from. Similarly, the product of two irreducible spherical tensors $T^{s_1 s_1'}_{\ell_1}$ and $T^{s_2 s_2'}_{\ell_2}$ can be decomposed into irreducible spherical compound tensors $T^{(s_1 s_2)(s_1' s_2')}_{\ell}$ using [67]

$$T^{(s_1 s_2)(s_1' s_2')}_{\ell m} = \sum_{m_1, m_2} T^{s_1 s_1'}_{\ell_1 m_1} T^{s_2 s_2'}_{\ell_2 m_2} (\ell_1 m_1, \ell_2 m_2 | \ell_1 \ell_2, \ell m), \tag{4}$$

where $(\ell_1 m_1, \ell_2 m_2 | \ell_1 \ell_2, \ell m)$ are Clebsch-Gordan coefficients. Given the ranks ℓ_1 and ℓ_2 of the tensors $T^{s_1 s_1'}_{\ell_1}$ and $T^{s_2 s_2'}_{\ell_2}$, the range of ranks ℓ is given by Eq. (3). Previous works [23,24,88] have considered a subset of the compound tensors (4) with $\ell = \ell_1 + \ell_2$; these compound tensors are also known as polarized harmonics [67,75]. Equation (4) allows one to derive, in a systematic way, *all* irreducible compound tensors that may be relevant for a physical system.

In a similar way, using the multiplication rules and Clebsch-Gordan coefficients for crystallographic point groups G [16], crystallographic tensors T_Γ transforming irreducibly according to IRs Γ of G can be combined to form crystallographic compound tensors transforming irreducibly under G.

D. Irreducible tensors representing multipole densities

In this section, we discuss in more detail irreducible tensors representing multipole densities. In finite systems, electric and magnetic multipoles can be formulated in powers of Cartesian components of position $\mathbf{r} = (x, y, z)$ [67,71,76,77], leading to alternating even and odd transformation behavior under SIS as ℓ is increased; see Table II. In contrast, the behavior under TIS is the same for all multipoles of a given kind (electric, magnetic, electrotoroidal, or magnetotoroidal) and coincides with the transformation property of the corresponding charge. Electric multipoles in finite systems thus can be written as polynomials in Cartesian components of position (in the following, collectively denoted r), while magnetic multipoles can be expressed using polynomials in r and components of spin (collectively denoted σ) representing magnetic dipole moments [77]. Multipole densities in infinite, periodic systems can be expressed as a function

TABLE V. Irreducible spherical tensors. In a simplified notation, we give the powers of Cartesian components of position (collectively denoted r), components of the wave vector (collectively denoted k), and components of spin (collectively denoted σ) required for a polynomial representation of irreducible spherical tensors $T_\ell^{ss'}$ transforming according to the IRs $D_\ell^{ss'}$ of $R_{i\times\theta}$. The symbol p denotes a non-negative integer. For the even-ℓ magnetotoroidal IRs D_ℓ^{+-}, polynomials in r, σ or k, σ can only be formed for $\ell > 0$, but no such polynomials exist that transform according to D_0^{+-}. Dots indicate that no such polynomials can be constructed for any ℓ. Terms $2p$ in the exponents reflect the fact that we can always multiply a tensor $T_\ell^{ss'}$ with a scalar r^{2p} or k^{2p} without changing its transformational properties.

	Electric	Magnetic	Electrotoroidal	Magnetotoroidal
ℓ even	$++: r^{\ell+2p}$	$--: r^{\ell\pm1+2p}\sigma$	$-+: \cdots$	$+-: r^{\ell+2p}\sigma$ (only $\ell > 0$)
ℓ odd	$-+: r^{\ell+2p}$	$+-: r^{\ell\pm1+2p}\sigma$	$++: \cdots$	$--: r^{\ell+2p}\sigma$
ℓ even	$++: k^{\ell+2p}$	$--: \cdots$	$-+: k^{\ell\pm1+2p}\sigma$	$+-: k^{\ell+2p}\sigma$ (only $\ell > 0$)
ℓ odd	$-+: k^{\ell+2p}\sigma$	$+-: k^{\ell\pm1+2p}\sigma$	$++: \cdots$	$--: k^{\ell+2p}$

of r, σ, or, equivalently, as a function of components of reciprocal lattice vectors (collectively denoted $\mathcal{G}$) and σ. Furthermore, the electronic band structure can be written as polynomials in components of the wave vector (collectively denoted k) and σ (see Table V and Sec. II F). Note that position $\mathbf{r}$ has the signature $-+$, whereas the wave vector $\mathbf{k}$ (representing crystal momentum $\hbar\mathbf{k}$) and reciprocal lattice vectors $\mathcal{G}$ have the signature $--$, and (spin) angular momentum has the signature $+-$.

Equation (4) implies that electric and magnetic multipoles can be combined to form *compound multipoles* that are likewise associated with tensors in Table V. These compound tensors can act as mediators for the observability of electric and magnetic multipoles. When constructing compound multipoles from electric and magnetic multipoles, we can view even-ℓ electric multipoles as *trivial* building blocks because such multipoles exist in any crystal structure (see Sec. II B). On the other hand, odd-ℓ electric and all magnetic multipoles are *nontrivial* as they arise only for certain categories of polarized matter. As shown in Appendix C, all toroidal tensors (except T_1^{++} [89]) can be obtained as products (4) combining one nontrivial and one or two trivial electromagnetic tensors such that the compound tensor inherits the signature of the nontrivial tensor. Of course, similar to electric and magnetic multipole densities, whether or not specific compound multipole densities are realized in a specific crystal structure also depends on the point group G of that structure. See Tables XXI and XXII in Appendix D.

Explicit expressions for the irreducible spherical tensors in Table V can be derived from the rank-1 tensors

$$T_{[r]1}^{-+} = \left[-\frac{1}{\sqrt{2}}(x+iy), z, \frac{1}{\sqrt{2}}(x-iy)\right], \tag{5a}$$

$$T_{[k]1}^{--} = \left[-\frac{1}{\sqrt{2}}(k_x+ik_y), k_z, \frac{1}{\sqrt{2}}(k_x-ik_y)\right], \tag{5b}$$

$$T_{[\sigma]1}^{+-} = \left[-\frac{1}{\sqrt{2}}(\sigma_x+i\sigma_y), \sigma_z, \frac{1}{\sqrt{2}}(\sigma_x-i\sigma_y)\right], \tag{5c}$$

using Eq. (4). However, it turns out that, using the rank-1 tensors $T_{[r]1}^{-+}, T_{[\sigma]1}^{+-}$ (upper part of Table V) and $T_{[k]1}^{--}, T_{[\sigma]1}^{+-}$ (lower part of Table V), such tensors can be realized for only six out of the eight multipole families, as indicated by dots in Table V. The missing two families reflect the fact that the sets of building blocks ($T_{[r]1}^{-+}, T_{[\sigma]1}^{+-}$ and $T_{[k]1}^{--}, T_{[\sigma]1}^{+-}$) are incomplete. To fill these gaps in Table V, we would need, e.g., (fictitious or engineered) electric dipole moments (signature $-+$) that complement the magnetic dipole moments σ (signature $+-$) as building blocks [27,89].

Specifically, it is impossible to form irreducible tensors in (k,σ) transforming according to the magnetic IRs D_ℓ^{--} with ℓ even. Tensors with signature $--$ can only be realized via odd powers k^{2n+1} representing magnetotoroidal tensors transforming according to the IRs D_ℓ^{--} with ℓ odd. In the electronic band structure, the antimagnetopolar category with signature $--$ thus can only be represented via magnetotoroidal terms proportional to k^{2n+1}. The remarkable consequences of this fact are discussed in Sec. II F when we examine the band structure for the different categories of polarizations.

Similar to the construction of irreducible spherical tensors using Eqs. (4) and (5), one can construct irreducible crystallographic tensors in r, σ and k, σ using the Clebsch-Gordan coefficients for the crystallographic point groups tabulated in Ref. [16]. This approach is known as the theory of invariants [14]. In the present context, this case was discussed in more detail in Ref. [18]. The essential difference between irreducible spherical tensors and irreducible crystallographic tensors lies in the fact that the index ℓ represents a good quantum number for the full rotation group $R_{i\times\theta}$ but not for the crystallographic point groups G; i.e., under groups G, the number of parities characterizing the multipole densities is reduced from three to two.

TABLE VI. Irreducible crystallographic tensors. In a simplified notation, we give the powers of Cartesian components of position (collectively denoted r), components of the wave vector (collectively denoted k), and components of spin (collectively denoted σ) required for a polynomial representation of irreducible crystallographic tensors with signature ss'. The symbol n denotes a non-negative integer. The first column indicates, in square brackets, the parity of the index ℓ of the spherical electric and magnetic tensors (as defined in Table II) that the respective crystallographic tensors correspond to.

	Electric	Magnetic
[ℓ even]	$++: r^{2n+2}$	$--: r^{2n+1}\sigma$
[ℓ odd]	$-+: r^{2n+1}$	$+-: r^{2n}\sigma$
[ℓ even]	$++: k^{2n+2}$	$--: k^{2n+1}$
[ℓ odd]	$-+: k^{2n+1}\sigma$	$+-: k^{2n}\sigma$

Therefore, in crystalline systems, the four toroidal families each must be merged with the respective electromagnetic family that has the same signature ss'. In crystalline systems, we thus have only four distinct families of tensors (see Table VI). This result reflects the fact that the electromagnetic and toroidal tensors are fundamentally distinct only under the full rotation group $R_{i\times\theta}$. In a crystalline environment characterized by a finite crystallographic point group G, electromagnetic and toroidal tensors cannot be differentiated anymore, as only the signature ss' remains a distinguishing feature of tensors [18]. The generic exponents listed in Table VI for the crystallographic tensors summarize the different exponents of the corresponding electromagnetic and toroidal spherical tensors in Table V with the same signature.

In physical terms, toroidal tensors as in Tables V and VI arise as compound tensors (4) representing products of electric and magnetic tensors; they describe the combined effect of electric and magnetic multipoles as commonly studied in quantum-mechanical perturbation theory. Interestingly, this case contrasts with the equations of classical electromagnetism that are linear [71], so, within the framework of classical electromagnetism, a superposition of electric and magnetic multipoles cannot give rise to such qualitatively new terms.

E. Absolute quantification of electric and magnetic multipole densities

For crystals, the definition of electric dipolarization as the dipole moment per unit cell is unsatisfactory; it depends on the arbitrary choice of the unit cell [31–34]. Similar difficulties arise, for example, with orbital magnetic dipoles [35] and higher multipole moments associated with clusters of atoms [23]. Important progress towards addressing this issue was made by the modern theories of electric dipolarization and magnetization that provide gauge-invariant expressions for the electric dipolarization and magnetization based on properties of Bloch functions, i.e., independent of individual atoms or ions constituting a crystal structure [32–34,90,91]. However, the modern theories still have a number of limitations. Their quantification of the electric dipolarization works only for insulators [92] and only pertains to polarization *changes* that must be evaluated relative to a reference state, though thermodynamics requires that a state variable such as the polarization in a ferroelectric crystal must have an absolute meaning independent of how a state has been reached [37]. Most importantly, the extension of the modern theories to higher-rank multipole densities beyond dipolar order turns out to be difficult [93,94].

Group theory provides not only a formal definition of multipole densities in crystals but also an absolute quantification of electric and magnetic multipole densities in crystals, as shown in Ref. [36]. In crystalline solids, lattice-periodic quantities q can be formulated in real space as continuous functions $q(\mathbf{r})$ or, equivalently, in terms of their discrete Fourier components $q(\mathcal{G})$ in reciprocal space. Here, q may represent, e.g., scalar quantities, such as the charge density ρ, or tensorial quantities, such as a magnetization density $\mathbf{m}$. In the following, we denote such quantities collectively as $q(\mathbf{x})$, where $\mathbf{x}$ may denote position $\mathbf{r}$ or reciprocal lattice vectors $\mathcal{G}$.

If G is the symmetry group of the crystal, observable quantities $q(\mathbf{x})$ must transform according to the identity IR Γ_1 of G. However, if G is a supergroup of the symmetry group of the crystal (see below), parts of $q(\mathbf{x})$ may transform according to different IRs Γ_α of G. To identify these parts, we can project $q(\mathbf{x})$ onto the IRs Γ_α of G [11],

$$q_\alpha(\mathbf{x}) = \Pi_\alpha q(\mathbf{x}) \equiv \frac{n_\alpha}{h}\sum_{g\in G}\chi_\alpha(g)^* P_g q(\mathbf{x}), \tag{6a}$$

such that $q_\alpha(\mathbf{x})$ transforms according to Γ_α. Here, $\chi_\alpha(g)$ are the characters of the IR Γ_α, P_g are the symmetry operators corresponding to the group elements $g\in G$, n_α is the dimension of Γ_α, and h is the order of G. The projectors Π_α can be formulated and evaluated independent of a particular choice of origin or unit cell [95]. The projection yields the decomposition

$$q(\mathbf{x}) = \sum_\alpha q_\alpha(\mathbf{x}) \tag{6b}$$

because the projection operators Π_α are orthogonal and complete [11]. Previously, the projection operators Π_α have been used, e.g., in electronic band-structure calculations for the method of symmetrized plane waves [95].

The symmetry group G used in Eqs. (6) need not be the symmetry group of the system. For example, if G is the parent point group above the critical temperature T_c of a ferroelastic or ferroelectric phase transition and $q(\mathbf{x})$ represents the charge density $\rho(\mathbf{x})$, the projection (6)

becomes a crystallographic multipole expansion, as introduced in Sec. II B, that allows one to quantitatively evaluate the crystallographic multipole densities $\rho_\alpha(\mathbf{x})$ arising in such ferroic phase transitions. Above T_c, the entire charge density $\rho(\mathbf{x}) = \rho_1(\mathbf{x})$ transforms according to the trivial IR Γ_1 of the parent point group G, whereas below T_c (when the new symmetry group U is a subgroup of G [38]), some fractions $\rho_\alpha(\mathbf{x})$ of the total density transform according to nontrivial IRs Γ_α of G (say, an electric dipole density in ferroelectric transitions and an electric quadrupole density in ferroelastic transitions). The quantities $q_\alpha(\mathbf{x})$ provide a complete characterization of the respective multipole density they represent. We can estimate the magnitude of $q_\alpha(\mathbf{x})$ by evaluating, for example,

$$Q_\alpha = \sum_{\mathbf{x}} |q_\alpha(\mathbf{x})|. \tag{7}$$

Numerical examples for electric and magnetic multipole densities in crystals based on Eqs. (6) have been given in Ref. [36].

The decomposition (6) provides a unified, quantitative theory of electric and magnetic multipole densities in crystalline media, treating all these quantities on the same footing. It is in line with established phenomenological (group-theory based) studies of electric dipolarization and magnetization in crystalline media [12,13,96] and also with the modern theory of polarization [32–34,90,91]. The decomposition (6) is valid for insulators, semimetals, and metals. The projected multipole densities $q_\alpha(\mathbf{x})$ and Q_α are gauge-invariant quantities with absolute values independent of a reference state. Therefore, these quantities are well suited as intensive state variables for thermodynamic theories [37], including the order parameters in Landau's theory of phase transitions [38]. The projection technique lends itself to be incorporated into the suite of computational materials-science tools, thus complementing current approaches that focus on the modern theories [34] and local multipole configurations [39,40,97].

F. Multipole densities and band structure

The irreducible crystallographic tensors listed in the bottom part of Table VI arise prominently in a Taylor expansion of the spin-dependent electronic band structure $E_\sigma(\mathbf{k})$ (obtained systematically via the theory of invariants [14]). Table VI implies that the spin-dependent electronic band structure $E_\sigma(\mathbf{k})$ in crystal structures is qualitatively different when some or all inversion symmetries are broken, as compared with the case where these symmetries are preserved [14,98,99].

More specifically, the spin-dependent band structure $E_\sigma(\mathbf{k})$ directly reflects the presence of multipolar order in solids [18,24,100]. This is illustrated for the five categories of polarization in Fig. 2, which juxtaposes typical band dispersions $E_\sigma(\mathbf{k})$ [101] with the multipole order (tensors $T_\ell^{ss'}$) allowed in these materials.

Among the tensors $T_\ell^{ss'}$ in a family ss', the tensors $\ell = 1$ stand out; for crystal structures, they define a unique *polar direction* with signature ss' [13]. Familiar examples include the vector of electric dipolarization in ferroelectric and pyroelectric media and the magnetization vector in ferromagnetic and pyromagnetic media. In Figs. 2(a)–2(i), using gray arrows and strikethrough arrows, we illustrate whether systems possess a polar direction or whether a polar direction is forbidden. Polar directions ss' are defined more accurately in Appendix B 2 via the IRs of the full axial group $D_\infty \times C_{i\times\theta}$.

Figures 2(b), 2(d), 2(f), and 2(h) consider the case $n = 0$, where the integer n is defined in Table VI, whereas panels (c), (e), (g), and (i) consider $n \geq 1$. No such distinction is needed for panel (a). We note that rows and columns of Fig. 2 each represent specific distinct subsets of the 122 magnetic crystal classes such that we obtain a complete classification of the 122 magnetic crystal classes and important physical properties they entail. The detailed classification of all 122 crystal classes is listed in Table XIX. See also Tables XXI and XXII.

In the following, we discuss in more detail the electronic band structure associated with the different categories of polarizations (upper part of Fig. 2).

(i) In parapolar materials, both SIS and TIS are good symmetries. According to Table V, we have only even-ℓ electric tensors k^{2n+2} that can be formed with signature $++$, but no odd-ℓ electrotoroidal tensors. Therefore, parapolar materials have a spin-degenerate dispersion, illustrated in Fig. 2(a), that is symmetric about $\mathbf{k} = 0$; i.e., we have $E(\mathbf{k}) = E(-\mathbf{k})$. A polar direction associated with a tensor T_1^{++} [28] cannot arise in the band structure of parapolar materials.

(ii) The electropolar category is characterized by a spin-split dispersion $E_\sigma(\mathbf{k})$ that does not break TIS. An example of a k-linear spin splitting depicted in Fig. 2(b) is the Rashba term $\propto \mathbf{k}\times\boldsymbol{\sigma}$ that reflects the electric dipolarization T_1^{-+} in ferroelectric or pyroelectric media such as the hexagonal wurtzite structure [102]. A k-linear spin splitting also arises in materials that permit an electrotoroidal scalar T_0^{-+} or an electrotoroidal quadrupole density T_2^{-+} (see Sec. III and Appendix C 2). The electropolar case with $n = 0$ can thus be realized with and without a polar direction $-+$.

A dispersion of the form sketched in Fig. 2(c) with $n > 0$ occurs in materials permitting odd-ℓ electropolarizations T_ℓ^{-+} with $\ell > 1$ such as the cubic zincblende structure, where the Dresselhaus term [103] represents an electric octupolarization T_3^{-+}. Further examples are discussed in Appendix C 2.

(iii) Magnetopolar materials break TIS. They can exhibit a finite spin-dependent splitting proportional to σ

around $\mathbf{k} = \mathbf{0}$ as illustrated in Fig. 2(d). Note that the spin matrices σ_j jointly transform like a vector T_1^{+-} [see Eq. (5)]. Therefore, the spin-dependent splitting of the band structure near $\mathbf{k} = \mathbf{0}$ due to terms proportional to σ reflects not just the signature $+-$ of any magnetopolar system but also the existence of a polar direction $+-$ that coincides with the macroscopic magnetization T_1^{+-}; i.e., these systems must be ferromagnetic. In contrast, magnetopolar systems that show a $\mathbf{k}$-dependent spin splitting as in Fig. 2(e), which vanishes for $\mathbf{k} = \mathbf{0}$, do not permit a magnetization T_1^{+-}. These systems are altermagnetic; they permit magnetic multipolarizations T_ℓ^{+-} with odd ℓ and $\ell > 1$ such as a magnetic octupolarization (see Sec. II G). Similar to the electropolar category, the electronic band structure of magnetopolar systems may also include terms that transform like magnetotoroidal tensors T_ℓ^{+-} with even ℓ.

(iv) Antimagnetopolar materials have a spin-degenerate $\mathbf{k}$-asymmetric dispersion that reflects the fact that these materials break both SIS and TIS, but CIS remains a good symmetry. As discussed in Sec. II D, the signature $--$ characteristic of antimagnetopolar order can only be realized via magnetotoroidal terms proportional to k^{2n+1}. If the system permits a magnetotoroidal dipolarization T_1^{--}, this is reflected in the band structure by a k-linear term that dominates the dispersion near $k = 0$, leading to a shifted parabola as depicted in Fig. 2(f) [18,29,104–106]. The magnetotoroidal octupolarization T_3^{--} present in a bulk diamond antiferromagnet is indicated by terms proportional to k^3 [18,106], so the dispersion is an example of the one shown in Fig. 2(g).

The fact that the electronic band structure in antimagnetopolar crystal structures only permits magnetotoroidal terms proportional to k^{2n+1} has remarkable consequences. The antimagnetopolar category is characterized by the presence of even-ℓ magnetic multipoles of the form $r^{2n+1}\sigma$ (see Table VI). Such even-ℓ magnetic multipoles T_ℓ^{--} do not possess a polar direction $--$ for any even ℓ. In the band structure, magnetotoroidal terms linear in k represent a polar direction for the antimagnetopolar category (with signature $--$) in the same way an electric dipole density defines a polar direction for the electropolar category $(-+)$ and a magnetic dipole density defines a polar direction for the magnetopolar category $(+-)$; i.e., each unipolar category permits a characteristic polar direction ss'. Among the antimagnetopolar crystal classes, we have no simple relation between the lowest even $\ell > 0$ permitting $T_\ell^{--} \neq 0$ and the lowest n of allowed magnetotoroidal terms k^{2n+1}. In Table XIX, all 122 crystal classes are ordered according to the lowest-rank multipole densities they permit. See also Tables XXI and XXII. As discussed in more detail in Appendix C, magnetotoroidal vectors arise as compound tensors.

(v) Multipolar materials break all inversion symmetries i, θ, and $i\theta$. Therefore, the band dispersions do not possess any symmetries, as shown in Figs. 2(h) and 2(i). These materials permit all families of multipoles. Similar to the electropolar case with $n = 0$ [Fig. 2(b)], the multipolar case with $n = 0$ can be realized with or without a polar direction. The multipolar case with $n \geq 1$ [Fig. 2(i)] always excludes the possibility of having a polar direction ss'.

An electric dipole density T_1^{-+} (ferroelectricity or pyroelectricity) may exist in 10 electropolar crystal classes and 21 multipolar crystal classes permitting a polar direction with signature $-+$. Similarly, a magnetic dipole density T_1^{+-} (ferromagnetism or pyromagnetism) may exist in 10 magnetopolar crystal classes and 21 multipolar crystal classes. A magnetotoroidal dipole density T_1^{--} (ferrotoroidicity or pyrotoroidicity) may exist in 10 antimagnetopolar crystal classes and 21 multipolar crystal classes. The electronic band structure of these ferroic systems generally corresponds to the case $n = 0$ shown in the upper row [panels (b), (d), (f), and (h)] of Fig. 2. Note that the higher-order terms $n > 0$ depicted in the lower row [panels (c), (e), (g), and (i)] of Fig. 2 require a higher crystal symmetry than the terms with $n = 0$. Therefore, the higher-order terms $n > 0$ are generally also present in the band structure of systems realizing the scenarios illustrated in the upper row. Weakly ferroic systems (see Sec. II H) are a subset of the systems permitting, by symmetry, the terms $n = 0$ shown in the upper row, though weak ferroicity implies that the band structure will be dominated by the higher-order terms $n > 0$ shown in the lower row. For example, the spin-dependent band structure of weak ferromagnets is dominated by the altermagnetic terms σk^{2n} with $n \geq 1$ [107].

G. Altermagnetism and piezomagnetism

The spin-dependent band dispersion shown in Fig. 2(e) that does not give rise to a macroscopic magnetization T_1^{+-} has recently been identified as a characteristic feature of altermagnets [3]. The presence of magnetopolarizations T_ℓ^{+-} with odd $\ell > 1$, while a magnetic dipolarization T_1^{+-} is forbidden by symmetry (no polar direction $+-$), can be considered a defining feature for altermagnets [18,82]. According to this definition, 11 magnetopolar and 12 multipolar crystal classes are altermagnetic.

Unlike recent theories [3,4], the above definition of altermagnetic systems does not depend on local configurations of magnetic and nonmagnetic atoms in a crystal structure. The altermagnetic band structure displayed in Fig. 2(e) can be realized in crystal structures made solely of magnetic atoms, as illustrated in Ref. [18]. The above definition applies both to collinear and to noncollinear magnetic structures.

Similarly, 11 electropolar and 12 multipolar crystal classes are alterelectric. These classes are characterized by the condition that they permit electropolarizations T_{ℓ}^{-+} with odd $\ell > 1$, while an electric dipolarization T_1^{-+} with polar direction $-+$ is forbidden. Zincblende is an example of a cubic alterelectric crystal structure that permits an electric octupolarization T_3^{-+} [18]. The spin-dependent band dispersion of electropolar alterelectric media is shown in Fig. 2(c). If alterelectric order arises in an order-disorder phase transition similar to the phase transition in ferroelectric media, it can be identified, e.g., by a specific-heat anomaly.

In addition, 11 antimagnetopolar and 12 multipolar crystal classes are altertoroidic. These classes are characterized by the condition that they permit magnetotoroidizations T_{ℓ}^{--} with odd $\ell > 1$, while a dipolarization T_1^{--} with polar direction $--$ is forbidden. The antiferromagnetic diamond structure that was studied in Refs. [18,106] is an example of an altertoroidic structure. The spin-degenerate band dispersion of antimagnetopolar altertoroidic media is shown in Fig. 2(g). Finally, we have 15 multialteric crystal classes.

All magnetopolar altermagnetic crystal classes except for the octahedral class $O_h = O \times C_i$ are also piezomagnetic. In piezomagnets, external stress (which does not change the signature ss') defines the polar direction that permits ferromagnetism and/or pyromagnetism. (Ferromagnets and pyromagnets are commonly likewise counted as piezomagnets [96].) In strained altermagnetic crystals, an external magnetic field can thus be used to manipulate the magnetic order. Similarly, all electropolar alterelectric crystal classes except for the octahedral class $O \times C_\theta$ are also piezoelectric, all antimagnetopolar altertoroidic classes except for the octahedral class $O_h(O) = O \times C_{i\theta}$ are also piezotoroidic, and all multialteric classes except for the octahedral class O are also multipiezoic.

H. Weak ferroicity and the anomalous Hall effect

The ferroic crystal classes summarized in Fig. 2 also include the possibility of weak ferroicity such as weak ferromagnetism [108,109]. In weakly ferroic systems, the symmetry of the magnetic crystal class *permits* ferroicity (i.e., symmetry permits a dipolarization $T_1^{ss'}$ representing, e.g., a magnetization); nonetheless, the ferroicity in a specific material may be very small or even zero. Generally, more crystal classes permit higher-rank spherical tensors than lower-rank tensors (see Table XIX). Thus, when a lower-rank tensor like $T_1^{ss'}$ becomes nonzero, this is generally accompanied by a symmetry reduction from some group G to a subgroup $U \subsetneq G$. However, in weak ferroics, the crystal class that permits a dipole density $T_1^{ss'}$ does not change when reorienting local moments on the atoms such that $T_1^{ss'} \to 0$ [108], while higher-rank odd-ℓ multipole densities $T_{\ell}^{ss'}$ remain nonzero. Therefore, even in the limit of a vanishing dipolarization $T_1^{ss'}$, these systems possess a polar direction that is realized, e.g., by an octupole density $T_3^{ss'}$; i.e., under the crystallographic point group G of the respective crystal class, some component of the octupole density $T_3^{ss'}$ transforms according to the same IR Γ_α of G as a dipole density $T_1^{ss'}$ [16]. For example, let $\mathbf{m}(\mathbf{x})$ denote the magnetization density due to the local distribution of magnetic moments in the crystal, and let Γ_α denote the IR under G of both a magnetic dipole density T_1^{+-} and (part of) an octupole density T_3^{+-}. In a weak ferromagnet, the projection of $\mathbf{m}(\mathbf{x})$ onto the IR Γ_α can be nonzero [compare Eq. (6)], yielding a projected density $\mathbf{m}_\alpha(\mathbf{x})$ that represents a magnetic octupole density T_3^{+-} [23], while the net magnetization density T_1^{+-} vanishes in the crystal, $\sum_{\mathbf{x}} \mathbf{m}_\alpha(\mathbf{x}) = 0$. This result reflects the fact discussed above that multiple IRs $D_{\ell}^{ss'}$ of the full rotation group $R_{i\times\theta}$ correspond to the same IR Γ_α of a crystallographic point group G [16].

The proper identification of the material's crystal class is relevant in the context of related effects such as the anomalous Hall effect (AHE). While the AHE has commonly been associated with ferromagnetic materials [111], recent studies have identified large anomalous Hall conductivities in antiferromagnetic materials [112–115]. It was shown early on in Ref. [116] that the AHE may exist only in materials belonging to one of the 31 ferromagnetic crystal classes, i.e., classes that *permit* by symmetry a macroscopic magnetization density T_1^{+-} (see also Ref. [117]). Indeed, consistent with Ref. [116] the antiferromagnetic materials showing nonzero anomalous Hall conductivities turn out to be weak ferromagnets, where the Hall vector is aligned with the polar direction permitted by the respective crystal class. For example, intermetallic ferromagnetic RGa (R = rare earth Pr, Nd, Sm, Gd, Tb, Dy, Ho, Er) [118,119], the collinear antiferromagnet MnTe [113], and the noncollinear antiferromagnets Mn_3Sn and Mn_3Ge [114,115] all belong to the ferromagnetic crystal class $D_{2h}(C_{2h}) = m'm'm$. Therefore, these materials share properties such as an AHE, even when the net magnetization in some of these materials may be zero, and the Hall vector must align parallel to the polar direction of the crystal class $D_{2h}(C_{2h})$. Furthermore, natural Faraday rotation (i.e., Faraday rotation in the absence of an external magnetic field) may exist in crystal structures for which ferromagnetism is permitted by symmetry [51], which includes weak ferromagnets. Weak ferroelectricity has previously been considered in Ref. [54].

I. Odd-parity magnets: Space-group symmetries versus point-group symmetries

The present work focuses on point-group symmetries of crystal structures that are responsible for macroscopic crystal properties, consistent with Neumann's principle. A more fine-grained classification of crystal symmetries is provided by the 1651 MSGs, where, generally, multiple

MSGs belong to the same crystal class; i.e., the respective MSGs have the same magnetic point group [120]. For example, all MSGs with black-white Bravais lattices (sometimes called type-IV MSGs) describe magnetically ordered structures. However, all type-IV MSGs belong to type-II (see Appendix A 2) crystal classes, which also describe nonmagnetic crystal structures. Therefore, magnetic crystals with type-IV MSGs only allow macroscopic tensor properties that would also be permitted in nonmagnetic crystal structures belonging to the same type-II crystal class [21,120]. In the standard model, crystals with type-IV MSGs thus belong to the parapolar and electropolar categories. Parapolar magnetic media include, e.g., NiO and MnO (point group $C_{2h} \times C_\theta = C_2 \times C_{i\times\theta}$ [121]). Every type-II crystal class has at least one realization in terms of type-IV MSGs.

The type-II crystal class of a magnetic type-IV crystal generally has a lower symmetry than the type-II crystal class of the same material in the absence of magnetic order (i.e., above the critical temperature for magnetic ordering). Therefore, the magnetic phase transition of type-IV materials can manifest itself via phenomena usually associated with phase transitions in nonmagnetic media. Recently, crystal structures with type-IV MSGs called odd-parity magnets have sparked renewed interest because their magnetic order can give rise to properties such as a Rashba effect [80,81]; i.e., odd-parity magnets fall into the electropolar category of the standard model. Previously, the Rashba effect had been discussed predominantly in the context of nonmagnetic materials. A more systematic discussion of how space-group symmetries relate to crystal properties within the standard model will be published elsewhere.

J. TIS breaking and spin-orbit coupling in magnetically ordered systems

The essence of the standard model developed in this work is a coarse-grained yet comprehensive classification of crystalline matter based on the three fundamental inversion symmetries i, θ, and $i\theta$. For example, broken TIS represents the fundamental cause for all physical phenomena that distinguish magnetic systems from nonmagnetic systems [51].

We want to compare our theory with recent complementary efforts, aiming for a more fine-grained classification of crystalline matter beyond the 122 magnetic point groups [3,4]. In the theory of magnetic groups, symmetry operations act jointly on orbital and spin (magnetic) degrees of freedom. The theory of spin groups [122] considers separate operations acting on orbital and spin degrees of freedom. Recent interest in this approach [3,4] is motivated by the fact that magnetic order is generally dominated by exchange coupling [123]. In the nonrelativistic Schrödinger theory, the electron spins are then completely decoupled from the electrons' orbital motion [124]. For collinear spins, this yields decoupled Schrödinger equations for spin up and down that preserve TIS, as noted previously in the context of electronic-structure calculations for magnetic systems in, e.g., Refs. [3,125,126]. Very generally, this result is due to the fact that the respective Hamiltonians for spin up and down are real [127]. Therefore, the Schrödinger-Pauli theory is fundamentally incomplete in its account of broken TIS in magnetically ordered systems. Spin-orbit coupling is needed in magnetically ordered systems to break TIS by making the Hamiltonian complex. For this reason, spin-orbit coupling has been an indispensable ingredient in microscopic theories of the anomalous Hall effect [111] and the magnetoelectric effect [128].

It is interesting to compare Schrödinger-Pauli theory with Dirac theory. Dirac theory provides a relativistically invariant formulation of quantum mechanics, while Schrödinger-Pauli theory is generally believed to give a faithful representation of the nonrelativistic and weakly relativistic limit of the Dirac theory. Indeed, unlike Schrödinger-Pauli theory, Dirac theory properly accounts for TIS breaking in magnetic systems even in the nonrelativistic limit [127]. This is closely related to the fact that the well-known electron magnetic moment $e\hbar/(2m)$ appears explicitly only in Schrödinger-Pauli theory. However, in Dirac theory, this moment is realized via orbital equilibrium currents that break TIS even in the nonrelativistic limit [129].

In consequence, a proper account of magnetic phenomena is naturally achieved in electronic-structure calculations based on Dirac theory. Such fully relativistic calculations of magnetic systems, though less common than calculations based on Schrödinger-Pauli theory, have been reported, e.g., in Refs. [130,131]. However, such a description does not lend itself to a decoupling of real-space order and magnetic order that is assumed in applications of spin-group theories [3,4,122].

III. CHIRALITY IN SOLIDS

Chirality literally means "handedness," referring to one of the most fundamental and ubiquitous types of asymmetry in nature [132]. On a conceptional level, chirality is associated with the existence of at least two inequivalent versions of a physical entity—called enantiomorphs—that cannot be superposed by proper rotations C and/or translations [43–50]. Instead, interconversion of enantiomorphs requires i-improper rotations iC, i.e., transformations that involve space inversion i such as a mirror reflection (which is a π rotation about an axis perpendicular to the reflection plane followed by space inversion i). Equivalently, an object has been called chiral if its symmetry group does not contain any i-improper rotation. An achiral object can be mapped onto itself by an i-improper rotation; i.e., it shows no enantiomorphism.

The space groups of chiral crystal structures allow two distinct cases. Either an enantiomorphic pair of crystal structures transforms according to an enantiomorphic pair of distinct space groups, or the pair of crystal structures transforms according to the same space group. In total, 65 nonmagnetic space groups describe chiral structures. These are the 65 Sohncke groups that were identified early on in crystallography and that represent a subset of the 230 nonmagnetic space groups [66]. However, in agreement with Neumann's principle, the macroscopically observable features of chirality only depend on the crystallographic point group G of the crystal class of a crystal structure [13]. The 65 Sohncke groups are exactly the space groups for which the respective point groups G are one of the 11 (nonmagnetic) chiral point groups; i.e., the distinction between the two cases described above is not relevant at the level of Neumann's principle. The Sohncke groups include symmorphic and nonsymmorphic space groups. Ignoring TIS, the 11 chiral point groups G are precisely the proper point groups G_{p} that form the roots for the 11 Laue classes $L(G_{\mathrm{p}})$ of crystallographic point groups [133].

Optical activity is often viewed as a unique hallmark of chirality. While this is correct for liquids and molecules in solution, crystal structures can be optically active though they are not chiral (point groups C_s, C_{2v}, S_4, and D_{2d}) [13,45,134]. This example shows how chirality in infinite crystal structures is qualitatively different from chirality in finite molecules. The surge of recent interest in understanding chirality in solids on a fundamental level [47–50] is one of the motivations for the present work.

The importance of TIS for chirality has been noted early on [135,136]. A distinction between two different types of chirality was suggested: So-called true chirality occurs in situations where only i-improper rotations, but not θ-improper rotations, can interconvert between enantiomorphs, whereas systems for which both i-improper and θ-improper rotations, but not $i\theta$-improper rotations, interconvert the enantiomorphs have been called false chiral [45,136,137]. Original discussions of false chirality only considered TIS-breaking external magnetic fields [45,136,137], but they did not consider magnetically ordered systems breaking TIS inherently. The utility of adopting a broader definition of enantiomorphism has also been emphasized [43].

In the following, we develop the most general description of enantiomorphism based on symmetry considerations. We start by introducing the five categories of chirality in Sec. III A. Experimental signatures for unichiral and multichiral systems are discussed in Sec. III B. Section III C focuses on the intricate way chirality manifests in the electronic band structure. A brief discussion of induced chirality is presented in Sec. III D. Materials candidates for the different categories of chirality are listed in Appendix F.

A. Categories of chirality

In the present work, we treat SIS, TIS, and CIS on an equal footing to obtain a more systematic understanding of chirality and to acquire a unified description of associated physical phenomena. In the lower part of Table IV, we identify five categories of chirality that are distinguished by which γ-improper rotations are present in the point group of a system. The parachiral category refers to systems that have all three kinds of γ-improper rotations among their symmetries. These systems have no enantiomorphism. The electrochiral, magnetochiral, and antimagnetochiral systems have θ-improper, i-improper, and $i\theta$-improper rotations, respectively, among their symmetries, so each of these categories has two distinct enantiomorphs. Finally, multichiral systems have only proper rotations among their symmetries, so these systems have four distinct enantiomorphs.

Clearly, the defining features of the five categories of chirality displayed in the lower part of Table IV follow a similar pattern as the defining features of the five categories of polarizations displayed in the upper part of Table IV. Therefore, each group type is associated with one category of multipole order and one category of chirality, which yields the symmetry classification of magnetic point groups presented in Fig. 1 (see also Appendix A 3, especially Table IX). The five categories of multipole order (polarizations) and the five categories of chirality thus represent two complementary classifications based on the presence or absence of the inversion symmetries i, θ, and $i\theta$. Polarizations reflect the presence or absence of i, θ, and $i\theta$ as *independent* elements in the symmetry group G of a physical system. Chiralities, on the other hand, reflect the presence or absence in G of any *composite* symmetry elements iC, θC, and $i\theta C$ (i.e., presence or absence of γ-improper rotations γC). See Fig. 1 and Table IV.

While the classifications of point groups with respect to the categories of polarizations and those of chirality are complementary, we nevertheless have an intricate connection between multipole order and chirality that may exist in a system. Specifically, the absence of γ-improper rotations in chiral systems implies that the respective monopoles $T_0^{ss'}$ become symmetry allowed (see Table IV). These monopoles thus represent chiral charges. They are signatures of chiral order, similar to how electric and magnetic multipoles are signatures of polar order [138]. (Below, we discuss more generally how configurations of polarizations can give rise to chirality.) Our naming of the five categories of chirality reflects the nature of the allowed scalars other than the universally allowed T_0^{++} (see Table IV). Compared with the existing nomenclature [45] comprising (true) chirality, false chirality, and achirality, the five mutually exclusive categories constitute a more comprehensive and systematic classification of chirality in solids [140].

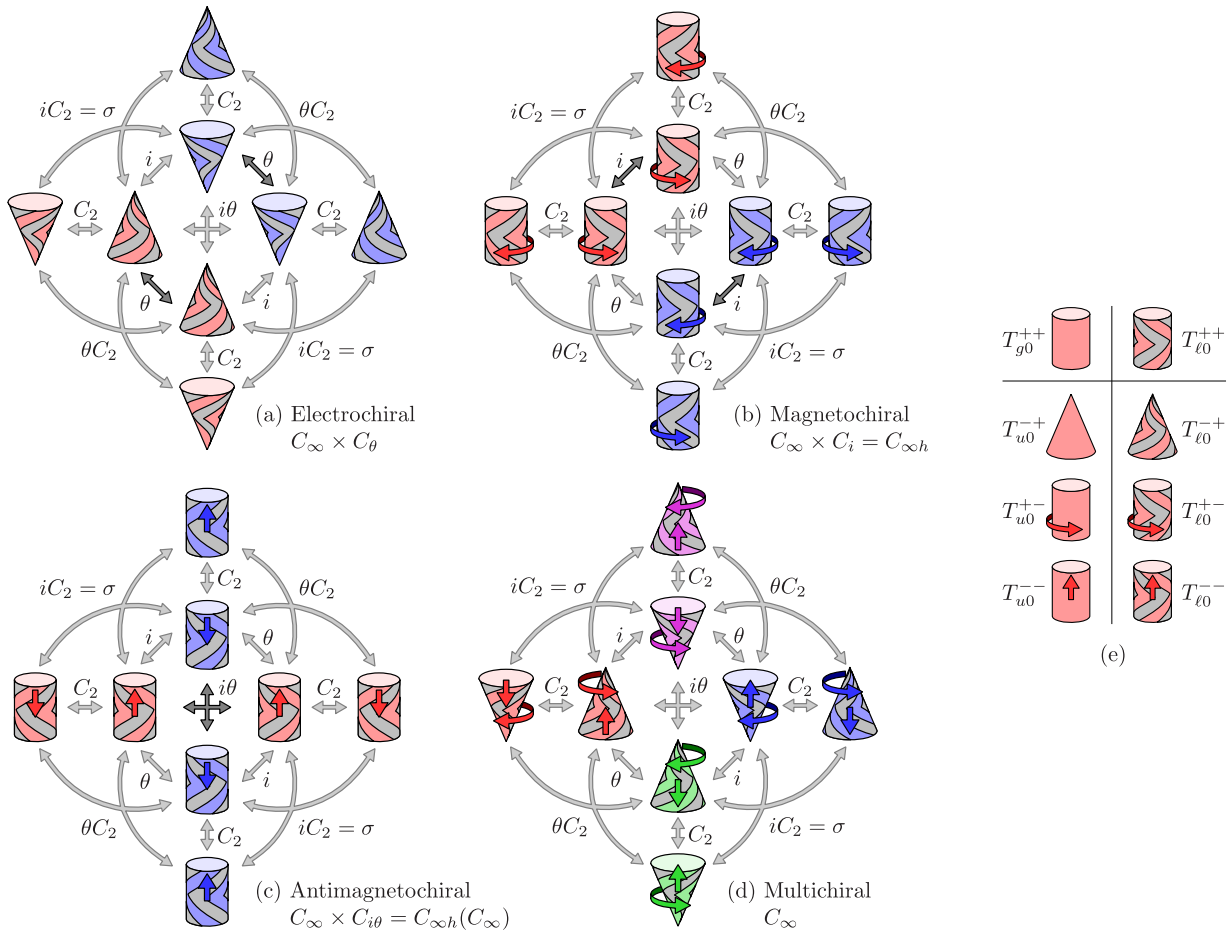


FIG. 4. Categories of chirality illustrated for axially symmetric objects representing the unipolar-unichiral and multipolar-multichiral groups in class $L(C_\infty)$ [133]. As a visual aid, different enantiomorphs are distinguished by color. Straight (curved) colored arrows indicate translational (rotational) motion of an object. Dark (light) gray double arrows connect two objects that transform into each other under the specified symmetry operation, which is (is not) a good symmetry of the object. Note that C_2 represents a π rotation about any axis perpendicular to the high-symmetry z axis. Panel (a) shows that, in electrochiral systems, space inversion i interconverts the enantiomorphs, but time inversion θ does not. In panel (b), the situation is reversed for magnetochiral systems. In panel (c), both i and θ separately interconvert enantiomorphs in antimagnetochiral systems, but their combination $i\theta$ leaves them invariant. In contrast, $i\theta$ interconverts the two enantiomorphs present in electro- and magnetochiral systems. In panel (d), all three inversions i, θ, and $i\theta$ interconvert the four enantiomorphs of a multichiral system. The chiral objects in panels (a) to (c) transform like tensor components $T^{ss'}_{\ell 0}$ as indicated in panel (e). These tensor components $T^{ss'}_{\ell 0}$ can be derived either by reducing the symmetry of tensor components $T^{ss'}_{u0}$ or by reducing the symmetry of tensor components $T^{++}_{\ell 0}$.

We now provide a brief overview of each category. Figures 4–6 give illustrative examples for these chiralities by exploring how different axially symmetric objects are either invariant (i.e., mapped onto themselves), mapped onto a rotated copy of themselves, or mapped onto distinct enantiomorphs. Such simple shapes, typically incorporating angular and/or linear momentum, provide generic representations for finite chiral systems [7,45,136]. Formally, this approach depicts categories of chirality for the continuous axial classes $L(C_\infty)$ and $L(D_\infty)$ discussed in more detail in Appendix B 2. The basic symmetry properties of the objects utilized in Figs. 4–6 are also reviewed in Appendix B 2 (see Table XVI).

1. Parachirality

Parachiral point groups contain γ-improper rotations γC for all three inversions $\gamma = i$, θ, and $i\theta$. Therefore, such systems do not allow enantiomorphism. No scalars of $R_{i\times\theta}$ other than T^{++}_0 are permitted under parachiral groups. In particular, the scalar T^{-+}_0 is forbidden, and parachiral systems are therefore achiral as per the definition in Ref. [45].

Examples of parachiral groups include the full axial rotation groups $C_\infty \times C_{i\times\theta}$ and $D_\infty \times C_{i\times\theta}$ permitting scalars $T^{++}_{\ell 0}$ and T^{++}_{g0}, respectively, as illustrated in Figs. 4(e), 5(e), and 6(e). See Fig. 3 for a crystallographic example (corundum Al_2O_3, point group $D_3 \times C_{i\times\theta} \equiv D_{3d} \times C_\theta$).

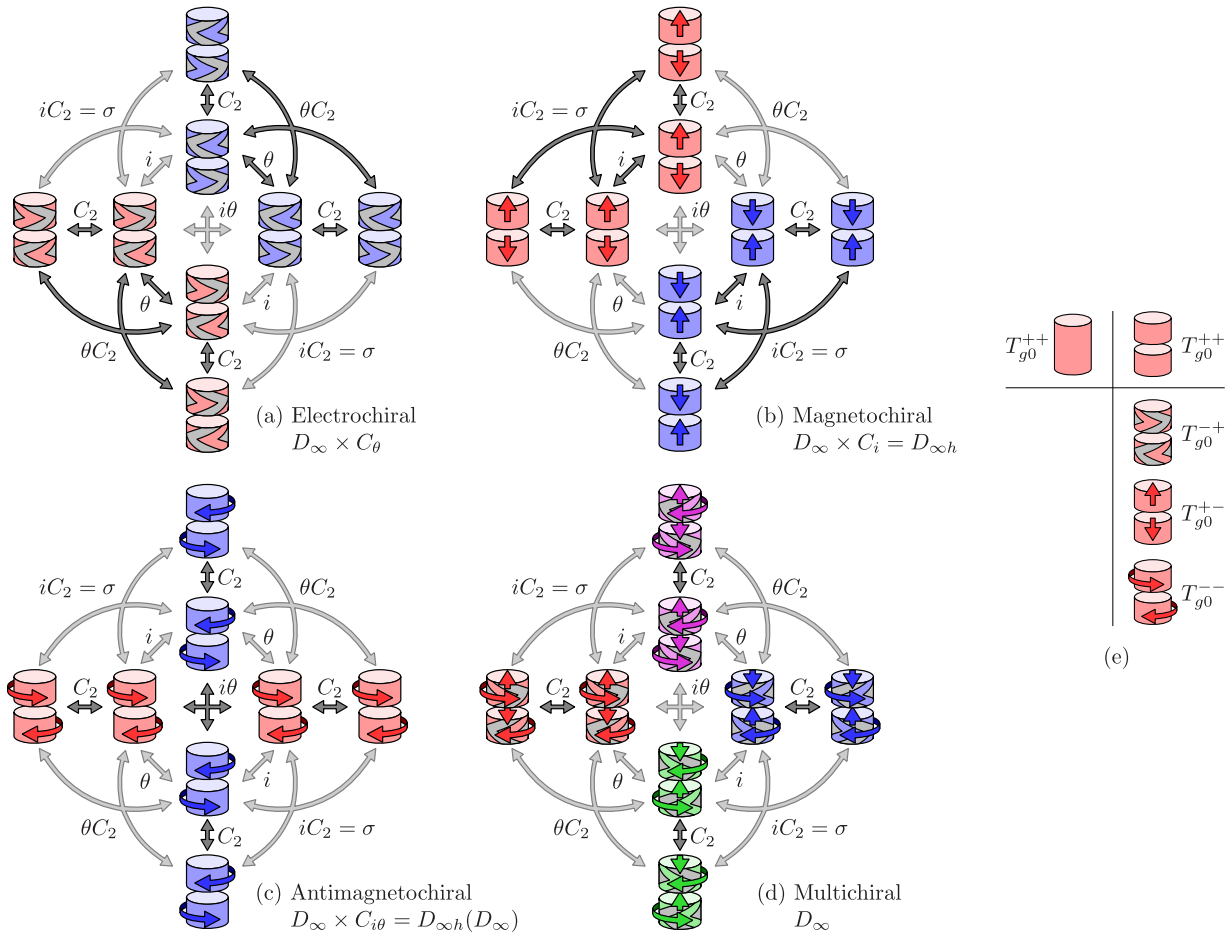


FIG. 5. Categories of chirality illustrated for axially symmetric objects representing the unipolar-unichiral and multipolar-multichiral groups in class $L(D_\infty)$ [133]. Conventions are the same as in Fig. 4. In panel (e), the chiral objects in panels (a) to (c) transform like tensor components $T_{g0}^{ss'}$ that can be derived by reducing the symmetry of tensor components T_{g0}^{++}.

2. Electrochirality

Electrochiral groups contain θ-improper rotations θC but no i-improper or $i\theta$-improper rotations; i.e., an inequivalent enantiomorph is generated when a transformation iC or $i\theta C$ is applied to the crystal. Electrochiral systems permit the pseudoscalar T_0^{-+}. See Figs. 4(a), 5(a), and 6(a) for illustrative examples.

As seen from Fig. 1, electrochiral groups are either electropolar or multipolar. Electrochiral magnets [141] belong to the latter type. Examples of nonmagnetic electrochiral systems are shown in Figs. 4(a) and 5(a). In these systems, chirality arises from the interplay of a parapolarization with an electropolarization, i.e., between even-ℓ and odd-ℓ electric-multipole densities. Crystallographic realizations of the scenarios from Figs. 4(a) and 5(a) have been encountered in Refs. [142,143] (with point groups $C_3 \times C_\theta$ and $D_4 \times C_\theta$, respectively). The situation depicted in Fig. 6(a) is equivalent to an electrochiral ferromagnet, where electrochirality emerges from the presence of collinear magnetic and magnetotoroidal dipolarizations [141], which is the crystal analog of electrochirality arising when a magnetic field is applied parallel to a beam of light [136]. In such multipolar electrochiral systems, the electrochiral enantiomorphs can be viewed as magnetic domains that are related via i-improper and $i\theta$-improper rotations but are each invariant under improper rotations of the form θC [141]. Such domains differ fundamentally from ordinary magnetic domains that can be superposed by proper rotations C.

3. Magnetochirality

Magnetochiral groups contain i-improper rotations iC, but θ-improper and $i\theta$-improper rotations are absent. Therefore, θ-improper or $i\theta$-improper rotations generate an inequivalent enantiomorph of a system described by such a group. See Figs. 4(b), 5(b), and 6(b) for illustrative examples.

The nontrivial scalar allowed in magnetochiral groups is T_0^{+-}, which has no indicator associated with it in the electronic band structure (see Table V and Sec. III C). Some

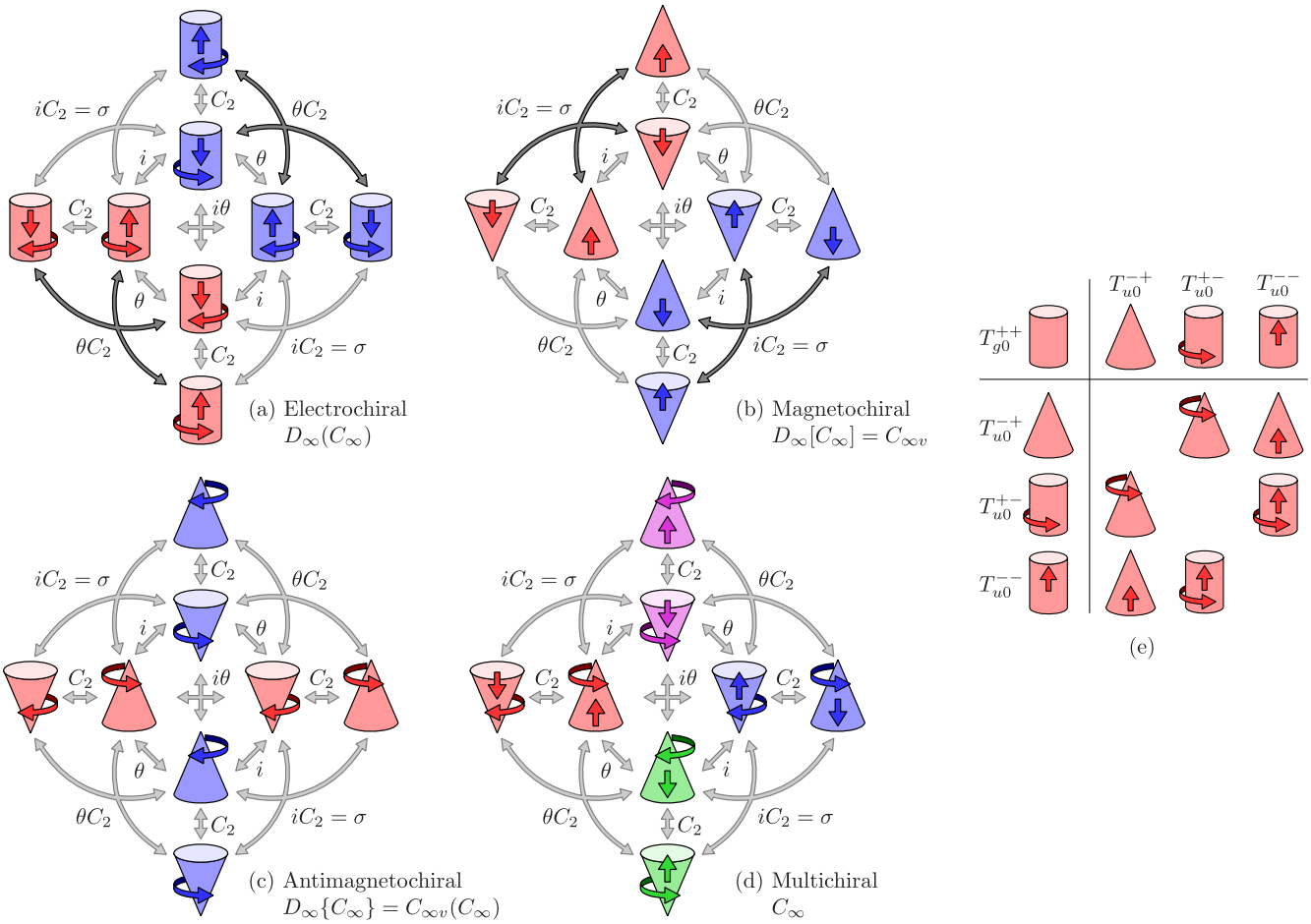


FIG. 6. Categories of chirality illustrated for axially symmetric objects representing the multipolar-unichiral groups in class $L(D_\infty)$ [133]. The multipolar-multichiral group C_∞ shown in panel (d) belongs to $L(C_\infty)$ [133]. Conventions are the same as in Fig. 4. The chiral objects in panels (a) to (d) can be viewed as superpositions of the parachiral objects in panel (e).

physical consequences arising from the presence of T_0^{+-} have recently been conjectured in Ref. [144]. As the scalar T_0^{-+} is forbidden under magnetochiral groups, magnetochiral systems would be considered achiral according to Ref. [45]. However, the enantiomorphism arising under θ-improper and $i\theta$-improper rotations makes magnetochiral systems fundamentally different from parachiral ones, as enantiomorphism is completely absent in the latter.

Magnetochirality requires magnetic order. Ordinary magnetic domains can be superposed by proper rotations C. Magnetochiral enantiomorphs can be considered as magnetic domains that are related by some improper rotations of the form θC and $i\theta C$, but these domains *cannot* be superposed by any proper rotation C, e.g., due to the presence of nonmagnetic atoms. See Fig. 3 for an example (hematite α-Fe_2O_3, point group $D_3 \times C_i \equiv D_{3d}$). Thus, magnetic domains that are magnetochiral enantiomorphs constitute fundamentally different, physically distinguishable entities, unlike ordinary magnetic domains that differ solely by the orientation of the magnetic order parameter.

Magnetochiral groups are either magnetopolar or multipolar (see Fig. 1). Examples of magnetopolar magnetochiral systems are shown in Figs. 4(b) and 5(b). Here, enantiomorphism arises from the interplay of a parapolarization with a magnetopolarization, i.e., even-ℓ electric and odd-ℓ magnetic multipole densities. In the example from Fig. 4(b), the magnetopolarization is a magnetization; i.e., this system is a ferromagnet. Alternatively, as exemplified by the system shown in Fig. 5(b), magnetochiral systems can also be altermagnets (having an odd-$\ell > 1$ magnetic multipole density). Hematite (α-Fe_2O_3, point group $D_3 \times C_i \equiv D_{3d}$, see Fig. 3) is such an altermagnetic magnetochiral materials candidate [145]. Its two enantiomorphs are the two different antiferromagnetic domains that are interrelated via TIS and CIS.

The scenario in Fig. 6(b) is an example of the multipolar magnetochiral type. In this scenario, magnetochirality arises from collinear electric and magnetotoroidal dipolarizations, which is analogous to magnetochirality realized in the situation where an electric field is applied parallel to a light beam.

4. Antimagnetochirality

Antimagnetochiral groups contain $i\theta$-improper rotations, but i-improper and θ-improper rotations are absent. Thus, γ-improper rotations γC, where $\gamma = i$ or θ, generate an inequivalent enantiomorph of an antimagnetochiral structure. See the examples depicted in Figs. 4(c), 5(c), and 6(c).

The antimagnetochiral category subsumes what has previously been referred to as false chirality [136,137]: Although such a system exhibits enantiomorphism, it does not permit a scalar T_0^{-+} and is therefore not considered to be truly chiral. Instead, a scalar T_0^{--} is allowed in antimagnetochiral systems, though this scalar has no indicator directly associated with it in the electronic band structure (see Table V and Sec. III C).

Antimagnetochiral groups are either antimagnetopolar or multipolar; see Fig. 1. Figures 4(c) and 5(c) show examples of antimagnetopolar antimagnetochiral systems, where antimagnetochirality arises from the combination of a parapolarization with an antimagnetopolarization. Figure 6(c) shows a multipolar system, representing the situation where antimagnetochirality arises from the presence of an electric polarization collinear with a magnetization or, equivalently, from parallel electric and magnetic fields [136].

Antimagnetochiral enantiomorphs can be viewed as magnetic domains that are related via i-improper and θ-improper rotations. See Fig. 3 for a crystallographic example [chromia Cr_2O_3, point group $D_3 \times C_{i\theta} \equiv D_{3d}(D_3)$]. Again, these should not be considered as ordinary magnetic domains—antimagnetochiral enantiomorphs cannot be superposed by proper rotations C and, therefore, constitute different physical entities [146,147].

5. Multichirality

Multichiral groups do not contain γ-improper rotations γC for any of the inversions $\gamma = i$, θ, or $i\theta$. Hence, these groups coincide with the proper point groups. See Figs. 4(d), 5(d), and 6(d) for illustrative examples. As indicated in these figures, multichiral systems have four distinct enantiomorphs, as all three improper rotations iC, θC, and $i\theta C$ yield distinct versions of the given object.

It is possible to group the four enantiomorphs of a multichiral system into two pairs so that members of a pair are transformed into each other by i-improper rotations. Based on the existence of enantiomorphs that interconvert via improper rotations iC, and the fact that a scalar T_0^{-+} is allowed, multichiral systems have been conventionally classified as showing true chirality [45,141]. However, the enantiomorphs forming a pair related by i-improper rotations are not invariant under θ-improper rotations, as is the case for electrochiral enantiomorphs. In fact, both θ-improper rotations and $i\theta$-improper rotations transform one pair of enantiomorphs related by i-improper rotations into the other pair of such enantiomorphs. Similarly, the four enantiomorphs could be divided into two other pairs where members of a pair interconvert via θ-improper rotations. While the same behavior is exhibited by magnetochiral enantiomorphs, members of such a multichiral-enantiomorph pair are again different because they are not invariant under i-improper rotations. Rather, the two pairs are switched by both i-improper rotations and $i\theta$-improper rotations. Lastly, for the third possible grouping of the four multichiral enantiomorphs into disjoint pairs, members of an individual pair can be superposed by improper rotations $i\theta C$, and the two pairs are interchanged by both θ-improper rotations and i-improper rotations. Thus, the enantiomorphism of multichiral systems is fundamentally different from the enantiomorphism of unichiral systems; it is not a mixture or superposition of the unichiral enantiomorphisms.

The lower symmetry of multichiral systems permits all four scalars $T_0^{ss'}$ to exist side by side. More generally, they simultaneously allow the same set of tensors $T_{lm}^{ss'}$ for all signatures ss'. Multichiral systems are therefore always multipolar (see Fig. 1). The interrelation of different multipolar orders with (conventional) chirality has been the focus of a recent experimental study [148] of a multichiral material ($BaCoSiO_4$, point group C_6). This system is a realization of the scenario depicted in Fig. 4(d). However, in such systems (having a point group C_n), the simultaneous presence of electric, magnetic, and magnetotoroidal dipolarizations can mask physical effects arising from multichirality, including optical nonreciprocity. More pristine realizations of multichiral systems are those with a point group D_{2n} [scenario depicted in Fig. 5(d)].

B. Experimental signatures of chirality

Very generally, the enantiomorphism realized in unichiral and multichiral media can be identified via observable effects such as natural optical activity [51] and nonreciprocal directional dichroism [52] that have opposite signs for the different enantiomorphs. The occurrence of these effects is not limited to chiral media; i.e., their observability represents a necessary but not a sufficient criterion for enantiomorphism [13,45,134]. However, in nonenantiomorphous media, these effects arise such that symmetry-equivalent directions of the media show the same effect with opposite signs [13,134]. If this case can be excluded experimentally, i.e., opposite signs are observed only for different enantiomorphs, a phenomenon like natural optical activity becomes a necessary and sufficient criterion for enantiomorphism.

This aspect of enantiomorphs clearly distinguishes, e.g., (anti)magnetochiral domains from ordinary magnetic domains. It also allows one to differentiate between opposite enantiomorphs. Multichiral systems require multiple such probes to distinguish all four enantiomorphs. In the following, we focus on optical nonreciprocities.

1. Optical nonreciprocity: General introduction

The reduced symmetry of chiral systems generally allows additional contributions to the dielectric tensor that give rise to distinctive optical effects [51]. To illustrate most clearly the dual and triadic relationships between unichiral systems, in the following, we focus on the phenomenon of nonreciprocal directional dichroism (NDD), i.e., the different rates of absorption for unpolarized light beams propagating in opposite directions. Fundamentally, NDD occurs in materials allowing a third-rank Cartesian tensor with signature $--$ [52]. A subset of these materials are crystals permitting a magnetotoroidal vector T_1^{--} [149]. In the remainder of this section, we focus on the emergence of NDD in chiral systems.

2. Electrochirality

Electrochirality gives rise to magnetochiral dichroism [150–152], which is the version of NDD characterized by the asymmetric absorption of unpolarized light parallel and antiparallel to an applied magnetic field. This phenomenon is currently attracting great interest [153]. It arises because an electrochiral system subject to a magnetic field or a magnetization has the reduced symmetries required for a nonzero tensor T_1^{--} [149,154]. This effect has equal magnitude but opposite sign for the two enantiomorphs and can therefore be used to differentiate between opposite enantiomorphs.

Electrochiral systems are also optically active [51], and they show a linear current-induced magnetization [6,155,156]. While these effects do not occur exclusively due to electrochirality [13,45,157], the magnitude of these effects is again equal for the two enantiomorphs but has the opposite sign.

3. Magnetochirality

Directional dichroism also arises when a magnetochiral system is placed into an electric field [149,154,158,159]. This electrochiral dichroism is characterized by an asymmetry in the absorption of light parallel and antiparallel to the applied electric field (or electric polarization). It can be considered as the dual of magnetochiral dichroism discussed above. Again, the asymmetry exhibited by the two magnetochiral enantiomorphs is equal in magnitude but has the opposite sign.

4. Antimagnetochirality

In antimagnetochiral materials that allow T_1^{--}, NDD occurs with equal magnitude and opposite sign for the two enantiomorphs, thus enabling their experimental differentiation [52,160]. Placing an antimagnetochiral material into an electric field generates the symmetry conditions for both the Faraday effect and magnetic circular dichroism to occur [161], with the associated nonreciprocities again having opposite sign for the two enantiomorphs [162].

5. Multichirality

Multichiral enantiomorphs are more profoundly different than unichiral enantiomorphs. For physical quantities and effects, it is generally the *sign* that can be opposite for different chiral domains. Therefore, to distinguish between all four enantiomorphs of a multichiral system, more than one physical quantity or effect must be considered. For example, multichiral systems show NDD when placed in a magnetic or an electric field [154], thus combining the experimental signatures of electrochiral and magnetochiral systems. Based on the sign of the directional dichroisms exhibited in applied magnetic and electric fields, the four multichiral enantiomorphs can be uniquely identified.

C. Chirality and band structure

As discussed in Sec. II, the spin-dependent electronic band structure $E_\sigma(\mathbf{k})$ directly reflects the categories of polarizations in solids. These categories manifest themselves via characteristic terms in the band structure that transform like irreducible tensors $T_\ell^{ss'}$. In the following, we argue that the band structure $E_\sigma(\mathbf{k})$ generally reflects the categories of chirality in solids via an *interplay* of parapolar and unipolar (i.e., electropolar, magnetopolar, or antimagnetopolar) terms.

The categories of chirality can be defined based on which monopoles $T_0^{ss'}$ are permitted in a system (see Table IV). For example, in electrochiral crystal structures, the electrotoroidal compound scalar T_0^{-+} becomes symmetry allowed. In a band structure, such a scalar is realized by a term $\boldsymbol{\sigma}\cdot\mathbf{k}$. The presence of this scalar in a band structure has thus been identified as a key feature of electrochiral systems [48]. It can be viewed as a minimal model of an effective low-energy Hamiltonian for electrochirality in solids.

In contrast, using the same building blocks k, σ, the charges T_0^{+-} and T_0^{--} have no band-structure indicators associated with them (see Table V). In magnetochiral systems (fictitious or engineered), we can envision compound scalars $T_0^{+-}\propto\mathbf{d}\cdot\mathbf{k}$ and, in antimagnetochiral systems, compound scalars $T_0^{--}\propto\boldsymbol{\sigma}\cdot\mathbf{d}$, where $\mathbf{d}$ is an electric dipole density (signature $-+$) similar to the magnetic dipole density $\boldsymbol{\sigma}$ (signature $+-$) [27].

However, for a crystal structure to be chiral, it is not decisive whether (and how) chiral charges $T_0^{ss'}$ are actually realized. Electropolarizations, magnetopolarizations, and antimagnetopolarizations $T_\ell^{ss'}$ with $\ell>0$ combined with parapolarizations T_ℓ^{++} with $\ell>0$ can likewise make a system chiral. In the following, we show how tensors $T_\ell^{ss'}$ with $\ell>0$ can be used to define minimal models of effective low-energy Hamiltonians for electrochirality, magnetochirality, and antimagnetochirality for all magnetic-point-group classes $L(G_\mathrm{p})$ [133].

Our theory is illustrated in Table VII, which lists the lowest-degree invariant tensors realizing chiralities in the

TABLE VII. Lowest-degree invariant tensors realizing chiralities in the continuous classes $L(R)$ and $L(D_\infty)$, the cubic classes $L(O)$ and $L(T)$, and the axial classes $L(D_n)$ and $L(C_n)$ with $n = 2, 4, 3, 6$ [133]. We have $R \supset O \supset T$ and $D_\infty \supset D_n \supset C_n$, so that terms allowed under the respective supergroup are also allowed under the respective subgroup. The symbol "cp" denotes cyclic permutation of indices x, y, z in the preceding term, and $(x \leftrightarrow y)$ denotes the preceding term with x and y interchanged. For the crystallographic classes, we denote in square brackets the degree ℓ of multipolar order represented by the respective terms as well as the maximal group that leaves this term invariant. For electrochirality and magnetochirality, we only consider electric and magnetic tensors with odd ℓ; we do not consider toroidal compound tensors with even ℓ. For antimagnetochirality, we consider the lowest-degree odd-ℓ magnetotoroidal compound tensors representing an antimagnetopolarization.

Class $L(G_\mathrm{p})$		$L(R)$		$L(O)$		$L(T)$
$G_\mathrm{p} \times C_{i\times\theta}$	PC	k^2	$[\ell = 4, O \times C_{i\times\theta}]$	$k_y^2 k_z^2 + \mathrm{cp}$		
			$[\ell = 6, O \times C_{i\times\theta}]$	$[k_x^4(k_y^2 + k_z^2) + \mathrm{cp}] - 8k_x^2 k_y^2 k_z^2$	$[\ell = 6, T \times C_{i\times\theta}]$	$(k_y^2 - k_z^2)(k_z^2 - k_x^2)(k_x^2 - k_y^2)$
$G_\mathrm{p} \times C_\theta$	EC	$\boldsymbol{\sigma} \cdot \mathbf{k}$	$[\ell = 9, O \times C_\theta]$	$\sigma_x k_x[k_y^2 k_z^2(3k_y^4 - 10k_y^2 k_z^2 + 3k_z^4) + k_x^2(k_x^2 - k_y^2 - k_z^2)(k_y^4 - 6k_y^2 k_z^2 + k_z^4)] + \mathrm{cp}$	$[\ell = 3, O[T] \times C_\theta]$	$\sigma_x k_x(k_y^2 - k_z^2) + \mathrm{cp}$
$G_\mathrm{p} \times C_i$	MC		$[\ell = 9, O \times C_i]$	$\sigma_x k_y k_z(k_y^2 - k_z^2)[5k_x^4 - 3k_x^2(k_y^2 + k_z^2) + k_y^2 k_z^2] + \mathrm{cp}$	$[\ell = 3, O(T) \times C_i]$	$\sigma_x k_y k_z + \mathrm{cp}$
$G_\mathrm{p} \times C_{i\theta}$	AMC		$[\ell = 9, O \times C_{i\theta}]$	$k_x k_y k_z(k_y^2 - k_z^2)(k_z^2 - k_x^2)(k_x^2 - k_y^2)$	$[\ell = 3, O(T) \times C_{i\theta}]$	$k_x k_y k_z$
Class $L(G_\mathrm{p})$		$L(D_\infty)$		$L(D_6)$		$L(C_6)$
$G_\mathrm{p} \times C_{i\times\theta}$	PC	$k_x^2 + k_y^2; k_z^2$	$[\ell = 6, D_6 \times C_{i\times\theta}]$	$k_x^2(k_x^2 - 3k_y^2)^2; k_y^2(k_y^2 - 3k_x^2)^2$	$[\ell = 6, C_6 \times C_{i\times\theta}]$	$k_x k_y(k_x^2 - 3k_y^2)(k_y^2 - 3k_x^2)$
$G_\mathrm{p} \times C_\theta$	EC	$\sigma_x k_x + \sigma_y k_y; \sigma_z k_z$	$[\ell = 7, D_{12}[D_6] \times C_\theta]$	$\sigma_x k_x[k_y^2(k_x^2 - 3k_y^2)(k_y^2 - 3k_x^2) + 3k_z^2(k_x^4 - 10k_x^2 k_y^2 + 5k_y^4)] - (x \leftrightarrow y) - 3\sigma_z k_z(k_x^2 - k_y^2)(k_x^4 - 14k_x^2 k_y^2 + k_y^4)$	$[\ell = 1, D_\infty[C_\infty] \times C_\theta]$	$\sigma_x k_y - \sigma_y k_x$
$G_\mathrm{p} \times C_i$	MC		$[\ell = 7, D_{12}(D_6) \times C_i]$	$3\sigma_x k_y k_z(5k_x^4 - 10k_x^2 k_y^2 + k_y^4) + (x \leftrightarrow y) - \sigma_z k_x k_y(k_x^2 - 3k_y^2)(k_y^2 - 3k_x^2)$	$[\ell = 1, D_\infty(C_\infty) \times C_i]$	σ_z
$G_\mathrm{p} \times C_{i\theta}$	AMC		$[\ell = 7, D_{12}(D_6) \times C_{i\theta}]$	$k_x k_y k_z(k_x^2 - 3k_y^2)(k_y^2 - 3k_x^2)$	$[\ell = 1, D_\infty(C_\infty) \times C_{i\theta}]$	k_z
Class $L(G_\mathrm{p})$				$L(D_3)$		$L(C_3)$
$G_\mathrm{p} \times C_{i\times\theta}$	PC		$[\ell = 4, D_3 \times C_{i\times\theta}]$	$k_y k_z(k_y^2 - 3k_x^2)$	$[\ell = 4, C_3 \times C_{i\times\theta}]$	$k_x k_z(k_x^2 - 3k_y^2)$
$G_\mathrm{p} \times C_\theta$	EC		$[\ell = 3, D_6[D_3] \times C_\theta]$	$2\sigma_x k_z k_x k_y + \sigma_y k_z(k_x^2 - k_y^2) + \sigma_z k_y(k_y^2 - 3k_x^2)$	$[\ell = 1, D_\infty[C_\infty] \times C_\theta]$	$\sigma_x k_y - \sigma_y k_x$
$G_\mathrm{p} \times C_i$	MC		$[\ell = 3, D_6(D_3) \times C_i]$	$\sigma_x(k_x^2 - k_y^2) - 2\sigma_y k_x k_y$	$[\ell = 1, D_\infty(C_\infty) \times C_i]$	σ_z
$G_\mathrm{p} \times C_{i\theta}$	AMC		$[\ell = 3, D_6(D_3) \times C_{i\theta}]$	$k_x(k_x^2 - 3k_y^2)$	$[\ell = 1, D_\infty(C_\infty) \times C_{i\theta}]$	k_z
Class $L(G_\mathrm{p})$				$L(D_4)$		$L(C_4)$
$G_\mathrm{p} \times C_{i\times\theta}$	PC		$[\ell = 4, D_4 \times C_{i\times\theta}]$	$k_x^2 k_y^2$	$[\ell = 4, C_4 \times C_{i\times\theta}]$	$k_x k_y(k_x^2 - k_y^2)$
$G_\mathrm{p} \times C_\theta$	EC		$[\ell = 5, D_8[D_4] \times C_\theta]$	$\sigma_x k_x[k_x^2(k_y^2 - k_z^2) - k_y^2(k_y^2 - 3k_z^2)] + (x \leftrightarrow y) + \sigma_z k_z(k_x^4 - 6k_x^2 k_y^2 + k_y^4)$	$[\ell = 1, D_\infty[C_\infty] \times C_\theta]$	$\sigma_x k_y - \sigma_y k_x$
$G_\mathrm{p} \times C_i$	MC		$[\ell = 5, D_8(D_4) \times C_i]$	$\sigma_x k_y k_z(k_y^2 - 3k_x^2) - (x \leftrightarrow y) - \sigma_z k_x k_y(k_x^2 - k_y^2)$	$[\ell = 1, D_\infty(C_\infty) \times C_i]$	σ_z
$G_\mathrm{p} \times C_{i\theta}$	AMC		$[\ell = 5, D_8(D_4) \times C_{i\theta}]$	$k_x k_y k_z(k_x^2 - k_y^2)$	$[\ell = 1, D_\infty(C_\infty) \times C_{i\theta}]$	k_z
Class $L(G_\mathrm{p})$				$L(D_2)$		$L(C_2)$
$G_\mathrm{p} \times C_{i\times\theta}$	PC		$[\ell = 2, D_2 \times C_{i\times\theta}]$	$k_x^2 - k_y^2; k_y^2 - k_z^2; k_z^2 - k_x^2$	$[\ell = 2, C_2 \times C_{i\times\theta}]$	$k_x k_y$
$G_\mathrm{p} \times C_\theta$	EC		$[\ell = 3, O[T] \times C_\theta]$	$\sigma_x k_x(k_y^2 - k_z^2) + \mathrm{cp}$	$[\ell = 1, D_\infty[C_\infty] \times C_\theta]$	$\sigma_x k_y - \sigma_y k_x$
$G_\mathrm{p} \times C_i$	MC		$[\ell = 3, O(T) \times C_i]$	$\sigma_x k_y k_z + \mathrm{cp}$	$[\ell = 1, D_\infty(C_\infty) \times C_i]$	σ_z
$G_\mathrm{p} \times C_{i\theta}$	AMC		$[\ell = 3, O(T) \times C_{i\theta}]$	$k_x k_y k_z$	$[\ell = 1, D_\infty(C_\infty) \times C_{i\theta}]$	k_z

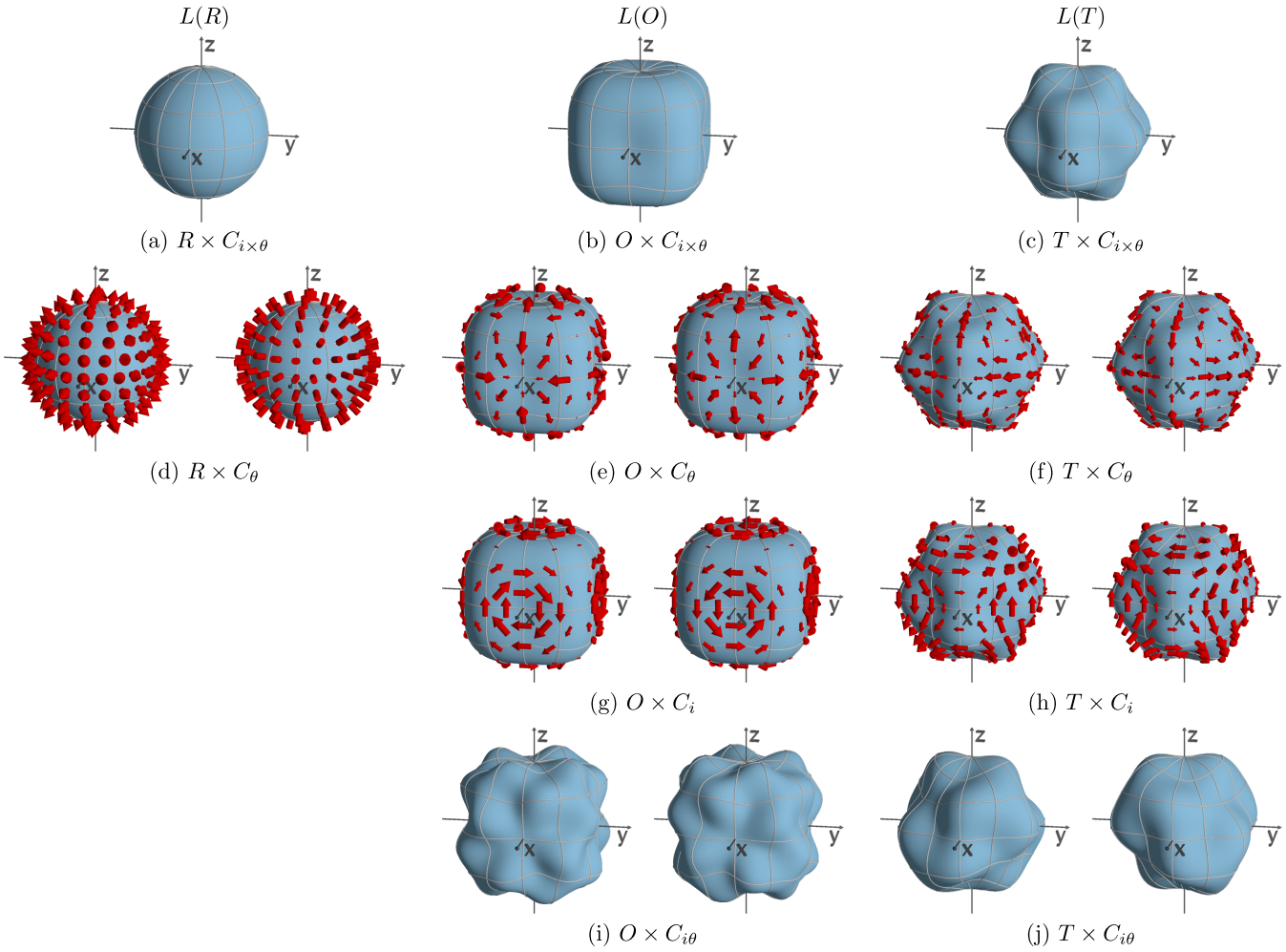


FIG. 7. Chirality exhibited in the band structure for unipolar-unichiral groups in classes $L(R)$ (left columns), $L(O)$ (center columns), and $L(T)$ (right columns) [133]. The first row shows energy surfaces of a parachiral system, whereas the second, third, and fourth rows show energy surfaces for the two enantiomorphs allowed under the indicated electrochiral, magnetochiral, and antimagnetochiral groups.

continuous classes $L(R)$ and $L(D_\infty)$, the cubic classes $L(O)$ and $L(T)$, and the axial classes $L(D_n)$ and $L(C_n)$ with $n = 2, 4, 3, 6$ [133].

1. Spherical class $L(R)$

The full rotation group $R_{i\times\theta}$ is parachiral. The only invariant tensor permitted by this group is T_0^{++}, which is realized by the scalar k^2 and functions thereof [Fig. 7(a)]. The electrochiral spherical group R_θ also permits a tensor $T_0^{-+} \propto \boldsymbol{\sigma}\cdot\mathbf{k}$ (and functions thereof). The latter term gives rise to two distinct enantiomorphs [18,163,164] [see Fig. 7(d)]. As discussed before, the magnetochiral group R_i and the antimagnetochiral group $R_{i\theta}$ have no band-structure indicators associated with them.

2. Cubic crystal system [classes $L(O)$ and $L(T)$]

Beyond the isotropic terms already permitted by the groups in the spherical class $L(R)$, all groups in the cubic class $L(O)$ also permit an electric hexadecapolarization ($\ell = 4$) that manifests itself in lowest order via a term [18]

$$H^{(\mathrm{e},4)} \propto k_x^2k_y^2 + k_y^2k_z^2 + k_z^2k_x^2. \tag{8}$$

This term represents a warping of the energy dispersion $E_\sigma(\mathbf{k})$ of band electrons in cubic crystal structures [165,166] [see Fig. 7(b)].

The group $O \times C_\theta$ is electrochiral. In lowest order ℓ, it permits an electropolarization with $\ell = 9$ that gives rise to a term

$$\begin{aligned} H^{(\mathrm{e},9)} \propto \sigma_x k_x[&k_y^2k_z^2(3k_y^4 - 10k_y^2k_z^2 + 3k_z^4) \\ &+ k_x^2(k_x^2 - k_y^2 - k_z^2)(k_y^4 - 6k_y^2k_z^2 + k_z^4)] + \mathrm{cp} \end{aligned} \tag{9}$$

[see Fig. 7(e)]. The electrotoroidal scalar $\boldsymbol{\sigma}\cdot\mathbf{k}$ that is generally likewise present in such systems can be interpreted as a compound moment density (4) due to the

combined effect of the electropolarization (9) and parapolarizations including the hexadecapolarization (8).

By SIS-TIS duality, the group $O \times C_i$ is magnetochiral. In lowest order ℓ, it permits a magnetopolarization with $\ell = 9$ that gives rise to a term

$$H^{(\mathrm{m},9)} \propto \sigma_x k_y k_z (k_y^2 - k_z^2)[5k_x^4 - 3k_x^2(k_y^2 + k_z^2) + k_y^2 k_z^2] + \mathrm{cp} \tag{10}$$

[see Fig. 7(g)]. Finally, the group $O \times C_{i\theta}$ is antimagnetochiral. It permits an antimagnetopolarization ($\ell = 0$) that manifests itself, in lowest order ℓ, via a magnetotoroidal density with $\ell = 9$ giving rise to a term

$$H^{(\mathrm{am},9)} \propto k_x k_y k_z (k_y^2 - k_z^2)(k_z^2 - k_x^2)(k_x^2 - k_y^2) \tag{11}$$

[see Fig. 7(i)].

Besides class $L(O)$, the cubic crystal system also includes class $L(T)$. As $T \subset O$, the polarizations permitted by the point groups G_O in $L(O)$ are also permitted by the respective groups $G_T \subset G_O$ in $L(T)$. Beyond that, the groups in $L(T)$ permit polarizations not present in $L(O)$, as listed in Table VII. These terms are of lower order than the terms permitted by $L(O)$.

Specifically, the electrochiral group $T \times C_\theta$ permits an electric octupolarization $\ell = 3$ that manifests itself via a Dresselhaus term

$$H^{(\mathrm{e},3)} \propto \sigma_x k_x (k_y^2 - k_z^2) + \mathrm{cp}. \tag{12}$$

As is well known [103], this term is already allowed for systems with the parachiral point group $T_d \times C_\theta = O[T] \times C_\theta$ [Fig. 8(a)] realized, e.g., by the zincblende structure; i.e., by itself, this term is not sufficient as an indicator for electrochirality in class $L(T)$. The Dresselhaus term (12) becomes an indicator for electrochirality [Fig. 7(f)] when combined with the parapolarization [$\ell = 6$, Fig. 7(c)]

$$H^{(\mathrm{e},6)} \propto (k_y^2 - k_z^2)(k_z^2 - k_x^2)(k_x^2 - k_y^2). \tag{13}$$

The parapolarization (13) is forbidden by the groups in class $L(O)$, but it is allowed in class $L(T)$. A parapolarization with $\ell = 6$ that is allowed already in class $L(O)$ is listed in Table VII.

Similarly, an altermagnetic magnetopolarization ($\ell = 3$),

$$H^{(\mathrm{m},3)} \propto \sigma_x k_y k_z + \mathrm{cp}, \tag{14}$$

may exist in systems with magnetochiral group $T \times C_i$ but also in parachiral systems with point group $O(T) \times C_i$. The magnetopolarization (14) becomes an indicator for magnetochirality when combined with the parapolarization (13) [see Fig. 7(h)]. Likewise, an antimagnetopolarization yields a magnetotoroidal term with $\ell = 3$,

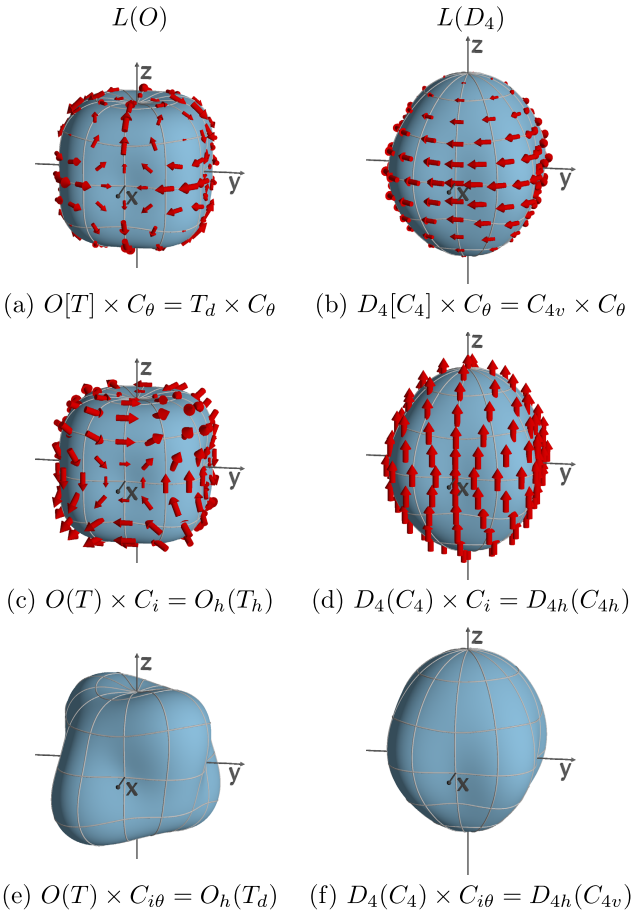


FIG. 8. Unipolarizations giving rise to unichirality in classes $L(T)$ (Fig. 7) and $L(C_4)$ (Fig. 9) may also exist in systems with point groups in classes $L(O)$ and $L(D_4)$ [133], respectively, where these terms, as shown here, *do not* give rise to unichirality.

$$H^{(\mathrm{am},3)} \propto k_x k_y k_z. \tag{15}$$

This term may exist in systems with antimagnetochiral group $T \times C_{i\theta}$ but also in parachiral systems with point group $O(T) \times C_{i\theta}$. The term (15) becomes an indicator for antimagnetochirality when combined with the parapolarization (13) [see Fig. 7(j)].

To summarize, in class $L(T)$, the unipolar terms (12), (14), and (15) become indicators of electrochirality, magnetochirality, and antimagnetochirality, respectively, only when each of these terms is combined with the parapolarization (13); i.e., jointly, the terms define minimal models for effective low-energy Hamiltonians realizing electrochirality (point group $T \times C_\theta$), magnetochirality ($T \times C_i$), and antimagnetochirality ($T \times C_{i\theta}$), respectively. This is discussed further in Sec. III C 4.

3. Axial systems [classes $L(D_n)$ and $L(C_n)$]

Similar to the preceding discussion of the cubic classes $L(O)$ and $L(T)$, Table VII also lists the lowest-order parapolar and unipolar tensors permitted by class

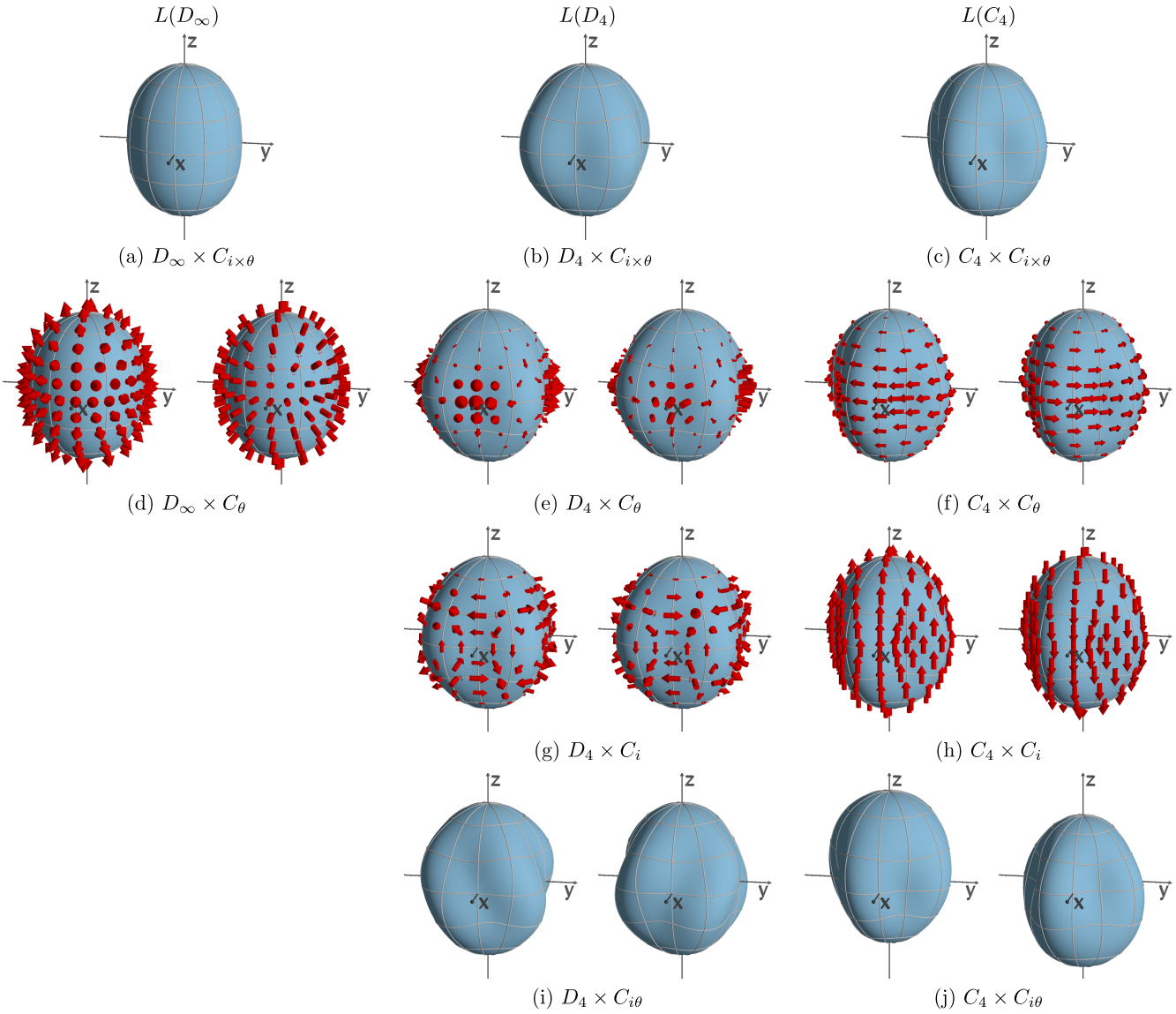


FIG. 9. Chirality exhibited in the band structure for unipolar-unichiral groups in classes $L(D_\infty)$ (left columns), $L(D_4)$ (center columns), and $L(C_4)$ (right columns) [133]. The first row shows energy surfaces of a parachiral system, whereas the second, third, and fourth rows show energy surfaces for the two enantiomorphs allowed under the indicated electrochiral, magnetochiral, and antimagnetochiral groups.

$L(D_\infty)$, as well as classes $L(D_n)$ and $L(C_n)$ with $n = 2$, 4, 3, 6. Figure 9 illustrates the chiral band structure for $L(D_\infty)$, $L(D_4)$, and $L(C_4)$. The corresponding set of plots for $L(D_3)$ is shown in Fig. 3. For the dihedral classes $L(D_6)$, $L(D_3)$, $L(D_4)$, and $L(D_2)$, unichirality is realized by combining suitable parapolar terms with unipolar terms with $\ell = 7$, 3, 5, and 3, respectively. Note that $D_2 \subset T$, so class $L(D_2)$ largely reproduces the features of class $L(T)$.

For magnetochiral α-Fe_2O_3 and antimagnetochiral Cr_2O_3 depicted in Fig. 3, the joint presence of an electric hexadecapolarization and a magnetic (for α-Fe_2O_3) or a magnetotoroidal (for Cr_2O_3) octupolarization generates chirality in the band structure. A hypothetical electrochiral corundum derivative (second column of Fig. 3) would similarly be characterized by having both the electric hexadecapolarization and an electric octupolarization present.

The electropolar cyclic groups $C_n \times C_\theta$ permit a spontaneous electric dipolarization ($\ell = 1$) that manifests itself via a Rashba term

$$H^{(\mathrm{e},1)} \propto \sigma_x k_y - \sigma_y k_x. \tag{16}$$

As is well known, this term is already allowed for systems with parachiral point groups $C_{nv} \times C_\theta = D_n[C_n] \times C_\theta$ realized, e.g., by the wurtzite structure ($C_{6v} \times C_\theta$) [102]. See also Fig. 8(b). When the Rashba term is combined with a suitable parapolar term forbidden by class $L(D_n)$ but

allowed by class $L(C_n)$ (see Table VII), jointly these terms describe an electrochiral system [Fig. 9(f)].

Similarly, the cyclic groups $C_n \times C_i$ are magnetopolar; i.e., they permit a spontaneous magnetization ($\ell = 1$) that manifests itself via an exchange (Zeeman) term

$$H^{(\mathrm{m},1)} \propto \sigma_z. \tag{17}$$

Such a term is already allowed for systems with the parachiral point groups $D_n(C_n) \times C_i$ [see Fig. 8(d)]. This term becomes an indicator of magnetochirality when combined with the respective parapolar terms listed for classes $L(C_n)$ in Table VII [Fig. 9(h)].

Finally, the cyclic groups $C_n \times C_{i\theta}$ are antimagnetopolar; i.e., they permit a spontaneous antimagnetopolarization that manifests itself via a magnetotoroidal term ($\ell = 1$)

$$H^{(\mathrm{am},1)} \propto k_z. \tag{18}$$

Again, such a term is already allowed for systems with the parachiral point groups $D_n(C_n) \times C_{i\theta}$ [see Fig. 8(f)]. This term becomes an indicator of antimagnetochirality when combined with the respective parapolar terms listed for classes $L(C_n)$ in Table VII [Fig. 9(j)].

4. Minimal effective models for chirality

For each tabulated tensor, Table VII lists its maximal group, i.e., the largest group that leaves the tensor invariant. For the odd-ℓ electropolar, magnetopolar, and antimagnetopolar tensors, the respective maximal group is always an improper group beyond class $L(G_\mathrm{p})$, so these tensors, by themselves, cannot serve as minimal effective models for chirality in class $L(G_\mathrm{p})$, as illustrated in Fig. 8.

Quite generally, a proper point group G_p is an invariant subgroup of i-minor groups $\tilde{G}_\mathrm{p}[G_\mathrm{p}]$,

$$G_\mathrm{p} \subset \tilde{G}_\mathrm{p}[G_\mathrm{p}] \tag{19a}$$

(see Appendix A 2). Specifically, we have ($n = 1, 2, 3, \ldots$)

$$T \subset T_d = O[T], \tag{19b}$$

$$D_{2n} \subset D_{(2n)d} = D_{4n}[D_{2n}], \tag{19c}$$

$$D_{2n+1} \subset D_{(2n+1)h} = D_{4n+2}[D_{2n+1}], \tag{19d}$$

$$C_{2n} \subset \begin{cases} S_{4n} = C_{4n}[C_{2n}] \\ C_{(2n)v} = D_{2n}[C_{2n}], \end{cases} \tag{19e}$$

$$C_{2n+1} \subset \begin{cases} C_{(2n+1)h} = C_{4n+2}[C_{2n+1}] \\ C_{(2n+1)v} = D_{2n+1}[C_{2n+1}], \end{cases} \tag{19f}$$

and similarly for the supergroups $\tilde{G}_\mathrm{p}(G_\mathrm{p})$ and $\tilde{G}_\mathrm{p}\{G_\mathrm{p}\}$ of G_p. Of course, while a group like D_4 is a crystallographic point group, the supergroup $D_{4d} = D_8[D_4] \supset D_4$ is not a crystallographic point group. Nonetheless, the improper point group D_{4d} is, ignoring TIS, the maximal group for the lowest-degree electropolar term permitted by the crystallographic point group D_4 (see Table VII), so this electropolar term, by itself, cannot serve as a minimal effective model for electrochirality in class $L(D_4)$.

Among the finite point groups, the octahedral group O is special as it does not appear as a subgroup of a finite group outside class $L(O)$. Therefore, the unipolar tensors with $\ell = 9$ listed in Table VII for class $L(O)$ represent, by themselves, minimal effective models for unichirality in class $L(O)$.

While the maximal groups for the unipolar tensors listed in Table VII generally go beyond the respective class $L(G_\mathrm{p})$, for each of the parapolar tensors in Table VII, the maximal group is the full group $G_\mathrm{p} \times C_{i\times\theta}$ of the respective class. Therefore, *jointly* the unipolar tensors combined with the respective parapolar tensors represent minimal, effective models for unichirality in class $L(G_\mathrm{p})$. Multichirality is realized by combining at least two different unipolar tensors in a class $L(G_\mathrm{p})$.

The cooperation of a parapolarization and a unipolarization to realize unichirality can also be recognized in Fig. 4. In Fig. 4(e), we can envision that polar properties have been added to the parapolar nonchiral object $T^{++}_{\ell 0}$. Alternatively, we could imagine that the unipolar nonchiral objects T^{-+}_{u0}, T^{+-}_{u0}, and T^{--}_{u0} have acquired a second nonpolar property, so, jointly, these properties realize chirality. These examples illustrate that we can generally have multiple pathways to realize chirality.

The multipolar-unichiral case in Fig. 6 is different from the unipolar-unichiral case in Figs. 4 and 5. The objects shown in Fig. 6(e) visualize the irreducible tensors T^{++}_{g0} and T^{-+}_{u0}, T^{+-}_{u0}, and T^{--}_{u0} as indicated. While individual objects $T^{ss'}_{u0}$ in Fig. 6(e) are unipolar but not chiral, it is the superposition of their polarizations that yields unichirality [Figs. 6(a)–6(c)] and multichirality [Fig. 6(d)].

This rule applies also to minimal effective models for chirality in multipolar-unichiral systems. For example, the multipolar-electrochiral group $D_4(C_4)$ permits the electropolar term

$$H^{(\mathrm{e},5)} \propto \sigma_x k_x[k_x^2(k_y^2 - k_z^2) - k_y^2(k_y^2 - 3k_z^2)] + (x \leftrightarrow y) + \sigma_z k_z(k_x^4 - 6k_x^2k_y^2 + k_y^4) \tag{20}$$

[because $D_4(C_4) \subset D_4 \times C_\theta \subset D_8[D_4] \times C_\theta$, see Table VII and Appendix A 3], the magnetopolar term (17) [because $D_4(C_4) \subset D_4(C_4) \times C_i$, see Table VII], and the antimagnetopolar term (18) [because $D_4(C_4) \subset D_4(C_4) \times C_{i\theta}$]. Any two of these terms are sufficient as a minimal model for electrochirality under $D_4(C_4)$ because the largest subgroup common to any two of the three groups $D_4 \times C_\theta$, $D_4(C_4) \times C_i$, and $D_4(C_4) \times C_{i\theta}$ is $D_4(C_4)$.

Of course, $D_4(C_4)$ permits not only the electropolar term (20) but also the parapolar term

$$H^{(\mathrm{e},4)} \propto k_x^2 k_y^2 \tag{21}$$

because $D_4(C_4) \subset D_4 \times C_{i\times\theta}$ (see Table VII). Jointly, the terms (20) and (21) can serve not only as a minimal model for electrochirality under $D_4 \times C_\theta$ but also under $D_4(C_4) \subset D_4 \times C_\theta$.

Using Table VII, minimal models for other multipolar-unichiral systems can be constructed in a similar way. Thus, we have a complete theory for minimal effective models describing chirality in crystals [101,167].

D. Induced chirality

From a symmetry point of view, an electropolar system with spontaneous electric dipolarization (16) is equivalent to a parapolar system placed into an external electric field. In parapolar systems with crystallographic point group $C_n \times C_{i\times\theta}$, electrochirality can therefore be induced by placing the system into an external electric field [28]. Similarly, magnetochirality can be induced by placing such a system into an external magnetic field. Finally, parallel electric and magnetic fields make such systems multichiral; i.e., they not only induce a Rashba term (16) and a Zeeman term (17), but, jointly, the fields also induce a magneto-toroidal term (18).

IV. CONCLUSIONS AND OUTLOOK

Our work introduces a standard model of electromagnetism and chirality in crystals that provides a comprehensive classification of broken symmetries and the physical properties they give rise to in all 122 magnetic crystal classes. The standard model is based on five categories of electric and magnetic multipole order and five categories of chirality that yield 12 types of crystal structures (see Fig. 1), each with distinctive electric and magnetic properties. Multiple versions of chirality that were previously overlooked, including multichirality with four distinct enantiomorphs, are novel rubrics underlying our complete classification. Our work shows explicitly how chirality is linked to electromagnetic order and band structure. In particular, we show how each category of chirality arises from distinct superpositions of electric and magnetic multipole densities. We also discuss band-structure indicators of chirality. For this purpose, we provide a complete theory of minimal effective models characterizing the different categories of chirality in different systems. These minimal models demonstrate explicitly how chirality in crystalline solids requires the interplay of multiple polarizations, either the interplay of unipolar and parapolar terms, or the interplay of multiple unipolar terms.

A. Macroscopic description of multipole order

An overarching goal of our work is to provide a general theory of electric and magnetic order in crystals that is freed from any reference to microscopic gauge-dependent degrees of freedom. To achieve this goal, we are generalizing the fundamental ideas developed earlier to discuss electric [12,34] and magnetic [20,21,34] dipole order to higher-rank multipoles. The five categories of multipole order (i.e., polarizations; see columns in Fig. 1) subsume phenomenology-based materials classifications and directly reflect distinctive features in the electronic band structure (Fig. 2).

We present a careful and comprehensive discussion of how compound multipoles arise in crystals, going beyond previous descriptions that utilized polarized harmonics [23,24,88]. These insights underpin the explanation for how antimagnetopolarizations (i.e., even-ℓ magnetic-multipole densities) are always represented by odd-ℓ magneto-toroidal terms in the spin-degenerate electronic band structure.

B. Hidden order parameters

The electric and magnetic dipole densities $\ell = 1$ (i.e., electric dipolarization and magnetization) represent the familiar order parameters in the thermodynamic description of ferroelectrics and ferromagnets, respectively [51]. Beyond these dipole densities $\ell = 1$ in ferroelectric and ferromagnetic media, multipole densities with rank $\ell > 1$ can serve as physically transparent order parameters of hidden orders in crystalline matter, thus facilitating their experimental detection [64,171,172]. To this end, our work establishes a direct association of multipole densities with the 122 magnetic crystal classes, as illustrated in Fig. 2. Generally, electric and magnetic multipole densities with odd $\ell > 1$ represent alterelectrics and altermagnets, respectively, i.e., electric and magnetic orders without a polar direction, while the even-ℓ antimagnetopolar (and odd-ℓ magnetotoroidal) multipole densities describe antimagnetopolar media. Application of methods developed in this work enables the absolute and gauge-invariant quantification of electric and magnetic multipole densities of any rank [36], which is a precondition for any well-defined order parameter [37,38].

Using multipole densities as order parameters presents an attractive alternative to utilizing staggered versions of electric or magnetic dipoles represented, e.g., by a Néel vector [51,110]. For example, the fundamental physical differences between magnetopolar antiferromagnets (i.e., altermagnets) and antimagnetopolar antiferromagnets (e.g., magnetoelectrics) are naturally captured by the different multipole densities representing these orders, which also allows for clear association with macroscopic physical properties (such as the distinctive band-structure features shown in Fig. 2). Making such connections based on Néel-vector constructions is typically less straightforward [173,174].

C. Response tensors

In the present work, we have focused on *irreducible* tensors; i.e., we have focused on tensors that transform irreducibly under point groups, including the spherical rotation groups and the crystallographic point groups. These irreducible tensors naturally lend themselves to the description of crystal *properties* such as the multipole densities that have been a central topic of the present work. We note that Cartesian tensors that are commonly reducible find widespread use as material tensors that describe crystal *responses* to external perturbations [13,96]. Recent works have studied nonequilibrium effects such as spin-dependent transport [175,176] and light-tailored multipole order [177–179]. A thorough analysis of such effects needs to consider Onsager's reciprocal relations accounting for the symmetry of fluctuations under time inversion θ when studying irreversible processes [38]. In the context of magnetic systems breaking TIS, such an analysis is not trivial. For example, following early work [180], the symmetry of the conductivity tensor describing the anomalous Hall effect in magnetically ordered systems was discussed intensely till a consensus was reached. See Ref. [117]. A proper discussion of this important point is beyond the scope of the present work. It will be the subject of a future publication.

D. More chirality from general improper rotations

The present work generalizes the concept of chirality, or enantiomorphism, to include noninvariance under improper rotations involving any one (or all three) among the inversions i, θ, and $i\theta$, leading to the identification of five categories of chirality (rows in Fig. 1, see also Fig. 3). This categorization settles previous arguments [43,45,137] about the place of TIS in definitions of chirality. We furthermore advance the search for band-structure indicators of enantiomorphism, presenting minimal models for each category of chirality realized in specific crystal classes (see Sec. III C, especially Table VII). Our findings make it evident that there is no universal indicator that is both necessary and sufficient for identifying chirality in all crystal classes. Rather, each unichiral or multichiral crystal class has its own interplay between parapolar and unipolar multipole densities that has its distinct fingerprints in the electronic band structure. The often-touted Dirac-like spin splitting term proportional to $\boldsymbol{\sigma}\cdot\mathbf{k}$ arises in electrochiral systems simply as a remnant of the electrotoroidal scalar T_0^{-+} having the Dirac term as an indicator already under the electrochiral rotation group R_θ.

The newly proposed (anti)magnetochiral and multichiral categories will be of particular interest for further experimental exploration. In Sec. III B 3, we describe the unusual nonreciprocal effects associated with magnetochiral systems (e.g., electrochiral dichroism), which have started to be explored experimentally [159]. Previous studies of multichiral systems focused on materials that are also multiferroic [148], where effects due to enantiomorphism are masked by multiferroic responses. We encourage future experimental investigations to focus on materials from the crystal classes D_2, D_4, D_3, D_6, T, or O [see Table XXVI], as the various nonreciprocities expected from multichirality should be more pristinely exhibited in these classes that do not support a polar direction.

ACKNOWLEDGMENTS

We thank the anonymous reviewers who helped us improve the presentation of this work. We also acknowledge stimulating discussions with D. F. Agterberg, S. Bhowal, P. M. R. Brydon, Y. Cao, R. M. Fernandes, D. M. Juraschek, Q. Niu, M. Norman, R. Resta, C. P. Romao, N. A. Spaldin, and X. H. Verbeek. R. W. also benefited from discussions with B. Assaf, S. Bey, T. Birol, L. Buiarelli, R. Cavanaugh, A. Hoffmann, N. Ghimire, L. Lurio, and J. Rau. U. Z. would like to thank S. Marsland for useful comments on an early version of the manuscript. Work at Argonne was supported by Department of Energy, Office of Basic Energy Sciences under Contract No. DE-AC02-06CH11357.

DATA AVAILABILITY

All data used for the research described in the article have been included in the article.

APPENDIX A: COMPOSITION OF MAGNETIC POINT GROUPS

The symmetry of a crystal structure is fully characterized by its (magnetic) space group S, which includes point symmetries, translations, and combinations thereof [10]. However, according to Neumann's principle [12–14], macroscopic properties of a crystal structure, such as material tensors and electric and magnetic polarization densities that may be realized in a structure, depend only on the magnetic point group G associated with the space group S. We therefore focus on point groups G in this work. For crystal structures transforming according to a symmorphic space group S_s, the point group G is the finite subgroup of S_s consisting of the elements of S_s that leave one point in space fixed. Nonsymmorphic space groups S_n also contain group elements that combine point-group symmetries g with nonprimitive translations. Here, the elements g are also elements of the point group G, although these symmetry operations are not, by themselves, elements of S_n. The latter case makes crystallographic point groups defining crystal classes qualitatively distinct from point groups of finite systems like molecules.

This appendix reviews the basic structure and properties of magnetic point groups and introduces a new classification scheme where SIS and TIS are systematically treated on the same footing. The relationships revealed through this classification underpin our comprehensive discussion

of multipole order (Sec. II) and chirality (Sec. III) in crystals.

1. Black-white symmetries and inversion groups

Rotation symmetries are represented by proper point groups $G_{\rm p}$ that only contain proper rotations as symmetry elements. In contrast, SIS and TIS are both examples of so-called black-white symmetries [11,181,182], which are represented by two-element groups of the form

$$C_\gamma = \{e, \gamma\}. \tag{A1}$$

Here, e is the identity, and γ is the single nontrivial group element that transforms between two qualities, represented abstractly by "black" and "white," satisfying $\gamma^2 = e$. Space inversion i is such an operation, as is time inversion θ (for our systems of interest [17]), and their combination $i\theta$ (CIS). We use the symbols C_i, C_θ, and $C_{i\theta}$ to refer to the inversion groups C_γ defined in Eq. (A1) when $\gamma = i, \theta$, and $i\theta$, respectively. For completeness and notational simplicity, we also define the full inversion group $C_{i\times\theta} \equiv C_i \times C_\theta = \{e, i, \theta, i\theta\}$ and the trivial inversion group $C_1 = \{e\}$. These groups are summarized in Table I. In the present work, the symbol C_ζ stands for any of the five inversion groups $C_{i\times\theta}$, C_θ, C_i, $C_{i\theta}$, or C_1.

2. Combining a black-white symmetry with other symmetries

There are three possible types of point groups G that arise from the combination of a black-white symmetry γ with other symmetries. As we consider multiple black-white symmetries in this work, we make their definitions specific:

(a) The γ-lacking groups $G^{(\rm a)}$ do not contain γ at all.

(b) The γ-major groups are of the form

$$G^{(\rm b)} = G^{(\rm a)} \times C_\gamma, \tag{A2}$$

so γ is, by itself, an element of $G^{(\rm b)}$.

(c) Suppose a γ-lacking group $G^{(\rm a)}$ contains an invariant subgroup of index 2 denoted $\tilde{G}^{(\rm a)}$, i.e.,

$$G^{(\rm a)} = \tilde{G}^{(\rm a)} + \bar{g}\tilde{G}^{(\rm a)}, \tag{A3a}$$

where $\bar{g} \in G^{(\rm a)}$, but $\bar{g} \notin \tilde{G}^{(\rm a)}$. Then, the γ-minor group is defined as

$$G^{(\rm c)} \equiv G^{(\rm a)}\langle\tilde{G}^{(\rm a)}\rangle_\gamma = \tilde{G}^{(\rm a)} + \gamma\bar{g}\tilde{G}^{(\rm a)}. \tag{A3b}$$

By definition, the major group $G^{(\rm a)} \times C_\gamma$ contains the γ-lacking group $G^{(\rm a)}$ and any minor group $G^{(\rm a)}\langle\tilde{G}^{(\rm a)}\rangle_\gamma$ as subgroups:

$$G^{(\rm a)} \subset G^{(\rm a)} \times C_\gamma, \tag{A4a}$$

$$G^{(\rm a)}\langle\tilde{G}^{(\rm a)}\rangle_\gamma \subset G^{(\rm a)} \times C_\gamma. \tag{A4b}$$

We adopt the convention established in the context of incorporating TIS, whereby, for $\gamma = \theta$, the resulting groups $G^{(\rm a)}$, $G^{(\rm b)}$, and $G^{(\rm c)}$ have been referred to as type I, type II, and type III, respectively [51,181], with the particular type-III notation

$$\gamma = \theta\colon\ G(\tilde{G}) \equiv G\langle\tilde{G}\rangle_\theta. \tag{A5a}$$

Similarly, we label groups $G^{(\rm a)}$, $G^{(\rm b)}$, and $G^{(\rm c)}$ arising in the process of incorporating SIS, i.e., when $\gamma = i$, as type i, type ii and type iii, respectively, and denote type-iii groups by

$$\gamma = i\colon\ G[\tilde{G}] \equiv G\langle\tilde{G}\rangle_i. \tag{A5b}$$

Groups that contain both i and θ can also be classified as major or minor groups with respect to $i\theta$. We indicate $i\theta$-minor groups by

$$\gamma = i\theta\colon\ G\{\tilde{G}\} \equiv G\langle\tilde{G}\rangle_{i\theta}. \tag{A5c}$$

See Table VIII for a summary of our nomenclature and specifics of notation.

3. Classes and types of magnetic point groups: Duality

Proper point groups $G_{\rm p}$ are both i-lacking and θ-lacking, and thus also $i\theta$-lacking. Combining these with SIS using the formalism described in Appendix A 2 yields the ordinary improper point groups [11,15] that can be either i-major or i-minor. These groups are still θ-lacking and $i\theta$-lacking. Combining these groups with TIS in the same way yields the magnetic point groups [19]. In this process of extending the proper point groups by adding SIS and TIS, each proper point group $G_{\rm p}$ spawns a *class* $L(G_{\rm p})$ of magnetic point groups G [57–60] defined via

$$L(G_{\rm p}) = \{G\colon G \mapsto G_{\rm p} \text{ when } i, \theta \mapsto e\}. \tag{A6}$$

By definition, each magnetic point group G belongs to one and only one class $L(G_{\rm p})$. We call the proper point group $G_{\rm p}$ the class root of class $L(G_{\rm p})$.

TABLE VIII. Combining an inversion symmetry $\gamma = i$, θ, and $i\theta$ with other symmetries. The group G does not contain γ at all.

			SIS: i		TIS: θ		CIS: $i\theta$	
(a)	γ-lacking	G	i	G	I	G	J	G
(b)	γ-major	$G \times C_\gamma$	ii	$G \times C_i$	II	$G \times C_\theta$	JJ	$G \times C_{i\theta}$
(c)	γ-minor	$G\langle\tilde{G}\rangle_\gamma$	iii	$G(\tilde{G})$	III	$G[\tilde{G}]$	JJJ	$G\{\tilde{G}\}$

The separate consideration of the two black-white properties i and θ yields overlapping group types; i.e., the full set of magnetic point groups can be viewed in terms of TIS as a collection of types I, II, and III, or seen equivalently [55,56] in terms of SIS as a collection of types i, ii, and iii. Yet another classification can be based on CIS. We now develop a scheme that treats SIS and TIS symmetrically and makes CIS explicit, thus providing a systematic and complete classification of the magnetic point groups. This approach also reveals a general structure underlying the composition of class $L(G_\mathrm{p})$ of magnetic point groups with class root G_p.

It has previously been observed [55] that exchanging $i \leftrightarrow \theta$ in all group elements of a magnetic point group G

TABLE IX. Classification of magnetic point groups based on the SIS-TIS duality relation (A7). We give the general form of each type and specify the number of groups of a given type among the 122 crystallographic magnetic point groups. Duality-related types are positioned underneath the self-dual type with which they form a triad. In addition to the short type label, we provide a full label indicating the types with respect to SIS (i, ii, or iii), TIS (I, II, or III) and CIS (J, JJ, or JJJ). Small 2×2 matrices mark congruences between tensors with signature ss' as discussed in detail in Appendix E. The categories of multipole order (i.e., polarization) and chirality are listed for each type. Notation: G_p denotes a proper point group, $\tilde{G}_\mathrm{p}$ is an index-2 subgroup of G_p, superscripts (j) distinguish distinct index-2 subgroups of G_p, and unprimed and primed groups denote versions of the same index-2 subgroup of G_p distinguished by different orientations of the coordinate system defining the group elements. The inversion groups C_ζ are defined in Appendix A 1 and listed for convenience in Table I. See also Fig. 10.

Self-dual type	J ≡ i-I-J	ii-II ≡ ii-II-JJ	JJJ" ≡ iii'-III'-JJJ'
General form	G_p	$G_\mathrm{p}\times C_{i\times\theta}$	$G_\mathrm{p}[\tilde{G}_\mathrm{p}](\tilde{G}''_\mathrm{p}[\tilde{\tilde{G}}_\mathrm{p}])$ $= G_\mathrm{p}(\tilde{G}'_\mathrm{p})\{\tilde{G}_\mathrm{p}(\tilde{\tilde{G}}_\mathrm{p})\}$ [a] $= G_\mathrm{p}\{\tilde{G}''_\mathrm{p}\}[\tilde{G}'_\mathrm{p}\{\tilde{\tilde{G}}_\mathrm{p}\}]$
Allowed tensors	$\begin{pmatrix}\circ&\circ\\ \circ&\circ\end{pmatrix}$	$\begin{pmatrix}\circ&\\ &\circ\end{pmatrix}$	$\begin{pmatrix}\circ&\star\\ \star&\star\end{pmatrix}$
Polarization	Multipolar	Parapolar	Multipolar
Chirality	Multichiral	Parachiral	Parachiral
Number of groups	11	11	1
Self-dual type	JJ ≡ i-I-JJ	JJ' ≡ iii-III-JJ	JJJ ≡ i-I-JJJ
General form	$G_\mathrm{p}\times C_{i\theta}$	$G_\mathrm{p}[\tilde{G}_\mathrm{p}]\times C_{i\theta} = G_\mathrm{p}(\tilde{G}_\mathrm{p})\times C_{i\theta}$	$G_\mathrm{p}\{\tilde{G}_\mathrm{p}\}$
Allowed tensors	$\begin{pmatrix}\circ&\\ &\circ\end{pmatrix}$	$\begin{pmatrix}\circ&\\ &\star\end{pmatrix}$	$\begin{pmatrix}\circ&\star\\ \star&\circ\end{pmatrix}$
Polarization	Antimagnetopolar	Antimagnetopolar	Multipolar
Chirality	Antimagnetochiral	Parachiral	Antimagnetochiral
Number of groups	11	10	10
Dual types	i-II-J ≡ i-II ↔ ii-I ≡ ii-I-J	iii-II-JJJ ≡ iii-II ↔ ii-III ≡ ii-III-JJJ	i-III-J ≡ i-III ↔ iii-I ≡ iii-I-J
General form	$G_\mathrm{p}\times C_\theta \leftrightarrow G_\mathrm{p}\times C_i$	$\left.\begin{matrix}G_\mathrm{p}[\tilde{G}_\mathrm{p}]\times C_\theta\\ = G_\mathrm{p}\{\tilde{G}_\mathrm{p}\}\times C_\theta\end{matrix}\right\} \leftrightarrow \left\{\begin{matrix}G_\mathrm{p}(\tilde{G}_\mathrm{p})\times C_i\\ = G_\mathrm{p}\{\tilde{G}_\mathrm{p}\}\times C_i\end{matrix}\right.$	$G_\mathrm{p}(\tilde{G}_\mathrm{p}) \leftrightarrow G_\mathrm{p}[\tilde{G}_\mathrm{p}]$
Allowed tensors	$\begin{pmatrix}\circ&\\ &\circ\end{pmatrix} \leftrightarrow \begin{pmatrix}\circ&\circ\\ \circ&\circ\end{pmatrix}$	$\begin{pmatrix}\circ&\\ &\star\end{pmatrix} \leftrightarrow \begin{pmatrix}\circ&\star\\ \star&\star\end{pmatrix}$	$\begin{pmatrix}\circ&\star\\ \star&\circ\end{pmatrix} \leftrightarrow \begin{pmatrix}\circ&\circ\\ \star&\star\end{pmatrix}$
Polarization	electropolar ↔ magnetopolar	electropolar ↔ magnetopolar	multipolar ↔ multipolar
Chirality	electrochiral ↔ magnetochiral	parachiral ↔ parachiral	electrochiral ↔ magnetochiral
Number of groups	11 ↔ 11	10 ↔ 10	10 ↔ 10
Self-dual type	JJJ' ≡ iii-III-JJJ'		
General form	$G_\mathrm{p}[\tilde{G}^{(1)}_\mathrm{p}](\tilde{G}^{(1')}_\mathrm{p}[\tilde{\tilde{G}}_\mathrm{p}]) = G_\mathrm{p}(\tilde{G}^{(1')}_\mathrm{p})[\tilde{G}^{(1)}_\mathrm{p}(\tilde{\tilde{G}}_\mathrm{p})] = G_\mathrm{p}\{\tilde{G}^{(1)}_\mathrm{p}\}(\tilde{G}^{(2)}_\mathrm{p}\{\tilde{\tilde{G}}_\mathrm{p}\})$ [a]		
Allowed tensors	$\begin{pmatrix}\circ&\diamond\\ \diamond&\star\end{pmatrix}$		
Polarization	Multipolar		
Chirality	Parachiral		
Number of groups	2		
Dual types	iii'-III-JJJ ≡ iii'-III ↔ iii-III' ≡ iii-III'-JJJ		
General form	$\left.\begin{matrix}G_\mathrm{p}\{\tilde{G}^{(1)}_\mathrm{p}\}[\tilde{G}^{(1')}_\mathrm{p}\{\tilde{\tilde{G}}\}] = G_\mathrm{p}[\tilde{G}^{(1')}_\mathrm{p}]\{\tilde{G}^{(1)}_\mathrm{p}[\tilde{\tilde{G}}_\mathrm{p}]\}\\ = G_\mathrm{p}[\tilde{G}^{(2)}_\mathrm{p}](\tilde{G}^{(1)}_\mathrm{p}[\tilde{\tilde{G}}_\mathrm{p}])^\mathrm{a}\}\end{matrix}\right\} \leftrightarrow \left\{\begin{matrix}G_\mathrm{p}(\tilde{G}^{(1)}_\mathrm{p})\{\tilde{G}^{(1')}_\mathrm{p}(\tilde{\tilde{G}})\} = G_\mathrm{p}\{\tilde{G}^{(1')}_\mathrm{p}\}(\tilde{G}^{(1)}_\mathrm{p}\{\tilde{\tilde{G}}_\mathrm{p}\})\\ = G_\mathrm{p}[\tilde{G}^{(1)}_\mathrm{p}](\tilde{G}^{(2)}_\mathrm{p}[\tilde{\tilde{G}}_\mathrm{p}])^\mathrm{a}\end{matrix}\right.$		
Allowed tensors	$\begin{pmatrix}\circ&\diamond\\ \star&\diamond\end{pmatrix} \leftrightarrow \begin{pmatrix}\circ&\star\\ \diamond&\diamond\end{pmatrix}$		
Polarization	multipolar ↔ multipolar		
Chirality	parachiral ↔ parachiral		
Number of groups	2 ↔ 2		

[a]The multipolar parachiral types can be expressed in multiple equivalent ways. We list only a few of these possibilities.

yields another magnetic point group $G_{\rm d}$. Clearly, the groups G and $G_{\rm d}$ are isomorphic. We call this relationship SIS-TIS duality or $i \leftrightarrow \theta$ duality,

$$G \leftrightarrow G_{\rm d}, \tag{A7}$$

with dual partners G and $G_{\rm d}$. It is easy to see that dual partners G and $G_{\rm d}$ belong to the same class $L(G_{\rm p})$; i.e., both G and $G_{\rm d}$ satisfy Eq. (A6) with the same class root $G_{\rm p}$. The concept of duality allows one to classify the groups in a given class $L(G_{\rm p})$ as follows.

Self-dual groups $G = G_{\rm d} \in L(G_{\rm p})$ are invariant under exchange $i \leftrightarrow \theta$. They belong to one (and only one) of the seven types J, ii-II, JJ, JJ', JJJ, JJJ', or JJJ" defined in Table IX. Besides the self-dual types, we have types associated with dual pairs $G \leftrightarrow G_{\rm d}$ with $G \neq G_{\rm d}$ and $G, G_{\rm d} \in L(G_{\rm p})$. We label these types by indicating their respective types under both SIS and TIS. See Table IX for the explicit definitions. In the following, we generally use short labels when referring to one of the new types, but an instructive full label indicating their types under SIS, TIS, and CIS is also given in Table IX.

Within each class, the groups of the types J, JJJ, JJJ', JJJ", i-III, iii-I, iii'-III, and iii-III' are all isomorphic. Furthermore, the groups of the types JJ, JJ', i-II, ii-I, ii-III, and iii-II are all isomorphic. A group of type ii-II is not isomorphic to any other group in the same class but contains all of these as its subgroups. See Fig. 10 for a description of general isomorphisms and subgroup relations between magnetic-point-group types in a given class. Isomorphisms formed the basis of a prior classification scheme of the 122 magnetic crystallographic groups [57,58].

Table IX provides comprehensive information about all magnetic-point-group types, including associated categories of multipole order and chirality. These latter properties have been elucidated in Secs. II and III. As is already apparent from Table IX, the 15 indicated group types map onto particular combinations of a category of polarization with a category of chirality. For 11 types, this mapping is unique; i.e., for each of these, the group type is synonymous with a distinct combination of polarization with chirality. The exception is the multipolar-parachiral combination that subsumes four (rare sub)types JJJ", JJJ', iii'-III, and iii-III'. Thus, Table IX and Fig. 10 constitute an alternative representation of the standard model illustrated by Fig. 1.

The present classification treats θ as a black-white symmetry like i so that $i^2 = \theta^2 = e$. This classification applies to states with integer spin angular momentum (transforming according to the single groups where $\theta^2 = e$), and it is relevant for all macroscopic properties of a crystal structure such as those characterized by Neumann's principle [12,13,17]. The single-group description is also sufficient for obtaining the invariant expansion of the electronic band structure near $k = 0$ [14] as in Fig. 2. This is illustrated by the fact that all building blocks in Eq. (5) for forming invariants in a spinful theory transform according to integer IRs of $R_{i\times\theta}$ with $\ell = 1$. This includes the operator of spin angular momentum $\boldsymbol{\sigma}$, Eq. (5c). There are other properties of systems with half-integer spin degrees of freedom that can only be properly discussed using double groups where $\theta^2 = -e$ [11]. For example, double groups are needed to understand certain degeneracies in the electronic band structure that may arise at the Brillouin zone boundary [14]. The typology and isomorphisms discussed here do not hold for the respective double groups.

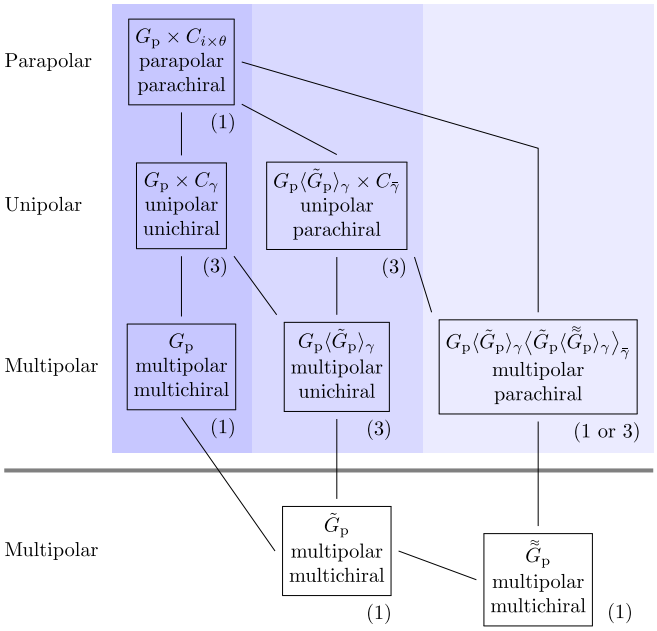


FIG. 10. Subgroup relations and isomorphisms between groups in a given class $L(G_{\rm p})$. Subgroup relations are depicted by lines. Groups placed within the same row are isomorphic. The categories of polarization and chirality for each group are also indicated, with the prefix "uni" representing "electro," "magneto," or "antimagneto." Numbers n at the lower right of a box specify how many groups represented by a box can be realized for inversion symmetries $\gamma, \bar{\gamma} = i, \theta$, and $i\theta$ with $\bar{\gamma} \neq \gamma$. When $n = 1$, these groups are self-triadic. When $n = 3$, these groups form a triad [Eq. (A10)]. When a line connects groups that depend on $\gamma, \bar{\gamma}$, the subgroup relation exists pairwise between the groups in the triads with the same $\gamma, \bar{\gamma}$. Every class $L(G_{\rm p})$ contains the groups shown in the left (dark-blue) column. If $G_{\rm p}$ has an index-2 subgroup $\tilde{G}_{\rm p}$, the class also includes the groups in the center (medium-blue) column. If $\tilde{G}_{\rm p}$ has an index-2 subgroup $\tilde{\tilde{G}}_{\rm p}$, the class also includes the groups in the right (light-blue) column. Below the dividing line at the bottom, subgroup relations between groups in class $L(G_{\rm p})$ and the groups $\tilde{G}_{\rm p}$ and $\tilde{\tilde{G}}_{\rm p}$ are shown. See also Table IX, which presents the groups that may exist in a class $L(G_{\rm p})$ in a more fine-grained way by indicating their types.

4. Triadic relationships

The SIS-TIS duality (A7) appears naturally when magnetic point groups are constructed in the usual way from proper point groups by adding the black-white symmetries space inversion i and time inversion θ [15,19] as reviewed at the beginning of Appendix A 3. The duality (A7) turns out to be useful to discuss physical phenomena involving electric and magnetic fields, and we make use of it throughout this work. Here, we briefly discuss the deeper mathematical structure from which this duality emerges.

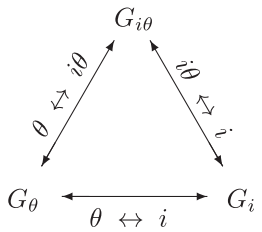
The full inversion group $C_{i\times\theta}$ has order 4. It is isomorphic to the Klein four-group,

$$K_4 = \{e, \gamma', \gamma'', \tilde{\gamma} = \gamma'\gamma'' \colon \gamma'^2 = \gamma''^2 = \tilde{\gamma}^2 = e\}, \tag{A8}$$

in abstract group theory [11]. This group treats the elements γ', γ'', and $\tilde{\gamma} = \gamma'\gamma''$ fully symmetrically. Indeed, one can express the full inversion group $C_{i\times\theta}$ in three equivalent forms,

$$C_{i\times\theta} = C_i \times C_\theta \equiv C_\theta \times C_{i\theta} \equiv C_{i\theta} \times C_i. \tag{A9}$$

Starting from a proper point group G_p, it is thus possible to construct all magnetic point groups in class $L(G_\mathrm{p})$ using any pair of inversion symmetries $\gamma', \gamma'' \in \{i, \theta, i\theta\}$ by first adding the black-white symmetry γ' and then adding γ''. Therefore, the concept of duality exists for any pair of inversion symmetries $\gamma', \gamma'' \in \{i, \theta, i\theta\}$. The resulting dualities are represented by the diagram



(A10)

with triadic partners G_i, G_θ, and $G_{i\theta}$ that are pairwise connected by duality relations similar to Eq. (A7).

Triadic partners G_i, G_θ, and $G_{i\theta}$ are isomorphic. A set of triadic partners G_i, G_θ, and $G_{i\theta}$ constitutes a triad of magnetic groups. Possibilities for forming triads are shown in Table IX. (See also Fig. 1 for an illustration.) Self-triadic groups are invariant under all dualities in the diagram (A10). They belong to the types J, ii-II, or JJJ". The remaining groups form triads with distinct partners G_i, G_θ, and $G_{i\theta}$ as indicated in Table IX. The index $\tilde{\gamma} = \gamma'\gamma''$ of a group $G_{\tilde{\gamma}}$ in the diagram (A10) indicates self-duality under the exchange $\gamma' \leftrightarrow \gamma''$. The equivalent expressions provided in Table IX for groups JJJ", iii-II, ii-III, JJ', iii'-III, iii-III', and JJJ' emphasize the respective self-dualities of these groups.

5. Subclasses of magnetic point groups

To classify the tensors permitted by different groups G in a class $L(G_\mathrm{p})$, the concept of subclasses of magnetic point groups turns out to be useful. Here, we discuss the construction of subclasses, details of their composition, and associated properties.

For $\gamma = i$, θ, and $i\theta$, the subclasses $L(G_0^\gamma, \gamma)$ of a class $L(G_\mathrm{p})$ are the subsets of groups G,

$$L(G_0^\gamma, \gamma) = \{G \colon G \mapsto G_0^\gamma \text{ when } \gamma \mapsto e\}. \tag{A11}$$

For given γ, the subclasses $L(G_0^\gamma, \gamma)$ of $L(G_\mathrm{p})$ are disjoint; i.e., each group $G \in L(G_\mathrm{p})$ belongs to one subclass $L(G_0^i, i)$, one subclass $L(G_0^\theta, \theta)$, and one subclass $L(G_0^{i\theta}, i\theta)$. The subclasses derived for $\gamma = i$, θ, and $i\theta$ hence represent alternative schemes for partitioning $L(G_\mathrm{p})$. Conversely, for a given class $L(G_\mathrm{p})$ and fixed $\gamma = i$, θ, or $i\theta$, the subclasses $L(G_0^\gamma, \gamma)$ spawn class $L(G_\mathrm{p})$, i.e.,

$$L(G_\mathrm{p}) = \bigcup_{G_0^\gamma} L(G_0^\gamma, \gamma) \quad \text{for fixed } \gamma = i, \theta, \text{ or } i\theta. \tag{A12}$$

The subclass root G_0^γ of the subclass $L(G_0^\gamma, \gamma)$ is γ-lacking by construction. If $G_0^\gamma = G_\mathrm{p}$, the subclass root G_0^γ is actually lacking all three inversions. The associated subclasses $L(G_\mathrm{p}, \gamma)$ for $\gamma = i$, θ, and $i\theta$ comprise G_p, $G_\mathrm{p} \times C_\gamma$ and all γ-minor groups $G_\mathrm{p}\langle\tilde{G}_\mathrm{p}\rangle_\gamma$.

If the subclass root G_0^γ still contains another black-white symmetry, it has to be different from γ. For the cases $\gamma = i$ or θ, the black-white symmetry present in G_0^γ will be

$$\gamma_\mathrm{d} = \begin{cases} i & \text{if } \gamma = \theta \\ \theta & \text{if } \gamma = i. \end{cases} \tag{A13}$$

The case $\gamma = i\theta$ requires a more elaborate discussion that is relegated to Appendix A 6. Here, we continue with a brief consideration of the cases $\gamma = i$ or θ.

If G_0^γ is a γ_d-major group, then $G_0^\gamma = G_\mathrm{p} \times C_{\gamma_\mathrm{d}}$. For $\gamma = i$ or θ, the subclass $L(G_\mathrm{p} \times C_{\gamma_\mathrm{d}}, \gamma)$ contains all the γ_d-major groups in class $L(G_\mathrm{p})$, as well as the type-JJ and type-JJ' groups in $L(G_\mathrm{p})$.

If G_0^γ is a γ_d-minor group, then $G_0^\gamma = G_\mathrm{p}\langle\tilde{G}_\mathrm{p}\rangle_{\gamma_\mathrm{d}}$. For $\gamma = i$ or θ, $L(G_\mathrm{p}\langle\tilde{G}_\mathrm{p}\rangle_{\gamma_\mathrm{d}}, \gamma)$ contains $G_\mathrm{p}\langle\tilde{G}_\mathrm{p}\rangle_{\gamma_\mathrm{d}}$, $G_\mathrm{p}\langle\tilde{G}_\mathrm{p}\rangle_{\gamma_\mathrm{d}} \times C_\gamma$, and $G_\mathrm{p}\{\tilde{G}_\mathrm{p}\}$. The subclass $L(G_\mathrm{p}[\tilde{G}_\mathrm{p}^{(1)}], \theta)$ furthermore contains $G_{\mathrm{JJJ}'} = G_\mathrm{p}[\tilde{G}_\mathrm{p}^{(1)}](\tilde{G}_\mathrm{p}^{(1')}[\tilde{\tilde{G}}_\mathrm{p}])$ (or the type-JJJ" group of the same form) and $G_{\text{iii-III}'} = G_\mathrm{p}[\tilde{G}_\mathrm{p}^{(1)}](\tilde{G}_\mathrm{p}^{(2)}[\tilde{\tilde{G}}_\mathrm{p}])$. Similarly, $L(G_\mathrm{p}(\tilde{G}_\mathrm{p}^{(1)}), i)$ contains $G_{\mathrm{JJJ}'}$ (or the type-JJJ" group of the same form) and $G_{\text{iii-III}'} = G_\mathrm{p}(\tilde{G}_\mathrm{p}^{(1)})[\tilde{G}_\mathrm{p}^{(2)}(\tilde{\tilde{G}}_\mathrm{p})]$.

The relation between group types and subclasses is summarized in Table X. Groups in a given row in the upper part of this table belong to the same subclass

TABLE X. Subclasses $L(G_0^\gamma,\gamma)$ and groups in a class $L(G_\mathrm{p})$. Here, $\tilde{G}_\mathrm{p}$ denotes an index-2 subgroup of the class root G_p. The groups in $L(G_\mathrm{p})$ are arranged in the upper part of the table according to the scheme shown in the center part of the table, where each group's type is indicated. For clarity, we omit groups of multipolar-parachiral type (i.e., JJJ", JJJ', iii'-III, and iii-III'). The subclass $L(G_0^\theta,\theta)$ for each group is specified in the header of its column. For groups of type JJ or JJ', their subclass $L(G_0^i,i)$ is also given in the column header. Groups of all other types have their subclass $L(G_0^i,i)$ specified in the header of their respective row. Small 2×2 matrices mark congruences between tensors with signature ss' as discussed in detail in Appendix E. The bottom part of the table lists the groups in the subclasses $L(G_0^{i\theta},i\theta)\equiv L(G_{0\mathrm{d}}^{i\theta},i\theta)$.

$L(G_0^{i\theta},i)\backslash L(G_0^\theta,\theta)$	$L(G_\mathrm{p},\theta)$		$L(G_\mathrm{p}[\tilde{G}_\mathrm{p}],\theta)$		$L(G_\mathrm{p}\times C_i,\theta)$		$L(G_\mathrm{p}\times C_i,\theta)$, $L(G_\mathrm{p}\times C_\theta,i)$	
$L(G_\mathrm{p},i)$	G_p	$\left(\begin{smallmatrix}\circ&\circ\\ \circ&\circ\end{smallmatrix}\right)$	$G_\mathrm{p}[\tilde{G}_\mathrm{p}]$	$\left(\begin{smallmatrix}\circ&\circ\\ \star&\star\end{smallmatrix}\right)$	$G_\mathrm{p}\times C_i$	$\left(\begin{smallmatrix}\circ&\circ\\ \circ&\circ\end{smallmatrix}\right)$	$G_\mathrm{p}\times C_{i\theta}$	$\left(\begin{smallmatrix}\circ&\circ\\ \circ&\star\end{smallmatrix}\right)$
$L(G_\mathrm{p}(\tilde{G}_\mathrm{p}),i)$	$G_\mathrm{p}(\tilde{G}_\mathrm{p})$	$\left(\begin{smallmatrix}\circ&\star\\ \circ&\star\end{smallmatrix}\right)$	$G_\mathrm{p}\{\tilde{G}_\mathrm{p}\}$	$\left(\begin{smallmatrix}\circ&\star\\ \star&\circ\end{smallmatrix}\right)$	$G_\mathrm{p}(\tilde{G}_\mathrm{p})\times C_i$	$\left(\begin{smallmatrix}\circ&\star\\ \circ&\star\end{smallmatrix}\right)$	$G_\mathrm{p}(\tilde{G}_\mathrm{p})\times C_{i\theta}$	$\left(\begin{smallmatrix}\circ&\star\\ \circ&\star\end{smallmatrix}\right)$
$L(G_\mathrm{p}\times C_\theta,i)$	$G_\mathrm{p}\times C_\theta$	$\left(\begin{smallmatrix}\circ&\circ\\ \circ&\circ\end{smallmatrix}\right)$	$G_\mathrm{p}[\tilde{G}_\mathrm{p}]\times C_\theta$	$\left(\begin{smallmatrix}\circ&\circ\\ \star&\star\end{smallmatrix}\right)$	$G_\mathrm{p}\times C_{i\times\theta}$	$\left(\begin{smallmatrix}\circ&\circ\\ \circ&\circ\end{smallmatrix}\right)$		
	J multipolar multichiral		iii-I multipolar magnetochiral		ii-I magnetopolar magnetochiral		JJ antimagnetopolar antimagnetochiral	
	i-III multipolar electrochiral		JJJ multipolar antimagnetochiral		ii-III magnetopolar parachiral		JJ' antimagnetopolar parachiral	
	i-II electropolar electrochiral		iii-II electropolar parachiral		ii-II parapolar parachiral			

$L(G_\mathrm{p},i\theta)$	$G_\mathrm{p}, G_\mathrm{p}\{\tilde{G}_\mathrm{p}\}, G_\mathrm{p}\times C_{i\theta}$
$L(G_\mathrm{p}(\tilde{G}_\mathrm{p}),i\theta)\equiv L(G_\mathrm{p}[\tilde{G}_\mathrm{p}],i\theta)$	$G_\mathrm{p}(\tilde{G}_\mathrm{p}), G_\mathrm{p}[\tilde{G}_\mathrm{p}], G_\mathrm{p}(\tilde{G}_\mathrm{p})\times C_{i\theta}\equiv G_\mathrm{p}[\tilde{G}_\mathrm{p}]\times C_{i\theta}$
$L(G_\mathrm{p}\times C_\theta,i\theta)\equiv L(G_\mathrm{p}\times C_i,i\theta)$	$G_\mathrm{p}\times C_\theta, G_\mathrm{p}\times C_i, G_\mathrm{p}\times C_{i\times\theta}, G_\mathrm{p}[\tilde{G}_\mathrm{p}]\times C_\theta, G_\mathrm{p}(\tilde{G}_\mathrm{p})\times C_i$

$L(G_0^i,i)$, with G_0^i being the group in the first column. Similarly, groups in a given column belong to the same subclass $L(G_0^\theta,\theta)$, with G_0^θ being the group in the first row. The groups of type JJ and JJ' belong to the same subclasses $L(G_0^i,i)$ and $L(G_0^\theta,\theta)$ as the group of type ii-II. Similarly, the groups of type JJJ' or JJJ" belong to the same subclasses $L(G_0^i,i)$ and $L(G_0^\theta,\theta)$ as the group of type JJJ. The composition of subclasses $L(G_0^{i\theta},i\theta)$ is discussed in Appendix A 6 and summarized in the lower part of Table X.

Application of the duality transformation $i\leftrightarrow\theta$ to the groups in a subclass $L(G_0^\gamma,\gamma)$ with $\gamma=i$ or θ generates the subclass $L(G_{0\mathrm{d}}^\gamma,\gamma_\mathrm{d})$, with the subclass roots $G_0^\gamma\leftrightarrow G_{0\mathrm{d}}^\gamma$ being dual partners. This corresponds to mapping rows onto columns and vice versa in the upper part of Table X. In contrast, every subclass $L(G_0^{i\theta},i\theta)\equiv L(G_{0\mathrm{d}}^{i\theta},i\theta)$ is mapped onto itself when the duality transformation is applied to the groups it comprises. Therefore, the subclass classifications $L(G_0^\gamma,\gamma)$ do not reflect a triadic relationship (A10). More generally, for each pair γ',γ'' of inversion symmetries, one can establish a pair of $\gamma'\leftrightarrow\gamma''$-dual subclasses $L(G_0^{\gamma'},\gamma')$ and $L(G_0^{\gamma''},\gamma'')$, as well as the $\gamma'\leftrightarrow\gamma''$-self-dual subclass $L(G_0^{\tilde{\gamma}},\tilde{\gamma})$ with $\tilde{\gamma}=\gamma'\gamma''$. In this work, we adhere to the nomenclature whereby the term duality without a specifier refers to SIS-TIS duality associated with the exchange $i\leftrightarrow\theta$.

6. Form of subclasses $L(G_0^{i\theta},i\theta)$

The concept of subclasses of magnetic point groups is introduced in Appendix A 5. While the form of subclasses $L(G_0^i,i)$ and $L(G_0^\theta,\theta)$ is straightforward, the form of subclasses $L(G_0^{i\theta},i\theta)$ discussed in the following is more subtle.

Every magnetic point group $G\in L(G_\mathrm{p})$ has the general form [56]

$$G=\tilde{G}_\mathrm{p}+i\{g_\nu^{(i)}\}+\theta\{g_\nu^{(\theta)}\}+i\theta\{g_\nu^{(i\theta)}\}. \tag{A14}$$

Here, $\tilde{G}_\mathrm{p}\subseteq G_\mathrm{p}$ is a proper point group, and $\{g_\nu^{(\gamma)}\}$ denotes the set of operations in the class root G_p that appears in G in combination with the black-white symmetry element $\gamma\in\{i,\theta,i\theta\}$. In the following, we assume $G\supsetneq G_\mathrm{p}$, i.e., at least one set $\{g_\nu^{(\gamma)}\}$ is nonempty. The relation $\gamma^2=e$ and general group properties of G imply the relations

$$g_\nu^{(\gamma)}g_\mu^{(\gamma)}\in\tilde{G}_\mathrm{p}\qquad\text{for any fixed }\gamma, \tag{A15a}$$

$$g_\nu^{(\gamma)}g_\mu^{(\gamma')}\in\{g_{\nu'}^{(\gamma\gamma')}\}\quad\text{for any pair }\gamma\neq\gamma'. \tag{A15b}$$

It follows from Eq. (A15) that either only one set $\{g_\nu^{(\gamma)}\}$ is nonempty or all three sets are nonempty.

To understand how the mapping $i\theta\mapsto e$ transforms the group G given in Eq. (A14), we first note

$$\theta=i^2\theta=ii\theta\overset{i\theta\mapsto e}{\mapsto}i \tag{A16a}$$

to find

$$G \overset{i\theta\mapsto e}{\longmapsto} G_0^{i\theta} \equiv \tilde{G}_\mathrm{p} + \{g_\nu^{(i\theta)}\} + i(\{g_\nu^{(i)}\} + \{g_\nu^{(\theta)}\}), \quad \text{(A16b)}$$

where clearly $G_0^{i\theta}$ is again a group. Alternatively, using

$$i = i\theta^2 = i\theta\theta \overset{i\theta\mapsto e}{\longmapsto} \theta \quad \text{(A17a)}$$

yields

$$G \overset{i\theta\mapsto e}{\longmapsto} G_{0\mathrm{d}}^{i\theta} \equiv \tilde{G}_\mathrm{p} + \{g_\nu^{(i\theta)}\} + \theta(\{g_\nu^{(i)}\} + \{g_\nu^{(\theta)}\}). \quad \text{(A17b)}$$

Thus, we can identify two equivalent subclass roots $G_0^{i\theta} \leftrightarrow G_{0\mathrm{d}}^{i\theta}$ that are related via the duality transformation $i \leftrightarrow \theta$, and

$$L(G_0^{i\theta}, i\theta) \equiv L(G_{0\mathrm{d}}^{i\theta}, i\theta). \quad \text{(A18)}$$

Applying the duality transformation $i \leftrightarrow \theta$ to G in Eq. (A14) yields the dual partner

$$G \leftrightarrow G_\mathrm{d} = \tilde{G}_\mathrm{p} + \theta\{g_\nu^{(i)}\} + i\{g_\nu^{(\theta)}\} + i\theta\{g_\nu^{(i\theta)}\}. \quad \text{(A19)}$$

Equations (A16) and (A17) show that G_d maps to the same subclass roots $G_0^{i\theta} \leftrightarrow G_{0\mathrm{d}}^{i\theta}$ as G; i.e., dual partners G and G_d belong to the same subclass $L(G_0^{i\theta}, i\theta) \equiv L(G_{0\mathrm{d}}^{i\theta}, i\theta)$.

Specializing the composition of a subclass $L(G_0^\gamma, \gamma)$ discussed generally in Appendix A 5 to the case $\gamma = i\theta$, we find that $L(G_\mathrm{p}, i\theta)$ contains not only G_p but also $G_\mathrm{JJ} = G_\mathrm{p} \times C_{i\theta}$ and all the type-JJJ groups $G_\mathrm{p}\{\tilde{G}_\mathrm{p}\} \in L(G_\mathrm{p})$. It follows from Eqs. (A16) and (A17) that the subclass $L(G_\mathrm{p} \times C_i, i\theta) \equiv L(G_\mathrm{p} \times C_\theta, i\theta)$ contains the groups of type ii-II, ii-I, and i-II as well as all type-ii-III and type-iii-II groups in $L(G_\mathrm{p})$. Groups in a subclass $L(G_\mathrm{p}[\tilde{G}_\mathrm{p}], i\theta) \equiv L(G_\mathrm{p}(\tilde{G}_\mathrm{p}), i\theta)$ contain not only $G_\mathrm{p}[\tilde{G}_\mathrm{p}]$ and $G_\mathrm{p}(\tilde{G}_\mathrm{p})$ but also the type-JJ' group $G_\mathrm{p}(\tilde{G}_\mathrm{p}) \times C_{i\theta}$. Furthermore, $G_{\mathrm{JJ}'} = G_\mathrm{p}[\tilde{G}_\mathrm{p}^{(1)}](\tilde{G}_\mathrm{p}^{(1')}[\tilde{\tilde{G}}_\mathrm{p}])$ is in $L(G_\mathrm{p}[\tilde{G}_\mathrm{p}^{(2)}], i\theta) \equiv L(G_\mathrm{p}(\tilde{G}_\mathrm{p}^{(2)}), i\theta)$, while $G_{\mathrm{iii\text{-}III}'} = G_\mathrm{p}[\tilde{G}_\mathrm{p}^{(1)}](\tilde{G}_\mathrm{p}^{(2)}[\tilde{\tilde{G}}_\mathrm{p}])$ and $G_{\mathrm{iii'\text{-}III}} = G_\mathrm{p}[\tilde{G}_\mathrm{p}^{(2)}](\tilde{G}_\mathrm{p}^{(1)}[\tilde{\tilde{G}}_\mathrm{p}])$ both belong to $L(G_\mathrm{p}[\tilde{G}_\mathrm{p}^{(1)}], i\theta) \equiv L(G_\mathrm{p}(\tilde{G}_\mathrm{p}^{(1)}), i\theta)$.

The combination of $L(G_\mathrm{p}, i\theta)$ with $L(G_\mathrm{p} \times C_i, i\theta) \equiv L(G_\mathrm{p} \times C_\theta, i\theta)$ and all subclasses $L(G_\mathrm{p}[\tilde{G}_\mathrm{p}], i\theta) \equiv L(G_\mathrm{p}(\tilde{G}_\mathrm{p}), i\theta)$ yield class $L(G_\mathrm{p})$ [Eq. (A12)].

APPENDIX B: CLASSIFICATION OF MAGNETIC POINT GROUPS

Having developed the classification of magnetic point groups within a given class, we now apply this classification to the known continuous and discrete point groups.

TABLE XI. Spherical magnetic point groups G_sp. Symmetry elements present (absent) in different groups G_sp are labeled "•" ("∘"). Here, C represents an arbitrary proper rotation. Labels in the first column refer to the classification of magnetic point groups introduced in Table IX. The last column gives invariant tensors for these groups expressed in terms of irreducible tensors $T_0^{ss'} = \{T_{00}^{ss'}\}$ of $R_{i\times\theta}$ (see Sec. II A) [183]. A superscript "any" indicates that invariant tensors may have any signature ss'.

	G_sp	C	i	iC	θ	θC	$i\theta$	$i\theta C$	$T_0^{ss'}$
ii-II	$R_{i\times\theta} = R \times C_{i\times\theta}$	•	•	•	•	•	•	•	T_0^{++}
i-II	$R_\theta = R \times C_\theta$	•	∘	∘	•	•	∘	∘	T_0^{-+}
ii-I	$R_i = R \times C_i$	•	•	•	∘	∘	∘	∘	T_0^{+-}
JJ	$R_{i\theta} = R \times C_{i\theta}$	•	∘	∘	∘	∘	•	•	T_0^{--}
J	$R = R \times C_1 \equiv R$	•	∘	∘	∘	∘	∘	∘	T_0^{any}

1. Continuous spherical groups

We have one spherical point group $R \equiv SO(3)$ of proper rotations C. By adding γ-improper rotations γC with $\gamma = i$, θ, or $i\theta$, we obtain the spherical magnetic groups G_sp listed in Table XI. These form class $L(R)$. As R lacks an index-2 subgroup, $L(R)$ contains only groups of type J, ii-II, JJ, ii-I, and i-II. See Table XII. We call $R_{i\times\theta} \equiv R \times C_{i\times\theta}$ the full rotation group. All continuous and discrete groups discussed in this work are subgroups of $R_{i\times\theta}$.

2. Continuous axial groups

There exist two proper continuous axial point groups, the cyclic group $C_\infty \equiv SO(2)$ and the dihedral group D_∞. By adding SIS and TIS to these groups, one obtains the cyclic magnetic groups $G_{c\infty}$ listed in Table XIII [class $L(C_\infty)$] and the dihedral magnetic groups $G_{d\infty}$ listed in Table XIV [class $L(D_\infty)$]. We call $D_\infty \times C_{i\times\theta}$ the full axial rotation group. See also Refs. [158,184–187] for related work on axial point groups.

TABLE XII. Class $L(R)$ of spherical magnetic point groups arranged according to the scheme in Table X and indicated at the bottom part of the table. See Table IX for the definitions of group types. The groups of type J, ii-I, i-II, and ii-II delineate the main block of groups in class $L(R)$, where the duality transformation $i \leftrightarrow \theta$ maps rows onto columns and vice versa. The type-JJ group outside the main block is self-dual, and so are the groups positioned on the main-block diagonal. Small 2×2 matrices mark congruences between tensors with signature ss' as discussed in detail in Appendix E.

R / $R \times C_\theta$	$\begin{pmatrix}\circ&\circ\\ \circ&\end{pmatrix}$ / $\begin{pmatrix}\circ&\\ \circ&\end{pmatrix}$	$R \times C_i$ / $R \times C_{i\times\theta}$	$\begin{pmatrix}\circ&\circ\\ &\end{pmatrix}$ / $\begin{pmatrix}\circ&\\ &\end{pmatrix}$	$R \times C_{i\theta}$	$\begin{pmatrix}\circ&\\ &\circ\end{pmatrix}$
J		ii-I		JJ	
i-II		ii-II			

TABLE XIII. Continuous cyclic magnetic groups $G_{c\infty}$. Symmetry elements present (absent) in different groups $G_{c\infty}$ are labeled "•" ("∘"). Here, C_z represents an arbitrary rotation about the fixed z axis. Labels in the first column refer to the classification of magnetic point groups introduced in Table IX. The last column gives invariant tensors for these groups expressed in terms of irreducible tensor components $T^{ss'}_{\ell 0}$ of $R_{i\times\theta}$ (see Sec. II A and Appendix B 2) [183].

	$G_{c\infty}$	C_z	i	iC_z	θ	θC_z	$i\theta$	$i\theta C_z$	$T^{ss'}_{\ell 0}$
ii-II	$C_\infty \times C_{i\times\theta} = C_{\infty h} \times C_\theta$	•	•	•	•	•	•	•	$T^{++}_{\ell 0}$
i-II	$C_\infty \times C_\theta$	•	∘	∘	•	•	∘	∘	$T^{-+}_{\ell 0}$
ii-I	$C_\infty \times C_i = C_{\infty h}$	•	•	•	∘	∘	∘	∘	$T^{+-}_{\ell 0}$
JJ	$C_\infty \times C_{i\theta} = C_{\infty h}(C_\infty)$	•	∘	∘	∘	∘	•	•	$T^{--}_{\ell 0}$
J	C_∞	•	∘	∘	∘	∘	∘	∘	$T^{\text{any}}_{\ell 0}$

Like R, the group C_∞ lacks an index-2 subgroup, so the structure of class $L(C_\infty)$ mirrors that of $L(R)$. See the upper part of Table XV. In contrast, group D_∞ has the index-2 subgroup C_∞. Class $L(D_\infty)$ thus has a richer composition that includes groups of type i-III, JJJ, ii-III, and JJ', i.e., the types indicated in the middle row of the scheme shown in the bottom part of Table XV.

The continuous axial groups are the maximal groups of many important physical quantities (see Table III). Therefore, in the following, we review, in more detail, the IRs of the continuous axial groups that we refer to repeatedly in this work. The cyclic groups $G_{c\infty}$ are Abelian so that all their IRs are one dimensional. Under these groups, the transformation behavior of tensor components $T^{ss'}_{\ell m}$ of $R_{i\times\theta}$ depends only on m but not on ℓ; for fixed m but different values of ℓ (with $|m| \le \ell$), the components $T^{ss'}_{\ell m}$ transform the same way under groups $G_{c\infty}$. The invariant tensors of groups $G_{c\infty}$ are then the tensor components $T^{ss'}_{\ell 0}$ (Table XIII). Similar to T^{++}_{00} under the spherical groups, tensor components $T^{++}_{\ell 0}$ are invariant under all cyclic groups $G_{c\infty}$.

The dihedral groups $G_{d\infty}$ are non-Abelian. Under groups $G_{d\infty}$, the tensor components $T^{ss'}_{\ell 0}$ of $R_{i\times\theta}$ transform according to one-dimensional IRs, whereas tensor components $T^{ss'}_{\ell,\pm m}$ with $m \neq 0$ pairwise transform according to two-dimensional IRs. More specifically, the transformation properties depend on the parity of ℓ. For even ℓ ("g"), tensor components $T^{ss'}_{g0}$ are even under π rotations C_2 about an axis perpendicular to the main axis of the dihedral

TABLE XIV. Continuous dihedral magnetic groups $G_{d\infty}$. Symmetry elements present (absent) in different groups $G_{d\infty}$ are labeled "•" ("∘"). Here, C_z represents an arbitrary rotation about the fixed z axis, and C_2 is a π rotation about an axis perpendicular to the z axis. Labels in the first column refer to the classification of magnetic point groups introduced in Table IX. The last two columns give invariant tensors for these groups expressed in terms of irreducible tensor components $T^{ss'}_{\ell 0}$ of $R_{i\times\theta}$ (see Sec. II A and Appendix B 2) [183]. Here, $T^{ss'}_{g0}$ stands for any $T^{ss'}_{\ell 0}$ with ℓ even, while $T^{ss'}_{u0}$ can be any $T^{ss'}_{\ell 0}$ with ℓ odd. The component T^{++}_{u0} is also included for completeness, even though it is not an invariant quantity for any continuous dihedral group $G_{d\infty}$.

	$G_{d\infty}$	C_z	i	iC_z	C_2	iC_2	θ	θC_z	$i\theta$	$i\theta C_z$	θC_2	$i\theta C_2$	$T^{ss'}_{\ell 0}$	
ii-II	$D_\infty \times C_{i\times\theta} = D_{\infty h} \times C_\theta$	•	•	•	•	•	•	•	•	•	•	•	T^{++}_{g0}	
i-II	$D_\infty \times C_\theta$	•	∘	∘	•	∘	•	•	∘	∘	•	∘	T^{-+}_{g0}	
ii-I	$D_\infty \times C_i = D_{\infty h}$	•	•	•	•	•	∘	∘	∘	∘	∘	∘	T^{+-}_{g0}	
JJ	$D_\infty \times C_{i\theta} = D_{\infty h}(D_\infty)$	•	∘	∘	•	∘	∘	∘	•	•	∘	•	T^{--}_{g0}	
		•	•	•	∘	∘	•	•	•	•	∘	∘		T^{++}_{u0}
iii-II	$D_\infty[C_\infty] \times C_\theta = C_{\infty v} \times C_\theta$	•	∘	∘	∘	•	•	•	∘	∘	∘	•		T^{-+}_{u0}
ii-III	$D_\infty(C_\infty) \times C_i = D_{\infty h}(C_{\infty h})$	•	•	•	∘	∘	∘	∘	∘	∘	•	•		T^{+-}_{u0}
JJ'	$D_\infty(C_\infty) \times C_{i\theta} = D_{\infty h}(C_{\infty v})$	•	∘	∘	∘	•	∘	∘	•	•	•	∘		T^{--}_{u0}
iii-I	$D_\infty[C_\infty] = C_{\infty v}$	•	∘	∘	∘	•	∘	∘	∘	∘	∘	∘	T^{+-}_{g0}	$T^{-\pm}_{u0}$
i-III	$D_\infty(C_\infty)$	•	∘	∘	∘	∘	∘	∘	∘	∘	•	∘	T^{-+}_{g0}	$T^{\pm-}_{u0}$
JJJ	$D_\infty\{C_\infty\} = C_{\infty v}(C_\infty)$	•	∘	∘	∘	∘	∘	∘	∘	∘	∘	•	T^{--}_{g0}	$T^{\mp\pm}_{u0}$
J	D_∞	•	∘	∘	•	∘	∘	∘	∘	∘	∘	∘	T^{any}_{g0}	

TABLE XV. Continuous axial magnetic point groups organized into classes. Within each class, the arrangement of groups follows the scheme in Table X, indicated in the bottom part of the table. See Table IX for the definitions of group types. The groups of type J, ii-I, i-II, and ii-II delineate the main block of groups in a given class, where the duality transformation $i \leftrightarrow \theta$ maps rows onto columns and vice versa. The type-JJ and type-JJ' groups outside the main block are self-dual, and so are the groups positioned on a main-block diagonal. Small 2×2 matrices mark congruences between tensors with signature ss' as discussed in detail in Appendix E. A group with exactly one filled symbol, pertaining to signature ss', represents the maximal group of the vector component $T_{10}^{ss'}$ (see Sec. II A).

C_∞	(:::)			$C_{\infty h} = C_\infty \times C_i$	(•••)	$C_{\infty h}(C_\infty) = C_\infty \times C_{i\theta}$	(•∘)
$C_\infty \times C_\theta$	(:)			$C_{\infty h} \times C_\theta = C_\infty \times C_{i\times\theta}$	(•)		
D_∞	(∘∘∘)	$C_{\infty v} = D_\infty[C_\infty]$	(∘★★)	$D_{\infty h} = D_\infty \times C_i$	(∘∘∘)	$D_{\infty h}(D_\infty) = D_\infty \times C_{i\theta}$	(∘∘)
$D_\infty(C_\infty)$	(∘★★)	$C_{\infty v}(C_\infty) = D_\infty\{C_\infty\}$	(∘★∘)	$D_{\infty h}(C_{\infty h}) = D_\infty(C_\infty) \times C_i$	(∘★★)	$D_{\infty h}(C_{\infty v}) = D_\infty(C_\infty) \times C_{i\theta}$	(∘★)
$D_\infty \times C_\theta$	(∘)	$C_{\infty v} \times C_\theta = D_\infty[C_\infty] \times C_\theta$	(★)	$D_{\infty h} \times C_\theta = D_\infty \times C_{i\times\theta}$	(∘)		
J		iii-I		ii-I		JJ	
i-III		JJJ		ii-III		JJ'	
i-II		iii-II		ii-II			

groups (chosen as the z axis in Table XIV), whereas for odd ℓ ("u"), tensor components $T_{u0}^{ss'}$ are odd under rotations C_2 [183]. The invariant tensor components $T_{\ell 0}^{ss'}$ under the dihedral groups $G_{d\infty}$ thus distinguish between ℓ even or odd (see Table XIV). But similar to tensor components $T_{\ell 0}^{ss'}$ under the cyclic groups, tensor components with different even or different odd values of ℓ behave the same.

The cyclic groups in Table XIII are subgroups of the dihedral groups in Table XIV. The maximal groups of tensor components $T_{\ell 0}^{ss'}$ are thus generally the dihedral groups that provide a more fine-grained classification of the symmetries of $T_{\ell 0}^{ss'}$ based on the parity of ℓ (see Table XIV). As noted above, tensor components $T_{u0}^{ss'}$ change sign under π rotations C_2 about an axis perpendicular to the z axis [183]. The transformation behavior of these tensor components under the full axial group $D_\infty \times C_{i\times\theta}$ as listed in Table XIV thus defines polar directions with signature ss'. For the three polar directions T_{u0}^{-+}, T_{u0}^{+-}, and T_{u0}^{--}, the respective maximal groups are listed in Table XIV.

Interestingly, inspection of Table XIV shows that an electrotoroidal tensor component T_{u0}^{++} is not invariant under any of the continuous dihedral groups. It is only invariant under continuous cyclic groups $G_{c\infty}$, including $C_\infty \times C_{i\times\theta}$, that do not distinguish between tensor components T_{u0}^{++} and electric tensor components T_{g0}^{++}. This fact has the remarkable consequence that, very generally, one cannot define a setting that would allow one to distinguish between electrotoroidal tensor components T_{u0}^{++} and electric tensor components T_{g0}^{++}. Beyond the fact that tensors T_u^{++} have no suitable building blocks in Table V, this is the reason why electrotoroidal tensors T_u^{++} are not studied further in this work.

According to the general definition of group types given in Table IX, the continuous dihedral groups have the group types listed in the first column of Table XIV. A comparison of Tables IV and XIV shows that the range of multipole densities $T_\ell^{ss'}$ permitted by these continuous dihedral groups falls short of the range of densities generally permitted by the categories of polarization associated with these group types. For example, the group $D_\infty \times C_\theta$ has the type i-II that belongs to the electropolar category. However, the group $D_\infty \times C_\theta$ does not allow odd-ℓ electric multipoles $(-+)$. This result can be traced back to the fact that the groups in class $L(D_\infty)$ can also be viewed as limiting groups $n \to \infty$ for the groups in class $L(D_n)$. The lowest degree $\ell_{\min}^{(e,u)}$ of odd-ℓ electric multipoles permitted by groups $D_n \times C_\theta$ grows monotonically with increasing n, with $\ell_{\min}^{(e,u)} \to \infty$ for $n \to \infty$ (see Table XXI). This does not affect our classification of categories of polarized matter as crystals are characterized by finite crystallographic point groups.

Continuous axial symmetries can be useful to represent the limiting symmetries of physical systems [184]. Illustrating these by simple geometrical shapes has a long history [184,185,187], and such simple objects can also be employed as depictions of finite chiral systems [136]. Inspired by these earlier approaches, we use axially symmetric objects (such as those shown in Table XVI) to explore the five categories of chirality (see Figs. 4–6). To ease cross-referencing between previous works [158,185] discussing axial quantities and ours, we provide Table XVII, relating respective notations for axial quantities.

3. Discrete groups

There are 11 proper crystallographic point groups: C_1, C_2, D_2, C_4, D_4, C_3, D_3, C_6, D_6, T, and O, representing the

TABLE XVI. Axially symmetric finite objects illustrating the categories of chirality for the classes $L(C_\infty)$ and $L(D_\infty)$, see Figs. 4–6.

Object	 Plain cylinder	 Marbled cylinder	 Plain cone	 Marbled cone	 Rotating cylinder	 Rotating marbled cylinder	 Moving cylinder	 Moving marbled cylinder
Point group	$D_\infty \times C_{i\times\theta}$	$C_\infty \times C_{i\times\theta}$	$D_\infty[C_\infty] \times C_\theta$	$C_\infty \times C_\theta$	$D_\infty(C_\infty) \times C_i$	$C_\infty \times C_i$	$D_\infty(C_\infty) \times C_{i\theta}$	$C_\infty \times C_{i\theta}$
Inversion symmetries	$i, \theta, i\theta$	$i, \theta, i\theta$	θ	θ	i	i	$i\theta$	$i\theta$
Improper rotations	$iC_2, \theta C_2, i\theta C_2,$ $iC_z, \theta C_z, i\theta C_z$	$iC_z, \theta C_z, i\theta C_z$	$iC_2, i\theta C_2, \theta C_z$	θC_z	$\theta C_2, i\theta C_2, iC_z$	iC_z	$iC_2, \theta C_2, i\theta C_z$	$i\theta C_z$
Category of chirality	Parachiral	Parachiral	Parachiral	Electrochiral	Parachiral	Magnetochiral	Parachiral	Antimagnetochiral
Object	 Plain divided cylinders	 Marbled divided cylinders	 Countermoving cylinders	 Counterrotating cylinders		 Moving rotating cylinder	 Moving cone	 Rotating cone
Point group	$D_\infty \times C_{i\times\theta}$	$D_\infty \times C_\theta$	$D_\infty \times C_i$	$D_\infty \times C_{i\theta}$		$D_\infty(C_\infty)$	$D_\infty[C_\infty]$	$D_\infty\{C_\infty\}$
Inversion symmetries	$i, \theta, i\theta$	θ	i	$i\theta$				
Improper rotations	$iC_2, \theta C_2, i\theta C_2,$ $iC_z, \theta C_z, i\theta C_z$	$\theta C_2, \theta C_z$	iC_2, iC_z	$i\theta C_2, i\theta C_z$		θC_2	iC_2	$i\theta C_2$
Category of chirality	Parachiral	Electrochiral	Magnetochiral	Antimagnetochiral		Electrochiral	Magnetochiral	Antimagnetochiral

TABLE XVII. Notation for axial quantities in the literature. Reference [185] uses the symbols from Ref. [73] for tensor components $T^{ss'}_{u0}$.

This work	T^{++}_{g0}	T^{-+}_{g0}	T^{+-}_{g0}	T^{--}_{g0}	T^{++}_{u0}	T^{-+}_{u0}	T^{+-}_{u0}	T^{--}_{u0}
Ref. [185]	**N**	**C**	**L**	**F**	**G**	**P**	**M**	**T**
Ref. [158]	$\mathscr{D}$	$\mathscr{D}$	$\mathscr{D}'$	$\mathscr{C}'$	$\mathscr{a}$	$\mathscr{P}$	$\mathscr{a}'$	$\mathscr{P}'$

roots for 11 classes. By adding SIS, one obtains 21 improper (with respect to SIS) point groups [11]; 11 of these are *i*-major groups, and 10 are *i*-minor groups. Jointly, these groups represent the familiar 32 nonmagnetic crystallographic point groups (ignoring TIS). By also adding TIS, the 122 magnetic crystallographic point groups are obtained [10,19,21,51]. The 32 type-II (i.e., θ-major) groups among these are the crystallographic point groups representing paramagnetic solids. The same groups also characterize antiferromagnetic crystals with nonsymmorphic space groups containing symmetry elements that combine nonprimitive translations with time inversion [21,120] (see Sec. II I). All other magnetic point groups describe crystals with magnetic order where TIS is broken.

The full set of 122 magnetic crystallographic point groups can be organized into 11 classes [57–60]. These classes are generalizations of the Laue classes that are usually defined in terms of the improper groups $G_{\rm p} \times C_i$ [66]. In a similar spirit, the Laue classes of magnetic crystallographic point groups have previously been defined in terms of the paramagnetic groups $G_{\rm p} \times C_{i\times\theta}$ [59]. Here, we find it more advantageous to organize these Laue classes in terms of their respective proper point groups $G_{\rm p}$ [58]. See Table XVIII.

The composition of the 11 (Laue) classes of magnetic point groups derived from the proper crystallographic point groups partly mirrors but also extends that of the continuous groups. In particular, the structure of $L(C_1)$, $L(C_3)$, and $L(T)$ is entirely analogous to that of $L(R)$ and $L(C_\infty)$ (compare Tables XV and XVIII), which is due to the fact that, like R and C_∞, the class roots C_1, C_3, and T have no index-2 subgroup. Similarly, the structure of $L(C_2)$, $L(C_4)$, $L(D_3)$, $L(C_6)$, and $L(O)$ mirrors that of $L(D_\infty)$ because the respective class roots all have one index-2 subgroup. Class $L(D_2)$ exhibits the basic $L(D_\infty)$ structure, but it contains, in addition, the group $C_{2v}(C_s) = D_2[C_2](C_2[C_1])$, which is the only crystallographic point group of type JJJ". Classes $L(D_4)$ and $L(D_6)$ exhibit greater complexity because they have two distinct index-2 subgroups, which doubles the possibilities for constructing groups of type iii-I, i-III, JJJ, iii-II, ii-III, and JJ' and also yields a triad of groups with respective types JJJ', iii'-III, and iii-III'.

Tables XII, XV, and XVIII systematize classes of magnetic point groups in terms of the SIS-TIS-symmetric group types summarized in Table IX. The placement of individual groups within rows and columns as per the schemes given at the bottom of each table illustrates SIS-TIS duality (see Appendix A 3). In particular, for each class $L(G_{\rm p})$, the *main block* has the groups of type J, ii-I, i-II, and ii-II at its four corners. Within this block, the duality transformation based on the exchange $i \leftrightarrow \theta$ maps rows on columns and vice versa. Groups placed on the diagonal of the main block are self-dual, and so are the type JJ, JJ', JJJ', and JJJ" groups positioned outside of the main block. Using SIS-TIS duality of magnetic point groups within a class as the organizing principle differentiates the arrangement of Table XVIII from the previously developed periodic arrangement of the 122 crystallographic magnetic point groups shown, e.g., in Table 2 of Ref. [59].

The organizing principle of Tables XII, XV, and XVIII follows that shown for a general class in the upper part of Table X. Thus, in all these tables, groups within the main block of a class $L(G_{\rm p})$ [188] are placed such that groups in a given row belong to the same subclass $L(G^i_0, i)$, where G^i_0 is the group in the first column. Groups in a given column of the main block belong to the same subclass $L(G^\theta_0, \theta)$, G^θ_0 being the group in the first row. See Appendixes A 5 and A 6 for a detailed discussion of subclass structures.

Subgroup relations and isomorphisms between groups in a given class $L(G_{\rm p})$ follow Fig. 10. See also explicit tabulations of subgroup relations for the ordinary crystallographic point groups [16,189] and for the magnetic groups [190,191]. Table IX lists the number of point groups of each type among the 122 crystallographic magnetic point groups. The triadic structure underlies the appearance of certain magic numbers [55,56,62] when groups are collated based on particular physical characteristics described by tensor quantities. See Appendix E for a detailed discussion of this point.

Table XIX lists the lowest rank $\ell_{\rm min}$ of nontrivial multipole densities permitted by all 122 crystallographic magnetic point groups.

TABLE XVIII. The 122 crystallographic magnetic point groups organized into (Laue) classes. Within each class, the arrangement of groups follows the scheme in Table X and indicated at the bottom part of the table. See Table IX for the definitions of group types. The groups of type J, ii-I, i-II, and ii-II delineate the main block of groups in a given class, where the duality transformation $i \leftrightarrow \theta$ maps rows onto columns and vice versa. The type-JJ, type-JJ', type-JJJ', and type-JJJ" groups outside the main block are self-dual, and so are the groups positioned on a main-block diagonal. Small 2×2 matrices mark congruences between tensors with signature ss' as discussed in detail in Appendix E.

Triclinic (5 groups)								
C_1	$\begin{pmatrix}\bullet&\bullet\\ \bullet&\bullet\end{pmatrix}$				$C_i = C_1 \times C_i$	$\begin{pmatrix}\bullet&\bullet\\ \bullet&\bullet\end{pmatrix}$	$C_i(C_1) = C_1 \times C_{i\theta}$	$\begin{pmatrix}\bullet&\bullet\\ \bullet&\bullet\end{pmatrix}$
$C_1 \times C_\theta$	$\begin{pmatrix}\bullet&\\ \bullet&\end{pmatrix}$				$C_i \times C_\theta = C_1 \times C_{i\times\theta}$	$\begin{pmatrix}\bullet&\\ \bullet&\end{pmatrix}$		
Monoclinic (11 groups)								
C_2	$\begin{pmatrix}\bullet&\bullet\\ \bullet&\bullet\end{pmatrix}$	$C_s = C_2[C_1]$	$\begin{pmatrix}\bullet&\bullet\\ \star&\star\end{pmatrix}$		$C_{2h} = C_2 \times C_i$	$\begin{pmatrix}\bullet&\bullet\\ \bullet&\bullet\end{pmatrix}$	$C_{2h}(C_2) = C_2 \times C_{i\theta}$	$\begin{pmatrix}\bullet&\bullet\\ \bullet&\bullet\end{pmatrix}$
$C_2(C_1)$	$\begin{pmatrix}\bullet&\star\\ \bullet&\star\end{pmatrix}$	$C_s(C_1) = C_2\{C_1\}$	$\begin{pmatrix}\bullet&\star\\ \star&\bullet\end{pmatrix}$		$C_{2h}(C_i) = C_2(C_1) \times C_i$	$\begin{pmatrix}\bullet&\star\\ \bullet&\star\end{pmatrix}$	$C_{2h}(C_s) = C_2(C_1) \times C_{i\theta}$	$\begin{pmatrix}\bullet&\star\\ \bullet&\star\end{pmatrix}$
$C_2 \times C_\theta$	$\begin{pmatrix}\bullet&\\ \bullet&\end{pmatrix}$	$C_s \times C_\theta = C_2[C_1] \times C_\theta$	$\begin{pmatrix}\bullet&\\ \star&\end{pmatrix}$		$C_{2h} \times C_\theta = C_2 \times C_{i\times\theta}$	$\begin{pmatrix}\bullet&\\ \bullet&\end{pmatrix}$		
(Ortho)rhombic (12 groups)								
D_2	$\begin{pmatrix}\circ&\circ\\ \circ&\circ\end{pmatrix}$	$C_{2v} = D_2[C_2]$	$\begin{pmatrix}\circ&\circ\\ \star&\star\end{pmatrix}$		$D_{2h} = D_2 \times C_i$	$\begin{pmatrix}\circ&\circ\\ \circ&\circ\end{pmatrix}$	$D_{2h}(D_2) = D_2 \times C_{i\theta}$	$\begin{pmatrix}\circ&\circ\\ \circ&\circ\end{pmatrix}$
$D_2(C_2)$	$\begin{pmatrix}\circ&\star\\ \circ&\star\end{pmatrix}$	$C_{2v}(C_2) = D_2\{C_2\}$	$\begin{pmatrix}\circ&\star\\ \star&\circ\end{pmatrix}$		$D_{2h}(C_{2h}) = D_2(C_2) \times C_i$	$\begin{pmatrix}\circ&\star\\ \circ&\star\end{pmatrix}$	$D_{2h}(C_{2v}) = D_2(C_2) \times C_{i\theta}$	$\begin{pmatrix}\circ&\star\\ \circ&\star\end{pmatrix}$
$D_2 \times C_\theta$	$\begin{pmatrix}\circ&\\ \circ&\end{pmatrix}$	$C_{2v} \times C_\theta = D_2[C_2] \times C_\theta$	$\begin{pmatrix}\circ&\\ \star&\end{pmatrix}$		$D_{2h} \times C_\theta = D_2 \times C_{i\times\theta}$	$\begin{pmatrix}\circ&\\ \circ&\end{pmatrix}$		
		$C_{2v}(C_s) = D_2[C_2](C_2'[C_1])$	$\begin{pmatrix}\circ&\star\\ \star&\star\end{pmatrix}$					
Tetragonal ($11 + 20$ groups)								
C_4	$\begin{pmatrix}\bullet&\bullet\\ \bullet&\bullet\end{pmatrix}$	$S_4 = C_4[C_2]$	$\begin{pmatrix}\bullet&\bullet\\ \star&\star\end{pmatrix}$		$C_{4h} = C_4 \times C_i$	$\begin{pmatrix}\bullet&\bullet\\ \bullet&\bullet\end{pmatrix}$	$C_{4h}(C_4) = C_4 \times C_{i\theta}$	$\begin{pmatrix}\bullet&\bullet\\ \bullet&\bullet\end{pmatrix}$
$C_4(C_2)$	$\begin{pmatrix}\bullet&\star\\ \bullet&\star\end{pmatrix}$	$S_4(C_2) = C_4\{C_2\}$	$\begin{pmatrix}\bullet&\star\\ \star&\bullet\end{pmatrix}$		$C_{4h}(C_{2h}) = C_4(C_2) \times C_i$	$\begin{pmatrix}\bullet&\star\\ \bullet&\star\end{pmatrix}$	$C_{4h}(S_4) = C_4(C_2) \times C_{i\theta}$	$\begin{pmatrix}\bullet&\star\\ \bullet&\star\end{pmatrix}$
$C_4 \times C_\theta$	$\begin{pmatrix}\bullet&\\ \bullet&\end{pmatrix}$	$S_4 \times C_\theta = C_4[C_2] \times C_\theta$	$\begin{pmatrix}\bullet&\\ \star&\end{pmatrix}$		$C_{4h} \times C_\theta = C_4 \times C_{i\times\theta}$	$\begin{pmatrix}\bullet&\\ \bullet&\end{pmatrix}$		
D_4	$\begin{pmatrix}\circ&\circ\\ \circ&\circ\end{pmatrix}$	$C_{4v} = D_4[C_4]$	$\begin{pmatrix}\circ&\circ\\ \star&\star\end{pmatrix}$	$D_{2d} = D_4[D_2]$	$\begin{pmatrix}\circ&\circ\\ \diamond&\diamond\end{pmatrix}$	$D_{4h} = D_4 \times C_i$	$\begin{pmatrix}\circ&\circ\\ \circ&\circ\end{pmatrix}$	$D_{4h}(D_4) = D_4 \times C_{i\theta}$	$\begin{pmatrix}\circ&\circ\\ \circ&\circ\end{pmatrix}$
$D_4(C_4)$	$\begin{pmatrix}\circ&\star\\ \circ&\star\end{pmatrix}$	$C_{4v}(C_4) = D_4\{C_4\}$	$\begin{pmatrix}\circ&\star\\ \star&\circ\end{pmatrix}$	$D_{2d}(S_4) = D_4[D_2](C_4[C_2])$	$\begin{pmatrix}\circ&\star\\ \diamond&\diamond\end{pmatrix}$	$D_{4h}(C_{4h}) = D_4(C_4) \times C_i$	$\begin{pmatrix}\circ&\star\\ \circ&\star\end{pmatrix}$	$D_{4h}(C_{4v}) = D_4(C_4) \times C_{i\theta}$	$\begin{pmatrix}\circ&\star\\ \circ&\star\end{pmatrix}$
$D_4(D_2)$	$\begin{pmatrix}\circ&\diamond\\ \circ&\diamond\end{pmatrix}$	$C_{4v}(C_{2v}) = D_4[C_4](D_2[C_2])$	$\begin{pmatrix}\circ&\diamond\\ \star&\diamond\end{pmatrix}$	$D_{2d}(D_2) = D_4\{D_2\}$	$\begin{pmatrix}\circ&\diamond\\ \circ&\diamond\end{pmatrix}$	$D_{4h}(D_{2h}) = D_4(D_2) \times C_i$	$\begin{pmatrix}\circ&\diamond\\ \circ&\diamond\end{pmatrix}$	$D_{4h}(D_{2d}) = D_4(D_2) \times C_{i\theta}$	$\begin{pmatrix}\circ&\diamond\\ \circ&\diamond\end{pmatrix}$
$D_4 \times C_\theta$	$\begin{pmatrix}\circ&\\ \circ&\end{pmatrix}$	$C_{4v} \times C_\theta = D_4[C_4] \times C_\theta$	$\begin{pmatrix}\circ&\\ \star&\end{pmatrix}$	$D_{2d} \times C_\theta = D_4[D_2] \times C_\theta$	$\begin{pmatrix}\circ&\\ \diamond&\end{pmatrix}$	$D_{4h} \times C_\theta = D_4 \times C_{i\times\theta}$	$\begin{pmatrix}\circ&\\ \circ&\end{pmatrix}$		
				$D_{2d}(C_{2v}) = D_4[D_2](D_2'[C_2])$	$\begin{pmatrix}\circ&\diamond\\ \diamond&\star\end{pmatrix}$				
Trigonal ($5 + 11$ groups)									
C_3	$\begin{pmatrix}\bullet&\bullet\\ \bullet&\bullet\end{pmatrix}$					$C_{3i} = C_3 \times C_i$	$\begin{pmatrix}\bullet&\bullet\\ \bullet&\bullet\end{pmatrix}$	$C_{3i}(C_3) = C_3 \times C_{i\theta}$	$\begin{pmatrix}\bullet&\bullet\\ \bullet&\bullet\end{pmatrix}$
$C_3 \times C_\theta$	$\begin{pmatrix}\bullet&\\ \bullet&\end{pmatrix}$					$C_{3i} \times C_\theta = C_3 \times C_{i\times\theta}$	$\begin{pmatrix}\bullet&\\ \bullet&\end{pmatrix}$		
D_3	$\begin{pmatrix}\circ&\circ\\ \circ&\circ\end{pmatrix}$	$C_{3v} = D_3[C_3]$	$\begin{pmatrix}\circ&\circ\\ \star&\star\end{pmatrix}$			$D_{3d} = D_3 \times C_i$	$\begin{pmatrix}\circ&\circ\\ \circ&\circ\end{pmatrix}$	$D_{3d}(D_3) = D_3 \times C_{i\theta}$	$\begin{pmatrix}\circ&\circ\\ \circ&\circ\end{pmatrix}$
$D_3(C_3)$	$\begin{pmatrix}\circ&\star\\ \circ&\star\end{pmatrix}$	$C_{3v}(C_3) = D_3\{C_3\}$	$\begin{pmatrix}\circ&\star\\ \star&\circ\end{pmatrix}$			$D_{3d}(C_{3i}) = D_3(C_3) \times C_i$	$\begin{pmatrix}\circ&\star\\ \circ&\star\end{pmatrix}$	$D_{3d}(C_{3v}) = D_3(C_3) \times C_{i\theta}$	$\begin{pmatrix}\circ&\star\\ \circ&\star\end{pmatrix}$
$D_3 \times C_\theta$	$\begin{pmatrix}\circ&\\ \circ&\end{pmatrix}$	$C_{3v} \times C_\theta = D_3[C_3] \times C_\theta$	$\begin{pmatrix}\circ&\\ \star&\end{pmatrix}$			$D_{3d} \times C_\theta = D_3 \times C_{i\times\theta}$	$\begin{pmatrix}\circ&\\ \circ&\end{pmatrix}$		

(Table continued)

TABLE XVIII. *(Continued)*

Hexagonal ($11 + 20$ groups)									
C_6	$\begin{pmatrix}\bullet & \bullet \\ \bullet & \bullet\end{pmatrix}$	$C_{3h} = C_6[C_3]$	$\begin{pmatrix}\bullet & \bullet \\ \star & \star\end{pmatrix}$			$C_{6h} = C_6 \times C_i$	$\begin{pmatrix}\bullet & \bullet \\ \circ & \circ\end{pmatrix}$	$C_{6h}(C_6) = C_6 \times C_{i\theta}$	$\begin{pmatrix}\bullet & \circ \\ \bullet & \circ\end{pmatrix}$
$C_6(C_3)$	$\begin{pmatrix}\bullet & \star \\ \bullet & \star\end{pmatrix}$	$C_{3h}(C_3) = C_6\{C_3\}$	$\begin{pmatrix}\bullet & \star \\ \star & \bullet\end{pmatrix}$			$C_{6h}(C_{3i}) = C_6(C_3) \times C_i$	$\begin{pmatrix}\bullet & \star \\ \circ & \star\end{pmatrix}$	$C_{6h}(C_{3h}) = C_6(C_3) \times C_{i\theta}$	$\begin{pmatrix}\bullet & \star \\ \star & \circ\end{pmatrix}$
$C_6 \times C_\theta$	$\begin{pmatrix}\bullet \\ \bullet\end{pmatrix}$	$C_{3h} \times C_\theta = C_6[C_3] \times C_\theta$	$\begin{pmatrix}\bullet \\ \star\end{pmatrix}$			$C_{6h} \times C_\theta = C_6 \times C_{i\times\theta}$	$\begin{pmatrix}\bullet \\ \circ\end{pmatrix}$		
D_6	$\begin{pmatrix}\circ & \circ \\ \circ & \circ\end{pmatrix}$	$C_{6v} = D_6[C_6]$	$\begin{pmatrix}\circ & \circ \\ \star & \star\end{pmatrix}$	$D_{3h} = D_6[D_3]$	$\begin{pmatrix}\circ & \circ \\ \diamond & \diamond\end{pmatrix}$	$D_{6h} = D_6 \times C_i$	$\begin{pmatrix}\circ & \circ \\ \circ & \circ\end{pmatrix}$	$D_{6h}(D_6) = D_6 \times C_{i\theta}$	$\begin{pmatrix}\circ & \circ \\ \circ & \circ\end{pmatrix}$
$D_6(C_6)$	$\begin{pmatrix}\circ & \star \\ \circ & \star\end{pmatrix}$	$C_{6v}(C_6) = D_6\{C_6\}$	$\begin{pmatrix}\circ & \star \\ \star & \circ\end{pmatrix}$	$D_{3h}(C_{3h}) = D_6[D_3](C_6[C_3])$	$\begin{pmatrix}\circ & \star \\ \diamond & \diamond\end{pmatrix}$	$D_{6h}(C_{6h}) = D_6(C_6) \times C_i$	$\begin{pmatrix}\circ & \star \\ \circ & \star\end{pmatrix}$	$D_{6h}(C_{6v}) = D_6(C_6) \times C_{i\theta}$	$\begin{pmatrix}\circ & \star \\ \star & \circ\end{pmatrix}$
$D_6(D_3)$	$\begin{pmatrix}\circ & \diamond \\ \circ & \diamond\end{pmatrix}$	$C_{6v}(C_{3v}) = D_6[C_6](D_3[C_3])$	$\begin{pmatrix}\circ & \diamond \\ \star & \diamond\end{pmatrix}$	$D_{3h}(D_3) = D_6\{D_3\}$	$\begin{pmatrix}\circ & \diamond \\ \circ & \diamond\end{pmatrix}$	$D_{6h}(D_{3d}) = D_6(D_3) \times C_i$	$\begin{pmatrix}\circ & \diamond \\ \circ & \diamond\end{pmatrix}$	$D_{6h}(D_{3h}) = D_6(D_3) \times C_{i\theta}$	$\begin{pmatrix}\circ & \diamond \\ \circ & \diamond\end{pmatrix}$
$D_6 \times C_\theta$	$\begin{pmatrix}\circ \\ \circ\end{pmatrix}$	$C_{6v} \times C_\theta = D_6[C_6] \times C_\theta$	$\begin{pmatrix}\circ \\ \star\end{pmatrix}$	$D_{3h} \times C_\theta = D_6[D_3] \times C_\theta$	$\begin{pmatrix}\circ \\ \diamond\end{pmatrix}$	$D_{6h} \times C_\theta = D_6 \times C_{i\times\theta}$	$\begin{pmatrix}\circ \\ \circ\end{pmatrix}$		
				$D_{3h}(C_{3v}) = D_6[D_3](D_3'[C_3])$	$\begin{pmatrix}\circ & \diamond \\ \diamond & \star\end{pmatrix}$				
Cubic ($5 + 11$ groups)									
T	$\begin{pmatrix}\circ & \circ \\ \circ & \circ\end{pmatrix}$					$T_h = T \times C_i$	$\begin{pmatrix}\circ & \circ \\ \circ & \circ\end{pmatrix}$	$T_h(T) = T \times C_{i\theta}$	$\begin{pmatrix}\circ & \circ \\ \circ & \circ\end{pmatrix}$
$T \times C_\theta$	$\begin{pmatrix}\circ \\ \circ\end{pmatrix}$					$T_h \times C_\theta = T \times C_{i\times\theta}$	$\begin{pmatrix}\circ \\ \circ\end{pmatrix}$		
O	$\begin{pmatrix}\circ & \circ \\ \circ & \circ\end{pmatrix}$	$T_d = O[T]$	$\begin{pmatrix}\circ & \circ \\ \star & \star\end{pmatrix}$			$O_h = O \times C_i$	$\begin{pmatrix}\circ & \circ \\ \circ & \circ\end{pmatrix}$	$O_h(O) = O \times C_{i\theta}$	$\begin{pmatrix}\circ & \circ \\ \circ & \circ\end{pmatrix}$
$O(T)$	$\begin{pmatrix}\circ & \star \\ \circ & \star\end{pmatrix}$	$T_d(T) = O\{T\}$	$\begin{pmatrix}\circ & \star \\ \star & \circ\end{pmatrix}$			$O_h(T_h) = O(T) \times C_i$	$\begin{pmatrix}\circ & \star \\ \circ & \star\end{pmatrix}$	$O_h(T_d) = O(T) \times C_{i\theta}$	$\begin{pmatrix}\circ & \star \\ \star & \circ\end{pmatrix}$
$O \times C_\theta$	$\begin{pmatrix}\circ \\ \circ\end{pmatrix}$	$T_d \times C_\theta = O[T] \times C_\theta$	$\begin{pmatrix}\circ \\ \star\end{pmatrix}$			$O_h \times C_\theta = O \times C_{i\times\theta}$	$\begin{pmatrix}\circ \\ \circ\end{pmatrix}$		
J			iii-I			ii-I		JJ	
i-III			JJJ, iii'-III, and iii-III'			ii-III		JJ'	
i-II			iii-II			ii-II			
			JJJ' and JJJ''						

TABLE XIX. Lowest rank $\ell_{\min}$ of nontrivial multipole densities permitted by the 122 crystallographic magnetic point groups. In the parapolar case, we consider even-ℓ electric multipole densities (signature $++$). In the remaining cases, we consider odd-ℓ electric ($-+$), odd-ℓ magnetic ($+-$), and odd-ℓ magnetotoroidal ($--$) multipole densities. Numbers in parentheses indicate that multiple multipolar groups $\gamma = i$, θ, and $i\theta$ permit the same rank-$\ell_{\min}$ multipole density.

$\ell_{\min}$	Parapolar	Unipolar		Multipolar		
1		$C_2\langle C_1\rangle_{\bar\gamma}\times C_\gamma$	$C_1\times C_\gamma$			C_1
		$D_2\langle C_2\rangle_{\bar\gamma}\times C_\gamma$	$C_2\times C_\gamma$	$D_2\langle C_2\rangle_\gamma(2)$	$C_2\langle C_1\rangle_\gamma(3)$	C_2
		$D_4\langle C_4\rangle_{\bar\gamma}\times C_\gamma$	$C_4\times C_\gamma$	$D_4\langle C_4\rangle_\gamma(2)$	$C_4\langle C_2\rangle_\gamma$	C_4
		$D_3\langle C_3\rangle_{\bar\gamma}\times C_\gamma$	$C_3\times C_\gamma$	$D_3\langle C_3\rangle_\gamma(2)$		C_3
		$D_6\langle C_6\rangle_{\bar\gamma}\times C_\gamma$	$C_6\times C_\gamma$	$D_6\langle C_6\rangle_\gamma(2)$	$C_6\langle C_3\rangle_\gamma$	C_6
				$D_2[C_2](C_2'[C_1])$		
				$D_4\langle D_2\rangle_\gamma\langle D_2'\langle C_2\rangle_\gamma\rangle_{\bar\gamma}$		
				$D_6\langle D_3\rangle_\gamma\langle D_3'\langle C_3\rangle_\gamma\rangle_{\bar\gamma}$		
2	$C_1\times C_{i\times\theta}, C_2\times C_{i\times\theta}, D_2\times C_{i\times\theta}$, $C_4\times C_{i\times\theta}, D_4\times C_{i\times\theta}, C_3\times C_{i\times\theta}$, $D_3\times C_{i\times\theta}, C_6\times C_{i\times\theta}, D_6\times C_{i\times\theta}$					
3		$C_4\langle C_2\rangle_{\bar\gamma}\times C_\gamma$				
		$D_4\langle D_2\rangle_{\bar\gamma}\times C_\gamma$	$D_2\times C_\gamma$	$D_4\langle D_2\rangle_\gamma(2)$		D_2
		$C_6\langle C_3\rangle_{\bar\gamma}\times C_\gamma$				
		$D_6\langle D_3\rangle_{\bar\gamma}\times C_\gamma$	$D_3\times C_\gamma$	$D_6\langle D_3\rangle_\gamma(2)$		D_3
		$O\langle T\rangle_{\bar\gamma}\times C_\gamma$	$T\times C_\gamma$	$O\langle T\rangle_\gamma(2)$		T
4	$T\times C_{i\times\theta}, O\times C_{i\times\theta}$					
5			$D_4\times C_\gamma$			D_4
7			$D_6\times C_\gamma$			D_6
9			$O\times C_\gamma$			O

APPENDIX C: COMPOUND MULTIPOLES

1. General theory

To illustrate how compound tensors can be formed from electric and magnetic tensors, Table XX gives the multiplication table for electric and magnetic IRs $D_\ell^{ss'}$ of the full rotation group $R_{i\times\theta}$ with $\ell \le 3$. The range of ranks ℓ contained in a product representation is given by Eq. (3).

For example, Table XX shows that a magnetic monopole T_0^{--} can arise as a product of an electric and a magnetic multipole with the same $\ell > 0$. These multipoles with $\ell > 0$ break spherical symmetry so that the symmetry group of a system realizing such a synthetic magnetic monopole cannot be the spherical magnetic group $R_{i\theta}$ (that would be the symmetry group of an elementary magnetic monopole if it existed). However, a product of electric and magnetic multipoles with large ℓ can be arbitrarily close to spherical symmetry, which indicates an avenue for realizing "realistic" synthetic magnetic monopoles [192,193].

Products (4) of electric and magnetic tensors yield not only electric and magnetic compound tensors but also electrotoroidal and magnetotoroidal compound tensors (marked with bold subscripts ℓ in Table XX). For example, an electric quadrupole T_2^{++} and an electric dipole T_1^{-+} jointly give rise to an electrotoroidal quadrupole $T_{\mathbf{2}}^{-+}$.

Note that an electrotoroidal compound tensor T_1^{++} does not appear in Table XX. Electrotoroidal compound tensors T_ℓ^{++} with odd ℓ are realized by antisymmetric (noncommuting) products $(T_{\ell_1}^{ss'}\times T_{\ell_1}^{ss'})_{\mathrm{a}}$ of the same tensor $T_{\ell_1}^{ss'}$ or by products $T_{\ell_1}^{ss'}\times\tilde T_{\ell_2}^{ss'}$ of two distinct tensors $T_{\ell_1}^{ss'}$ and $\tilde T_{\ell_2}^{ss'}$ with the same signature ss' [67]. However, odd-ℓ IRs D_ℓ^{++} appearing off-diagonally in the multiplication table have $\ell \ge 3$. The IR D_1^{++} arises only on the diagonal. Assuming that for each ℓ a system has only one electric and one magnetic multipole $T_\ell^{ss'}$, second-order products of these multipoles thus cannot realize an electrotoroidal compound tensor T_1^{++}. This is in line with the difficulties encountered in Table V and Appendix B 2 to realize and interpret such tensors.

Toroidal scalars $T_0^{\mp\pm}$ likewise do not arise as second-order products of electric and magnetic tensors (see Table XX), but they do arise in third-order products of electric and magnetic tensors, for example,

$$\left.\begin{matrix} T_2^{++} \\ T_4^{++} \\ T_3^{\mp\pm} \end{matrix}\right\} T_3^{++} \Bigg\} T_0^{\mp\pm}. \tag{C1}$$

TABLE XX. Multiplication table for electric and magnetic IRs $D_\ell^{ss'}$ of the full rotation group $R_{i\times\theta}$ with $\ell \le 3$. We have $D_{1,2,3}^{ss'} \equiv D_1^{ss'} + D_2^{ss'} + D_3^{ss'}$, etc. Bold subscripts ℓ indicate that an IR contained in the product representation represents a toroidal multipole.

D_0^{++}	D_0^{--}	D_1^{-+}	D_1^{+-}	D_2^{++}	D_2^{--}	D_3^{-+}	D_3^{+-}	$D_\ell^{ss'}$
D_0^{++}	D_0^{--}	D_1^{-+}	D_1^{+-}	D_2^{++}	D_2^{--}	D_3^{-+}	D_3^{+-}	D_0^{++}
	D_0^{++}	D_1^{+-}	D_1^{-+}	D_2^{--}	D_2^{++}	D_3^{+-}	D_3^{-+}	D_0^{--}
		$D_{0,\mathbf{1},2}^{++}$	$D_{0,\mathbf{1},2}^{--}$	$D_{1,\mathbf{2},3}^{-+}$	$D_{1,\mathbf{2},3}^{+-}$	$D_{2,\mathbf{3},4}^{++}$	$D_{2,\mathbf{3},4}^{--}$	D_1^{-+}
			$D_{0,1,2}^{++}$	$D_{1,\mathbf{2},3}^{+-}$	$D_{1,\mathbf{2},3}^{-+}$	$D_{2,\mathbf{3},4}^{--}$	$D_{2,\mathbf{3},4}^{++}$	D_1^{+-}
				$D_{0,1,2,3,4}^{++}$	$D_{0,\mathbf{1},2,\mathbf{3},4}^{--}$	$D_{1,\mathbf{2},3,\mathbf{4},5}^{-+}$	$D_{1,\mathbf{2},3,\mathbf{4},5}^{+-}$	D_2^{++}
					$D_{0,1,2,3,4}^{++}$	$D_{1,\mathbf{2},3,\mathbf{4},5}^{+-}$	$D_{1,\mathbf{2},3,\mathbf{4},5}^{-+}$	D_2^{--}
						$D_{0,1,2,3,4,5,6}^{++}$	$D_{0,\mathbf{1},2,\mathbf{3},4,\mathbf{5},6}^{--}$	D_3^{-+}
							$D_{0,1,2,3,4,5,6}^{++}$	D_3^{+-}

Similar to magnetic scalars T_0^{--}, the toroidal scalars T_0^{-+} and T_0^{+-} can only arise in electromagnetic media that break spherical symmetry.

Inspection of Table XX and Eq. (C1) shows that all nontrivial compound tensors (except T_1^{++} [89]) can be obtained as products combining one nontrivial and one or two trivial tensors. By definition, trivial tensors have the signature $++$. Therefore, toroidal compound tensors inherit the signature of the nontrivial electromagnetic tensor they are composed of, while the index ℓ' of toroidal compound tensors has the opposite parity as the index ℓ of the nontrivial tensor they are composed of. Consistent with Tables V and VI, we thus interpret toroidal compound tensors as manifestations of the nontrivial electromagnetic tensor they are composed of.

The above group-theoretical analysis of compound tensors is independent of specific realizations of the tensors $T_\ell^{ss'}$ as discussed in Table V. It is equally applicable to finite and infinite periodic systems.

Consistent with our definition of categories of multipole order based on the signature ss', the terms electropolarization (signature $-+$), magnetopolarization ($+-$), and antimagnetopolarization ($--$) refer jointly to the respective odd-ℓ electric, odd-ℓ magnetic, and even-ℓ magnetic multipoles, as well as the corresponding toroidal compound moments with the same signature, unless we want to emphasize the composition of toroidal compound tensors.

2. Examples of compound moments

Reference [18] contains a detailed study of how electric and magnetic multipoles manifest themselves via characteristic terms in the electronic band structure of a crystal, using variations of lonsdaleite and diamond as examples. A careful inspection shows that a number of examples discussed in that work rely on compound moments.

For instance, we can have three qualitatively distinct homogeneous polynomials in k, σ of degree 2 in a crystal, two of which are compound moments. (i) Crystal structures with point groups T and O permit the crystallographic tensor $\boldsymbol{\sigma}\cdot\mathbf{k}$. This term transforms like an electrotoroidal compound scalar T_0^{-+} that arises as a product (C1) of a nontrivial odd-ℓ electric multipole and two trivial even-ℓ electric multipoles. See also Sec. III. (ii) Electropolar crystal structures such as wurtzite (point group C_{6v}, ignoring TIS) permit an electric dipole density that manifests itself via the Rashba term $k_x\sigma_y - k_y\sigma_x$ [102]. Under $R_{i\times\theta}$, this term transforms like the component T_{10}^{-+} of an electric dipole density. (iii) The cubic zincblende structure (point group T_d) permits an electric octupole density ($\ell = 3$) that manifests itself via the Dresselhaus term $\sigma_x k_x(k_y^2 - k_z^2) + \text{cp}$, where cp denotes cyclic permutation [103]. Under $R_{i\times\theta}$, this term transforms like the component $T_{3,-2}^{-+} + T_{3,2}^{-+}$ of an electric octupole density ($\ell = 3$). When uniaxial strain is applied to a zincblende structure (in the [001] direction, thus reducing the crystal symmetry from T_d to D_{2d}), we obtain the crystallographic tensor $k_x\sigma_x - k_y\sigma_y$. Under $R_{i\times\theta}$, this term transforms like the component $T_{2,-2}^{-+} + T_{2,2}^{-+}$ of an electrotoroidal quadrupole density that arises as a product (4) of the nontrivial electric octupole density ($\ell = 3$) that exists already in unstrained zincblende and a trivial strain-induced electric quadrupole density ($\ell = 2$). The electrotoroidal quadrupole density represents the lowest even-rank electrotoroidal moment density permitted in a structure with point group D_{2d} (Appendix D, Table XXI).

Pristine lonsdaleite has four identical atoms per unit cell; its crystallographic point group is $D_{6h} = D_6 \times C_i$ (ignoring TIS). If the four sublattices are occupied by two types of atoms as in Fig. 2(b) of Ref. [18], this results in an electric octupolarization ($\ell = 3$), and the point-group symmetry is reduced to D_{3h}. In addition, two new invariants arise in the band structure (to lowest order in $\mathbf{k}$) [18],

$$H_1 = c_1\sigma_z k_y(3k_x^2 - k_y^2), \tag{C2a}$$

$$H_2 = c_2 k_z\left[\sigma_x k_x k_y + \frac{1}{2}\sigma_y(k_x^2 - k_y^2)\right], \tag{C2b}$$

where c_1 and c_2 are material-specific prefactors. These terms can be rearranged as

$$H^{(3)} = \frac{5}{8}(H_1 - 2H_2), \tag{C3a}$$

$$H^{(4)} = \frac{3}{8}(H_1 + 6H_2). \tag{C3b}$$

Here, the first term transforms like the component $T^{-+}_{3,-3} + T^{-+}_{3,3}$ of an electric octupole density ($\ell = 3$), while the second term transforms like the component $T^{-+}_{4,-3} + T^{-+}_{4,3}$ of an electrotoroidal hexadecapole density ($\ell = 4$). The latter represents the lowest even-rank electrotoroidal moment density permitted in a structure with point group D_{3h} (Appendix D, Table XXI). It is realized as a compound moment density that combines the nontrivial electric octupole density ($\ell = 3$) with the trivial electric quadrupole density ($\ell = 2$) present already in pristine lonsdaleite.

An important example of compound moments arises in the context of antimagnetopolarizations. Very generally, unlike electropolarizations and magnetopolarizations, even-ℓ antimagnetopolarizations T^{--}_{ℓ} have no indicators in the band structure associated with them (see Table V). However, antimagnetopolarizations combined with trivial even-ℓ parapolarizations give rise to odd-ℓ magnetotoroidal densities T^{--}_{ℓ} that manifest themselves in the band structure via terms proportional to odd powers in k (Table V). Therefore, we associate antimagnetopolarizations with such terms k^{2n+1}. While odd-ℓ electropolarizations and odd-ℓ magnetopolarizations permit a simple correspondence between the rank ℓ and a minimal-degree polynomial representation of the associated tensors (Table V), no such correspondence exists for even-ℓ antimagnetopolarizations.

For example, in a diamond crystal structure, a magnetic quadrupole density ($\ell = 2$) gives rise to a term $k_z(k_x^2 - k_y^2)$ [18,106]. Under $R_{i\times\theta}$, this term transforms like the component $T^{--}_{3,-2} + T^{--}_{3,2}$ of a magnetotoroidal octupole density ($\ell = 3$). This term arises as a product (4) of a nontrivial magnetic quadrupole density ($\ell = 2$) and a trivial electric hexadecapole density ($\ell = 4$) present already in pristine diamond.

A complete review of the examples in Ref. [18] is beyond the scope of the present work. Tables XXI and XXII in Appendix D give the lowest ranks of electromagnetic multipoles and toroidal compound multipoles in crystal structures with different crystallographic point groups G.

APPENDIX D: SPHERICAL TENSORS AND MULTIPOLE ORDER PERMITTED BY THE 122 CRYSTALLOGRAPHIC MAGNETIC POINT GROUPS

This appendix provides explicit details about which spherical tensors $T^{ss'}_{\ell}$ are permitted by the 122 crystallographic magnetic point groups. The information given here is directly relevant for discussing electric, magnetic, and toroidal multipole order in crystals [see Sec. II B]. As discussed below, the information is furthermore relevant for materials and property tensors that are commonly represented by Cartesian rank-N tensors.

Table XXI is devoted to θ-even tensors T^{s+}_{ℓ}. It lists the number of independent components such tensors with rank $\ell \leq 3$ have under the nonmagnetic (type-II) groups belonging to the 11 Laue classes $L(G_{\rm p})$. For comparison, the same information is also provided for type-II groups in the three classes of continuous cyclic, dihedral, and spherical point groups. To streamline the presentation, the universally allowed electric monopolarization T^{++}_0 has been omitted. Basic physical properties can be read off from this table. For example, groups allowing T^{-+}_0 represent electrochiral systems (see Sec. III A 2), and groups allowing T^{-+}_1 represent pyroelectric and ferroelectric systems [13].

Table XXI, together with Table XVIII, can be used to infer the properties of tensors T^{s+}_{ℓ} in all 122 magnetic point groups. Specifically, Table XXI gives the properties of tensors for the crystallographic point groups $G^{\theta}_0 \times C_{\theta}$ that appear in Table XVIII in the last row of the main block [188] for a class $L(G_{\rm p})$. The structure of tensors T^{s+}_{ℓ} allowed under $G^{\theta}_0 \times C_{\theta}$ is repeated for all members of the subclass $L(G^{\theta}_0, \theta) \subset L(G_{\rm p})$, which are the groups positioned in the column headed by G^{θ}_0 within the same class's main block. The formal basis for these congruences is elaborated in detail in Appendix E.

Table XXI also tabulates the lowest even ("g") and odd ("u") orders ℓ of electric ("e") and electrotoroidal ("et") multipole densities permitted in each crystal class. The electric monopolarization T^{++}_0 is trivially allowed under all point groups and, therefore, is not considered for determining $\ell^{(\rm e,g)}_{\rm min}$. Instead, to convey information that is specific to each group, we tabulate the lowest *nonzero* even order of parapolarizations allowed under each group.

Table XXII pertains to θ-odd tensors T^{s-}_{ℓ}. It lists the number of independent components for such tensors with rank $\ell \leq 3$ under the type-III magnetic point groups (58 crystallographic, 7 continuous). According to the classification introduced in Appendix A 3, these comprise the groups of type i-III, ii-III, iii'-III, iii-III', JJJ, JJJ', JJJ", JJ, and JJ'. In the other types, θ-odd tensors are either equivalent to the θ-even ones listed in Table XXI (types J, ii-I, and iii-I), or they are forbidden by symmetry (types i-II, ii-II, and iii-II). More generally, the entries in Table XXII

TABLE XXI. Number of independent components of θ-even spherical tensors T_ℓ^{s+} permitted by type-II magnetic point groups (considering ranks $\ell \leq 3$). Tensors T_ℓ^{++} represent parapolarizations, and T_ℓ^{-+} are electropolarizations. A "0" indicates that the tensor is forbidden by symmetry. The electric monopolarization T_0^{++} has been omitted, as it is trivially always allowed. The quantities $\ell_{\rm min}^{(\rm e/et,g/u)}$ indicate, respectively, for each group, the lowest symmetry-allowed even ("g") and odd ("u") orders ℓ of electric ("e") and electrotoroidal ("et") multipole densities $\ell > 0$, i.e., again ignoring the electric and electrotoroidal monopolarizations T_0^{++} and T_0^{-+}. Both the Schönflies and Hermann-Mauguin notations [194] are given for each group, as well as the group's type according to the classification in Table IX.

				Parapolar					Electropolar					
Crystal system	Schönflies	Hermann-Mauguin	Type	$\ell_{\rm min}^{(e,g)}$	$\ell_{\rm min}^{(et,u)}$	T_1^{++}	T_2^{++}	T_3^{++}	$\ell_{\rm min}^{(et,g)}$	$\ell_{\rm min}^{(e,u)}$	T_0^{-+}	T_1^{-+}	T_2^{-+}	T_3^{-+}
Triclinic	$C_1 \times C_\theta = C_1 \times C_\theta$	$1'$	i-II	2	1	3	5	7	2	1	1	3	5	7
	$C_1 \times C_{i\times\theta} = C_i \times C_\theta$	$\bar{1}1'$	ii-II	2	1	3	5	7	∞	∞	0	0	0	0
Monoclinic	$C_2 \times C_\theta = C_2 \times C_\theta$	$21'$	i-II	2	1	1	3	3	2	1	1	1	3	3
	$C_2[C_1] \times C_\theta = C_s \times C_\theta$	$m1'$	iii-II	2	1	1	3	3	2	1	0	2	2	4
	$C_2 \times C_{i\times\theta} = C_{2h} \times C_\theta$	$2/m1'$	ii-II	2	1	1	3	3	∞	∞	0	0	0	0
Orthorhombic	$D_2 \times C_\theta = D_2 \times C_\theta$	$2221'$	i-II	2	3	0	2	1	2	3	1	0	2	1
	$D_2[C_2] \times C_\theta = C_{2v} \times C_\theta$	$mm21'$	iii-II	2	3	0	2	1	2	1	0	1	1	2
	$D_2 \times C_{i\times\theta} = D_{2h} \times C_\theta$	$mmm1'$	ii-II	2	3	0	2	1	∞	∞	0	0	0	0
Tetragonal	$C_4 \times C_\theta = C_4 \times C_\theta$	$41'$	i-II	2	1	1	1	1	2	1	1	1	1	1
	$C_4[C_2] \times C_\theta = S_4 \times C_\theta$	$\bar{4}1'$	iii-II	2	1	1	1	1	2	3	0	0	2	2
	$C_4 \times C_{i\times\theta} = C_{4h} \times C_\theta$	$4/m1'$	ii-II	2	1	1	1	1	∞	∞	0	0	0	0
	$D_4 \times C_\theta = D_4 \times C_\theta$	$4221'$	i-II	2	5	0	1	0	2	5	1	0	1	0
	$D_4[C_4] \times C_\theta = C_{4v} \times C_\theta$	$4mm1'$	iii-II	2	5	0	1	0	4	1	0	1	0	1
	$D_4[D_2] \times C_\theta = D_{2d} \times C_\theta$	$\bar{4}2m1'$	iii-II	2	5	0	1	0	2	3	0	0	1	1
	$D_4 \times C_{i\times\theta} = D_{4h} \times C_\theta$	$4/mmm1'$	ii-II	2	5	0	1	0	∞	∞	0	0	0	0
Trigonal	$C_3 \times C_\theta = C_3 \times C_\theta$	$31'$	i-II	2	1	1	1	3	2	1	1	1	1	3
	$C_3 \times C_{i\times\theta} = C_{3i} \times C_\theta$	$\bar{3}1'$	ii-II	2	1	1	1	3	∞	∞	0	0	0	0
	$D_3 \times C_\theta = D_3 \times C_\theta$	$321'$	i-II	2	3	0	1	1	2	3	1	0	1	1
	$D_3[C_3] \times C_\theta = C_{3v} \times C_\theta$	$3m1'$	iii-II	2	3	0	1	1	4	1	0	1	0	2
	$D_3 \times C_{i\times\theta} = D_{3d} \times C_\theta$	$\bar{3}m1'$	ii-II	2	3	0	1	1	∞	∞	0	0	0	0
Hexagonal	$C_6 \times C_\theta = C_6 \times C_\theta$	$61'$	i-II	2	1	1	1	1	2	1	1	1	1	1
	$C_6[C_3] \times C_\theta = C_{3h} \times C_\theta$	$\bar{6}1'$	iii-II	2	1	1	1	1	4	3	0	0	0	2
	$C_6 \times C_{i\times\theta} = C_{6h} \times C_\theta$	$6/m1'$	ii-II	2	1	1	1	1	∞	∞	0	0	0	0
	$D_6 \times C_\theta = D_6 \times C_\theta$	$6221'$	i-II	2	7	0	1	0	2	7	1	0	1	0
	$D_6[C_6] \times C_\theta = C_{6v} \times C_\theta$	$6mm1'$	iii-II	2	7	0	1	0	6	1	0	1	0	1
	$D_6[D_3] \times C_\theta = D_{3h} \times C_\theta$	$\bar{6}m21'$	iii-II	2	7	0	1	0	4	3	0	0	0	1
	$D_6 \times C_{i\times\theta} = D_{6h} \times C_\theta$	$6/mmm1'$	ii-II	2	7	0	1	0	∞	∞	0	0	0	0
Cubic	$T \times C_\theta = T \times C_\theta$	$231'$	i-II	4	3	0	0	1	4	3	1	0	0	1
	$T \times C_{i\times\theta} = T_h \times C_\theta$	$m\bar{3}1'$	ii-II	4	3	0	0	1	∞	∞	0	0	0	0
	$O \times C_\theta = O \times C_\theta$	$4321'$	i-II	4	9	0	0	0	4	9	1	0	0	0
	$O[T] \times C_\theta = T_d \times C_\theta$	$\bar{4}3m1'$	iii-II	4	9	0	0	0	6	3	0	0	0	1
	$O \times C_{i\times\theta} = O_h \times C_\theta$	$m\bar{3}m1'$	ii-II	4	9	0	0	0	∞	∞	0	0	0	0
Number of crystallographic groups allowing tensor						13	27	21			11	10	13	18
Axial	$C_\infty \times C_\theta = C_\infty \times C_\theta$	$\infty 1'$	i-II	2	1	1	1	1	2	1	1	1	1	1
	$C_\infty \times C_{i\times\theta} = C_{\infty h} \times C_\theta$	$\infty/m1'$	ii-II	2	1	1	1	1	∞	∞	0	0	0	0
	$D_\infty \times C_\theta = D_\infty \times C_\theta$	$\infty 21'$	i-II	2	∞	0	1	0	2	∞	1	0	1	0
	$D_\infty[C_\infty] \times C_\theta = C_{\infty v} \times C_\theta$	$\infty m1'$	iii-II	2	∞	0	1	0	∞	1	0	1	0	1
	$D_\infty \times C_{i\times\theta} = D_{\infty h} \times C_\theta$	$\infty/mm1'$	ii-II	2	∞	0	1	0	∞	∞	0	0	0	0
Spherical	$R \times C_\theta = R_\theta$	$\infty\infty 1'$	i-II	∞	∞	0	0	0	∞	∞	1	0	0	0
	$R \times C_{i\times\theta} = R_{i\times\theta}$	$\infty\infty m1'$	ii-II	∞	∞	0	0	0	∞	∞	0	0	0	0

TABLE XXII. Number of independent components of θ-odd spherical tensors T^{s-}_{ℓ} permitted by type-III magnetic point groups (considering ranks $\ell \leq 3$). Tensors T^{+-}_{ℓ} represent magnetopolarizations, and T^{--}_{ℓ} are antimagnetopolarizations. A "0" indicates that the corresponding tensor is forbidden by symmetry. The magnetic monopolarization T^{+-}_{0} has been omitted, as it is universally forbidden under type-III groups. The quantities $\ell^{(\mathrm{m/mt,g/u})}_{\mathrm{min}}$ indicate, respectively, for each group, the lowest symmetry-allowed even ("g") and odd ("u") orders ℓ of magnetic ("m") and magnetotoroidal ("mt") multipole densities $\ell > 0$, i.e., ignoring monopolarizations. Both the Schönflies and Hermann-Mauguin notations [194] are given for each group, as well as the group's type according to the classification in Table IX.

				Magnetopolar					Antimagnetopolar					
Crystal system	Schönflies	Hermann-Mauguin	Type	$\ell^{(mt,g)}_{\mathrm{min}}$	$\ell^{(m,u)}_{\mathrm{min}}$	T^{+-}_{1}	T^{+-}_{2}	T^{+-}_{3}	$\ell^{(m,g)}_{\mathrm{min}}$	$\ell^{(mt,u)}_{\mathrm{min}}$	T^{--}_{0}	T^{--}_{1}	T^{--}_{2}	T^{--}_{3}
Triclinic	$C_1 \times C_{i\theta} = C_i(C_1)$	$\bar{1}'$	JJ	∞	∞	0	0	0	2	1	1	3	5	7
Monoclinic	$C_2(C_1) = C_2(C_1)$	$2'$	i-III	2	1	2	2	4	2	1	0	2	2	4
	$C_2\{C_1\} = C_s(C_1)$	m'	JJJ	2	1	2	2	4	2	1	1	1	3	3
	$C_2(C_1) \times C_i = C_{2h}(C_i)$	$2'/m'$	ii-III	2	1	2	2	4	∞	∞	0	0	0	0
	$C_2 \times C_{i\theta} = C_{2h}(C_2)$	$2/m'$	JJ	∞	∞	0	0	0	2	1	1	1	3	3
	$C_2(C_1) \times C_{i\theta} = C_{2h}(C_s)$	$2'/m$	JJ'	∞	∞	0	0	0	2	1	0	2	2	4
Orthorhombic	$D_2(C_2) = D_2(C_2)$	$2'2'2$	i-III	2	1	1	1	2	2	1	0	1	1	2
	$D_2\{C_2\} = C_{2v}(C_2)$	$m'm'2$	JJJ	2	1	1	1	2	2	3	1	0	2	1
	$D_2[C_2](C'_2[C_1]) = C_{2v}(C_s)$	$2'm'm$	JJJ"	2	1	1	1	2	2	1	0	1	1	2
	$D_2(C_2) \times C_i = D_{2h}(C_{2h})$	$mm'm'$	ii-III	2	1	1	1	2	∞	∞	0	0	0	0
	$D_2 \times C_{i\theta} = D_{2h}(D_2)$	$m'm'm'$	JJ	∞	∞	0	0	0	2	3	1	0	2	1
	$D_2(C_2) \times C_{i\theta} = D_{2h}(C_{2v})$	mmm'	JJ'	∞	∞	0	0	0	2	1	0	1	1	2
Tetragonal	$C_4(C_2) = C_4(C_2)$	$4'$	i-III	2	3	0	2	2	2	3	0	0	2	2
	$C_4\{C_2\} = S_4(C_2)$	$\bar{4}'$	JJJ	2	3	0	2	2	2	1	1	1	1	1
	$C_4(C_2) \times C_i = C_{4h}(C_{2h})$	$4'/m$	ii-III	2	3	0	2	2	∞	∞	0	0	0	0
	$C_4 \times C_{i\theta} = C_{4h}(C_4)$	$4/m'$	JJ	∞	∞	0	0	0	2	1	1	1	1	1
	$C_4(C_2) \times C_{i\theta} = C_{4h}(S_4)$	$4'/m'$	JJ'	∞	∞	0	0	0	2	3	0	0	2	2
	$D_4(D_2) = D_4(D_2)$	$4'22'$	i-III	2	3	0	1	1	2	3	0	0	1	1
	$D_4(C_4) = D_4(C_4)$	$42'2'$	i-III	4	1	1	0	1	4	1	0	1	0	1
	$D_4[C_4](D_2[C_2]) = C_{4v}(C_{2v})$	$4'mm'$	iii'-III	2	3	0	1	1	2	3	0	0	1	1
	$D_4\{C_4\} = C_{4v}(C_4)$	$4m'm'$	JJJ	4	1	1	0	1	2	5	1	0	1	0
	$D_4\{D_2\} = D_{2d}(D_2)$	$\bar{4}'2m'$	JJJ	2	3	0	1	1	2	5	1	0	1	0
	$D_4[D_2](D'_2[C_2]) = D_{2d}(C_{2v})$	$\bar{4}'m2'$	JJJ'	2	3	0	1	1	4	1	0	1	0	1
	$D_4[D_2](C_4[C_2]) = D_{2d}(S_4)$	$\bar{4}2'm'$	iii-III'	4	1	1	0	1	2	3	0	0	1	1
	$D_4(D_2) \times C_i = D_{4h}(D_{2h})$	$4'/mmm'$	ii-III	2	3	0	1	1	∞	∞	0	0	0	0
	$D_4(C_4) \times C_i = D_{4h}(C_{4h})$	$4/mm'm'$	ii-III	4	1	1	0	1	∞	∞	0	0	0	0
	$D_4 \times C_{i\theta} = D_{4h}(D_4)$	$4/m'm'm'$	JJ	∞	∞	0	0	0	2	5	1	0	1	0
	$D_4(C_4) \times C_{i\theta} = D_{4h}(C_{4v})$	$4/m'mm$	JJ'	∞	∞	0	0	0	4	1	0	1	0	1
	$D_4(D_2) \times C_{i\theta} = D_{4h}(D_{2d})$	$4'/m'm'm$	JJ'	∞	∞	0	0	0	2	3	0	0	1	1

(Table continued)

TABLE XXII. *(Continued)*

				Magnetopolar					Antimagnetopolar					
Crystal system	Schönflies	Hermann-Mauguin	Type	$\ell_{\min}^{(mt,g)}$	$\ell_{\min}^{(m,u)}$	T_1^{+-}	T_2^{+-}	T_3^{+-}	$\ell_{\min}^{(m,g)}$	$\ell_{\min}^{(mt,u)}$	T_0^{--}	T_1^{--}	T_2^{--}	T_3^{--}
Trigonal	$C_3 \times C_{i\theta} = C_{3i}(C_3)$	$\bar{3}'$	JJ	∞	∞	0	0	0	2	1	1	1	1	3
	$D_3(C_3) = D_3(C_3)$	$32'$	i-III	4	1	1	0	2	4	1	0	1	0	2
	$D_3\{C_3\} = C_{3v}(C_3)$	$3m'$	JJJ	4	1	1	0	2	2	3	1	0	1	1
	$D_3(C_3) \times C_i = D_{3d}(C_{3i})$	$\bar{3}m'$	ii-III	4	1	1	0	2	∞	∞	0	0	0	0
	$D_3 \times C_{i\theta} = D_{3d}(D_3)$	$\bar{3}'m'$	JJ	∞	∞	0	0	0	2	3	1	0	1	1
	$D_3(C_3) \times C_{i\theta} = D_{3d}(C_{3v})$	$\bar{3}'m$	JJ'	∞	∞	0	0	0	4	1	0	1	0	2
Hexagonal	$C_6(C_3) = C_6(C_3)$	$6'$	i-III	4	3	0	0	2	4	3	0	0	0	2
	$C_6\{C_3\} = C_{3h}(C_3)$	$\bar{6}'$	JJJ	4	3	0	0	2	2	1	1	1	1	1
	$C_6(C_3) \times C_i = C_{6h}(C_{3i})$	$6'/m'$	ii-III	4	3	0	0	2	∞	∞	0	0	0	0
	$C_6 \times C_{i\theta} = C_{6h}(C_6)$	$6/m'$	JJ	∞	∞	0	0	0	2	1	1	1	1	1
	$C_6(C_3) \times C_{i\theta} = C_{6h}(C_{3h})$	$6'/m$	JJ'	∞	∞	0	0	0	4	3	0	0	0	2
	$D_6(D_3) = D_6(D_3)$	$6'22'$	i-III	4	3	0	0	1	4	3	0	0	0	1
	$D_6(C_6) = D_6(C_6)$	$62'2'$	i-III	6	1	1	0	1	6	1	0	1	0	1
	$D_6[C_6](D_3[C_3]) = C_{6v}(C_{3v})$	$6'mm'$	iii'-III	4	3	0	0	1	4	3	0	0	0	1
	$D_6\{C_6\} = C_{6v}(C_6)$	$6m'm'$	JJJ	6	1	1	0	1	2	7	1	0	1	0
	$D_6\{D_3\} = D_{3h}(D_3)$	$\bar{6}'2m'$	JJJ	4	3	0	0	1	2	7	1	0	1	0
	$D_6[D_3](D_3'[C_3]) = D_{3h}(C_{3v})$	$\bar{6}'m2'$	JJJ'	4	3	0	0	1	6	1	0	1	0	1
	$D_6[D_3](C_6[C_3]) = D_{3h}(C_{3h})$	$\bar{6}m'2'$	iii-III'	6	1	1	0	1	4	3	0	0	0	1
	$D_6(D_3) \times C_i = D_{6h}(D_{3d})$	$6'/m'mm'$	ii-III	4	3	0	0	1	∞	∞	0	0	0	0
	$D_6(C_6) \times C_i = D_{6h}(C_{6h})$	$6/mm'm'$	ii-III	6	1	1	0	1	∞	∞	0	0	0	0
	$D_6 \times C_{i\theta} = D_{6h}(D_6)$	$6/m'm'm'$	JJ	∞	∞	0	0	0	2	7	1	0	1	0
	$D_6(C_6) \times C_{i\theta} = D_{6h}(C_{6v})$	$6/m'mm$	JJ'	∞	∞	0	0	0	6	1	0	1	0	1
	$D_6(D_3) \times C_{i\theta} = D_{6h}(D_{3h})$	$6'/mmm'$	JJ'	∞	∞	0	0	0	4	3	0	0	0	1
Cubic	$T \times C_{i\theta} = T_h(T)$	$m'\bar{3}'$	JJ	∞	∞	0	0	0	4	3	1	0	0	1
	$O(T) = O(T)$	$4'32'$	i-III	6	3	0	0	1	6	3	0	0	0	1
	$O\{T\} = T_d(T)$	$\bar{4}'3m'$	JJJ	6	3	0	0	1	4	9	1	0	0	0
	$O(T) \times C_i = O_h(T_h)$	$m\bar{3}m'$	ii-III	6	3	0	0	1	∞	∞	0	0	0	0
	$O \times C_{i\theta} = O_h(O)$	$m'\bar{3}'m'$	JJ	∞	∞	0	0	0	4	9	1	0	0	0
	$O(T) \times C_{i\theta} = O_h(T_d)$	$m'\bar{3}'m$	JJ'	∞	∞	0	0	0	6	3	0	0	0	1
Number of crystallographic groups allowing tensor						18	15	37			21	21	29	40
Axial	$C_\infty \times C_{i\theta} = C_{\infty h}(C_\infty)$	∞/m'	JJ	∞	∞	0	0	0	2	1	1	1	1	1
	$D_\infty(C_\infty) = C_\infty(C_\infty)$	$\infty 2'$	i-III	∞	1	1	0	1	∞	1	0	1	0	1
	$D_\infty(C_\infty) = C_{\infty v}(C_\infty)$	$\infty m'$	JJJ	∞	1	1	0	1	2	∞	1	0	1	0
	$D_\infty(C_\infty) \times C_i = C_{\infty h}(C_{\infty h})$	∞/mm'	ii-III	∞	1	1	0	1	∞	∞	0	0	0	0
	$D_\infty(C_{i\theta}) = D_{\infty h}(D_\infty)$	$\infty/m'm'$	JJ	∞	∞	0	0	0	2	∞	1	0	1	0
	$D_\infty(C_\infty) \times C_{i\theta} = D_{\infty h}(C_{\infty v})$	$\infty/m'm$	JJ'	∞	∞	0	0	0	∞	1	0	1	0	1
Spherical	$R \times C_{i\theta} = R_{i\theta}$	$\infty\infty m'$	JJ	∞	∞	0	0	0	∞	∞	1	0	0	0

are related to those given in Table XXI as per the relationships illustrated by small 2×2 matrices in Tables XII, XV, and XVIII, and further elucidated in Appendix E. As the magnetotoroidal monopolarization T_0^{+-} is forbidden by symmetry under all type-III groups, it has been omitted to simplify the presentation. Table XXII also lists the lowest even- and odd-ℓ magnetic and magnetotoroidal multipole densities with $\ell > 0$ permitted under a given type-III magnetic point group.

A variety of magnetism-related physical properties can be inferred from Table XXII. For example, ferromagnetism occurs for groups allowing the tensor T_1^{+-} [20,21]. In groups where T_1^{+-} is forbidden, the presence of T_ℓ^{+-} with odd $\ell \geq 3$ signals altermagnetism [18,82]. Axion electrodynamics can be associated with a finite T_0^{--} [195].

APPENDIX E: RATIONALIZING SYMMETRY-ALLOWED TENSOR COMPONENTS FOR MAGNETIC POINT GROUPS

This appendix discusses commonalities regarding the shape of tensors describing systems belonging to the same Laue class $L(G_p)$. Combining rotations in a proper point group G_p with space inversion i and time inversion θ yields the magnetic point groups of class $L(G_p)$. The relations between symmetry transformations for these groups manifest in commonalities regarding the form of symmetry-allowed tensors. Similarities in the form of crystal-property matrices are apparent from their tabulations (see, e.g., Refs. [13,59,96] and Appendix D above), and they also underpin the observation of Opechowski's magic relations [58].

We visualize the commonalities between tensor configurations for groups within a class via small 2×2 matrices such as $\left(\begin{smallmatrix}\circ & \star \\ \diamond & \diamond\end{smallmatrix}\right)$ shown in Tables IX, X, XII, XV, and XVIII. Symbols in these matrices mark congruences between tensors with signature $++$ (upper left), $+-$ (upper right), $-+$ (lower left), and $--$ (lower right) for a given group and between different groups within a given class. Filled symbols indicate that a rank-1 tensor is allowed (compare Tables XXI and XXII); i.e., filled symbols reflect the fact that a group possesses a polar direction as discussed in Sec. II F. A missing symbol indicates that tensors with the respective signature are forbidden for any ℓ. For example, the matrix $\left(\begin{smallmatrix}\circ & \star \\ \diamond & \diamond\end{smallmatrix}\right)$ listed in Table XVIII for the group $D_{2d}(S_4) = D_4[D_2](C_4[C_2])$ [class $L(D_4)$] indicates that this group allows tensors $T_\ell^{ss'}$ for all four signatures ss'. In particular, this group allows rank-1 tensors with signature $+-$, and rank-ℓ tensors with signature $-+$ have the same structure as rank-ℓ tensors with signature $--$ (for $\ell \geq \ell_{\min}$ as listed in Tables XXI and XXII). Finally, repeated appearances of the symbol $\circ$ in the matrices listed for other groups in class $L(D_4)$ indicate that the respective tensors $T_\ell^{ss'}$ allowed for these groups have the same structure as the tensors T_ℓ^{++} allowed for the group $D_{2d}(S_4)$ [and similarly for the other symbols in $\left(\begin{smallmatrix}\circ & \star \\ \diamond & \diamond\end{smallmatrix}\right)$]. These congruences of tensor configurations for groups within a given class $L(G_p)$ imply that knowing the structure of rank-ℓ tensors for nonmagnetic groups of type J and iii-I (as discussed, e.g., by Nye [13]) is sufficient to infer the structure of rank-ℓ tensors for all groups in $L(G_p)$.

In the following, we use the concepts of duality (A7) and triadic relationships (A10) between magnetic point groups to formally derive, for each signature ss', the congruences of tensors $T_\ell^{ss'}$ among the groups in a given class $L(G_p)$. In particular, we show how it is possible to relate the structure of tensors T_ℓ^{s-} allowed for magnetic groups in $L(G_p)$ to the structure of the tensors T_ℓ^{s+} allowed for nonmagnetic groups in $L(G_p)$. While our discussion focuses on spherical tensors $T_\ell^{ss'}$ [67,68] that are relevant, e.g., for describing multipole order in solids (see discussion in Sec. II), the congruences also apply to Cartesian tensors representing materials properties [13,14,56–61] (see Appendix D).

1. Tensors T_ℓ^{++}: Parapolarizations

Parapolarizations, having signature $++$, are agnostic with respect to both SIS and TIS; hence, their structure is determined by symmetry under proper rotations only. Tensors T_ℓ^{++} thus have the same structure for all groups in a given class $L(G_p)$, and this structure depends only on the symmetries present in the class root G_p.

2. Tensors T_ℓ^{-+}: Electropolarizations

Tensors that are odd under SIS and even under TIS are unaffected by whether TIS may be broken. Tensors T_ℓ^{-+} thus have the same structure for all groups in a subclass $L(G_0^\theta, \theta) \subset L(G_p)$, coinciding with the structure of T_ℓ^{-+} for the subclass root G_0^θ. For the groups in the subclass $L(G_p, \theta)$, the structure of tensors T_ℓ^{-+} is the same as the structure of tensors T_ℓ^{++} because these tensors have the same structure for the subclass root G_p.

In contrast, the structure of tensors T_ℓ^{-+} for the groups in $L(G_p[\tilde{G}_p], \theta)$ is, in general, different from the structure of the tensors T_ℓ^{++}. No tensors of the form T_ℓ^{-+} are allowed for any groups in a subclass $L(G_p \times C_i, \theta)$. Table X illustrates the congruence of tensors T_ℓ^{-+} between groups in a given subclass $L(G_0^\theta, \theta)$ (corresponding to columns in the upper part of the table).

3. Tensors T_ℓ^{+-}: Magnetopolarizations

Tensors with signature $+-$ are unaffected by whether SIS may be broken. For all groups in a subclass $L(G_0^i, i) \subset L(G_p)$ (corresponding to rows in the upper part of Table X), tensors T_ℓ^{+-} thus have the same

structure, coinciding with the structure of T_ℓ^{+-} for the subclass root G_0^i. In particular, for the groups in $L(G_\mathrm{p}, i)$, tensors T_ℓ^{+-} have the same structure as tensors T_ℓ^{++}, while tensors of the form T_ℓ^{+-} are forbidden by symmetry for all groups in $L(G_\mathrm{p} \times C_\theta, i)$.

For the groups in $L(G_\mathrm{p}(\tilde{G}_\mathrm{p}), i)$, the structure of tensors T_ℓ^{+-} is, in general, different from that of the tensors T_ℓ^{++}. However, by virtue of the SIS-TIS duality relation under exchange $i \leftrightarrow \theta$, the structure of magnetopolarizations T_ℓ^{+-} permitted by the groups in $L(G_\mathrm{p}(\tilde{G}_\mathrm{p}), i)$ coincides with the structure of electropolarizations T_ℓ^{-+} permitted by the groups in $L(G_\mathrm{p}[\tilde{G}_\mathrm{p}], \theta)$.

4. Tensors T_ℓ^{--}: Antimagnetopolarizations

While tensors T_ℓ^{--} are odd under i and θ applied individually, these tensors are even under the combination $i\theta$. For all groups in a Laue subclass $L(G_0^{i\theta}, i\theta) \subset L(G_\mathrm{p})$, tensors T_ℓ^{--} thus have the same structure, coinciding with the structure of T_ℓ^{--} for the subclass root $G_0^{i\theta}$. For the groups in $L(G_\mathrm{p}, i\theta)$, the structure of tensors T_ℓ^{--} is the same as the structure of tensors T_ℓ^{++}, and such tensors are forbidden for all groups in $L(G_\mathrm{p} \times C_\theta, i\theta) \equiv L(G_\mathrm{p} \times C_i, i\theta)$.

For the groups in $L(G_\mathrm{p}(\tilde{G}_\mathrm{p}), i\theta) \equiv L(G_\mathrm{p}[\tilde{G}_\mathrm{p}], i\theta)$, the structure of tensors T_ℓ^{--} is, in general, different from the structure of the tensors T_ℓ^{++}. However, for the type-i-III group $G_\mathrm{p}(\tilde{G}_\mathrm{p})$, tensors T_ℓ^{+-} and T_ℓ^{--} have the same structure. This group is in the subclass $L(G_\mathrm{p}(\tilde{G}_\mathrm{p}), i\theta)$. We thus find that for the groups in $L(G_\mathrm{p}(\tilde{G}_\mathrm{p}), i\theta)$, the structure of tensors T_ℓ^{--} is the same as the structure of tensors T_ℓ^{+-} for the groups in $L(G_\mathrm{p}(\tilde{G}_\mathrm{p}), i)$ and the structure of tensors T_ℓ^{-+} for the groups in $L(G_\mathrm{p}[\tilde{G}_\mathrm{p}], \theta)$. See the bottom part of Table X for the composition of subclasses $L(G_0^{i\theta}, i\theta)$.

5. Inferences facilitated by triadic relationships

By itself, the concept of SIS-TIS duality is insufficient to infer congruences of tensors T_ℓ^{--} for different groups in a class $L(G_\mathrm{p})$, as the signature $--$ is mapped onto itself under the duality transformation $i \leftrightarrow \theta$. Nevertheless, in the preceding subsection, we leveraged the identical properties of T_ℓ^{+-} and T_ℓ^{--} tensors under type-i-III groups to predict the form of the tensors for all groups in the subclass $L(G_\mathrm{p}(\tilde{G}_\mathrm{p}), i\theta)$. Here, we utilize the notion of triadic relationships discussed in Appendix A 4 to reveal further close links between the properties of tensors T_ℓ^{--} and tensors with mixed signatures $+-$ and $-+$.

A triad of magnetic point groups consists of a dual pair $G_\theta \leftrightarrow G_i$ augmented by a self-dual group $G_{i\theta}$. The diagram (A10) illustrates our notation, and Table IX displays the general form of magnetic point groups forming a triad. For triadic partners, the structure of tensors with signature $-+$, $+-$, and $--$ is permuted. As a simple nontrivial example, consider the triad formed by groups of type JJ', iii-II, and ii-III within a class, according to their general forms given in Table IX. Here, the form of tensors T_ℓ^{--} permitted by the type-JJ' member $G_{i\theta}$ of this triad mirrors the form of the tensors T_ℓ^{+-} allowed under the group G_i of type ii-III, and the tensors T_ℓ^{-+} associated with G_i's dual partner G_θ of type iii-II. Thus, the triads embody a close interrelation of tensors with signatures $-+$, $+-$, and $--$ for magnetic point groups within a given class.

APPENDIX F: CHIRAL MATERIALS CANDIDATES

This appendix tabulates examples of materials candidates realizing the categories of chirality introduced in Sec. III A.

1. Electrochiral materials

The physical property of electropolar electrochiral materials that is currently attracting the most interest is the expected radial spin texture $\boldsymbol{\sigma} \cdot \mathbf{k}$ [163] and the associated phenomenon of a current-induced magnetization [156,196]. Typical illustrations of the chirality-dependent spin texture look like Fig. 7(d). The crucial importance of crystallographic symmetries for shaping spin textures arising from electrochirality has only recently been recognized [164,197]. Insights from Ref. [164] and our more detailed discussion above are useful for interpreting and guiding precision measurements such as those performed recently for the paradigmatic chiral metal Te [198,199]. More electropolar electrochiral materials candidates are shown in Table XXIII. Selected examples for symmetry-appropriate spin textures are shown in Figs. 7 and 9. See also Ref. [164].

As opposed to the nonmagnetic electropolar electrochiral materials, multipolar electrochiral materials show either ferromagnetism or antiferromagnetism. The topological properties of the chiral antiferromagnets have been discussed in Refs. [202,203]. Materials candidates for this type are also listed in Table XXIII.

2. Magnetochiral materials

The presence of a magnetotoroidal scalar T_0^{+-} is a sufficient condition for magnetochirality. Some physical consequences of having T_0^{+-} are discussed in

TABLE XXIII. Materials candidates for the electrochiral category of chirality. Examples for electropolar electrochiral materials are taken from Ref. [163]. For the multipolar electrochiral category, candidate materials were extracted from the Bilbao magnetic-materials database [200,201]. Some of the latter have been shown previously in Table I of Ref. [202]. The electrochiral magnetic-point-group types exhibit true chirality according to the conventional classification [45].

Crystal system	Electropolar electrochiral		Multipolar electrochiral	
Cubic	Mg_3Ru_2	$O \times C_\theta$	$BaCuTe_2O_6$	$O(T)$
	β-RhSi	$T \times C_\theta$		
Hexagonal	Hf_5Ir_3	$D_6 \times C_\theta$	$EuIn_2As_2$	$D_6(C_6)$
			⋯	$D_6(D_3)$
	α-In_2Se_3	$C_6 \times C_\theta$	$YMnO_3$	$C_6(C_3)$
Trigonal	$SrIr_2P_2$	$D_3 \times C_\theta$	$BaCu_3V_2O_8(OD)_2$	$D_3(C_3)$
	$LaBSiO_5$	$C_3 \times C_\theta$		
Tetragonal	$MgAs_4$	$D_4 \times C_\theta$	$CeMn_2Ge_2$	$D_4(C_4)$
			$Er_2Ge_2O_7$	$D_4(D_2)$
	$Sr_2As_2O_7$	$C_4 \times C_\theta$	⋯	$C_4(C_2)$
Orthorhombic	α-Ag_2Se	$D_2 \times C_\theta$	$Ca_2CoSi_2O_7$	$D_2(C_2)$

Ref. [144], focusing on the effect of terms coupling T_0^{+-} to scalar products of dipoles transforming like T_0^{+-} (i.e., $T_1^{ss'} \cdot T_1^{s(-s')}$).

A more explicit electronic-structure implication of magnetochirality is altermagnetism in materials candidates where ferromagnetism is forbidden ("inadmissible" magnetochiral antiferromagnets). Candidates for magnetochiral materials (both magnetopolar and multipolar types) are listed in Table XXIV. A recently investigated magnetochiral materials example is Co_2SiO_4 [159].

3. Antimagnetochiral materials

Prominently discussed materials examples for this category are antimagnetopolar $LiMnPO_4$ [39] and multipolar $LuFeO_3$ [204]. Interest in these compounds has been fueled by their realization of a monopolization T_0^{--} whose value has been estimated using computational-chemistry approaches [39,204]. The main physical implication is the isotropic linear magnetoelectric response ("axion electrodynamics" [195,205]). Candidates for antimagnetochiral materials (both

TABLE XXIV. Materials candidates for the magnetochiral category of chirality. All materials examples have been extracted from the Bilbao magnetic-materials database [200,201]. See also Ref. [144] (especially Table I in that work) for a related discussion. The category of magnetochirality introduced in our work subsumes point-group types that have previously been considered as achiral [45]. They are also different from preexisting notions of magnetic chirality [141].

Crystal system	Magnetopolar magnetochiral		Multipolar magnetochiral	
Cubic	⋯	$O_h = O \times C_i$	⋯	$T_d = O[T]$
	NiS_2	$T_h = T \times C_i$		
Hexagonal	⋯	$D_{6h} = D_6 \times C_i$	$HoMnO_3$	$C_{6v} = D_6[C_6]$
			$Ba_3CoSb_2O_9$	$D_{3h} = D_6[D_3]$
	FeF_3	$C_{6h} = C_6 \times C_i$	⋯	$C_{3h} = C_6[C_3]$
Trigonal	α-Fe_2O_3	$D_{3d} = D_3 \times C_i$	$PbNiO_3$	$C_{3v} = D_3[C_3]$
	$CaFe_3Ti_4O_{12}$	$C_{3i} = C_3 \times C_i$		
Tetragonal	$CdYb_2S_4$	$D_{4h} = D_4 \times C_i$	⋯	$C_{4v} = D_4[C_4]$
			$Ba_2MnSi_2O_7$	$D_{2d} = D_4[D_2]$
	MnV_2O_4	$C_{4h} = C_4 \times C_i$	⋯	$S_4 = C_4[C_2]$
Orthorhombic	Co_2SiO_4	$D_{2h} = D_2 \times C_i$	$HoCrWO_6$	$C_{2v} = D_2[C_2]$

TABLE XXV. Materials candidates for the antimagnetochiral categories of chirality. All examples have been extracted from the Bilbao magnetic-materials database [200,201]. The antimagnetochiral magnetic-point-group types coincide with those considered to be falsely chiral according to prior convention [45].

Crystal system	Antimagnetopolar antimagnetochiral		Multipolar antimagnetochiral	
Cubic	⋯	$O_h(O) = O \times C_{i\theta}$	⋯	$T_d(T) = O\{T\}$
	⋯	$T_h(T) = T \times C_{i\theta}$		
Hexagonal	⋯	$D_{6h}(D_6) = D_6 \times C_{i\theta}$	$LuFeO_3$	$C_{6v}(C_6) = D_6\{C_6\}$
			TmAgGe	$D_{3h}(D_3) = D_6\{D_3\}$
	$PbMn_2Ni_6Te_3O_{18}$	$C_{6h}(C_6) = C_6 \times C_{i\theta}$	$Cu_{0.82}Mn_{1.18}As$	$C_{3h}(C_3) = C_6\{C_3\}$
Trigonal	Cr_2O_3	$D_{3d}(D_3) = D_3 \times C_{i\theta}$	$CaBaCo_2Fe_2O_7$	$C_{3v}(C_3) = D_3\{C_3\}$
	$MnTiO_3$	$C_{3i}(C_3) = C_3 \times C_{i\theta}$		
Tetragonal	GdB_4	$D_{4h}(D_4) = D_4 \times C_{i\theta}$	$CeCoGe_3$	$C_{4v}(C_4) = D_4\{C_4\}$
			Pb_2MnO_4	$D_{2d}(D_2) = D_4\{D_2\}$
	$TlFe_{1.6}Se_2$	$C_{4h}(C_4) = C_4 \times C_{i\theta}$	$CsCoF_4$	$S_4(C_2) = C_4\{C_2\}$
Orthorhombic	$LiMnPO_4$	$D_{2h}(D_2) = D_2 \times C_{i\theta}$	$SrMnSb_2$	$C_{2v}(C_2) = D_2\{C_2\}$

TABLE XXVI. Materials candidates for the multichiral category of chirality. These candidates were extracted from the Bilbao magnetic-materials database [200,201], and some of them have been shown previously in Table I of Ref. [202]. The multichiral magnetic-point-group types exhibit true chirality according to the conventional classification [45].

Crystal system	Multipolar multichiral	
Cubic	$SrCuTe_2O_6$	O
	Mn_3CoGe	T
Hexagonal	⋯	D_6
	$BaCoSiO_4$	C_6
Trigonal	$La_{0.33}Sr_{0.67}FeO_3$	D_3
	Cu_2OSeO_3	C_3
Tetragonal	$Ho_2Ge_2O_7$	D_4
	Ce_5TeO_8	C_4
Orthorhombic	$FePO_4$	D_2

antimagnetopolar and multipolar types) are listed in Table XXV.

4. Multichiral materials

Candidates for multichiral materials are listed in Table XXVI. These are necessarily multipolar (see Table IX). The existence of four enantiomorphs is a distinctive property of such materials. A recently investigated multichiral materials example is $BaCoSiO_4$ [148].

[1] M. Fiebig, T. Lottermoser, D. Meier, and M. Trassin, *The evolution of multiferroics*, Nat. Rev. Mater. **1**, 16046 (2016).

[2] G. Aeppli, A. V. Balatsky, H. M. Rønnow, and N. A. Spaldin, *Hidden, entangled and resonating order*, Nat. Rev. Mater. **5**, 477 (2020).

[3] L. Šmejkal, J. Sinova, and T. Jungwirth, *Beyond conventional ferromagnetism and antiferromagnetism: A phase with nonrelativistic spin and crystal rotation symmetry*, Phys. Rev. X **12**, 031042 (2022).

[4] L. Šmejkal, J. Sinova, and T. Jungwirth, *Emerging research landscape of altermagnetism*, Phys. Rev. X **12**, 040501 (2022).

[5] R. M. Fernandes, V. S. de Carvalho, T. Birol, and R. G. Pereira, *Topological transition from nodal to nodeless Zeeman splitting in altermagnets*, Phys. Rev. B **109**, 024404 (2024).

[6] Q. Yang, Y. Li, C. Felser, and B. Yan, *Chirality-induced spin selectivity and current-driven spin and orbital polarization in chiral crystals*, Newton **1**, 100015 (2025).

[7] D. M. Juraschek *et al.*, *Chiral phonons*, Nat. Phys. **21**, 1532 (2025).

[8] S. Willenbrock, *Symmetries of the standard model*, in *Proceedings of the Theoretical Advanced Study Institute in Elementary Particle Physics*, edited by J. Terning, C. E. M. Wagner, and D. Zeppenfeld (World Scientific, Singapore, 2006), pp. 3–38.

[9] N. W. Ashcroft and N. D. Mermin, *Solid State Physics* (Holt, Rinehart, Winston, Philadelphia, 1976).

[10] C. J. Bradley and A. P. Cracknell, *The Mathematical Theory of Symmetry in Solids* (Clarendon, Oxford, 1972).

[11] W. Ludwig and C. Falter, *Symmetries in Physics*, 2nd ed. (Springer, Berlin, 1996).

[12] W. Voigt, *Lehrbuch der Kristallphysik* (B. G. Teubner, Leipzig, 1910).

[13] J. F. Nye, *Physical Properties of Crystals* (Oxford University Press, Oxford, 1985).

[14] G. L. Bir and G. E. Pikus, *Symmetry and Strain-Induced Effects in Semiconductors* (Wiley, New York, 1974).

[15] H. Weyl, *Symmetry* (Princeton University Press, Princeton, NJ, 1952).

[16] G. F. Koster, J. O. Dimmock, R. G. Wheeler, and H. Statz, *Properties of the Thirty-Two Point Groups* (MIT, Cambridge, MA, 1963).

[17] For TIS to be a black-white symmetry requires $\theta^2 = e$, whereas $\theta^2 = -1$ for half-integer spin states [11]. The case $\theta^2 = e$ is relevant for a range of important quantities and phenomena. The present work focuses on macroscopically observable quantities such as electric and magnetic multipoles that must transform according to the integer IRs of the full rotation group $R_{i\times\theta}$ for which $i^2 = \theta^2 = e$. Moreover, we are interested in electronic band structures as in Fig. 2. Double-group IRs where $\theta^2 = -e$ are relevant when analyzing eigenstates like Bloch functions in a spinful theory. However, the operator of spin angular momentum $\boldsymbol{\sigma}$ by itself transforms like a vector ($\ell = 1$) [see Eq. (5c)]. Therefore, single-group IRs are sufficient when the relevant effective Hamiltonians for a spinful band theory are derived, e.g., via the theory of invariants [14]. Hence, for the range of quantities that are of interest here, the group theory of the symmetries i and θ is the same.

[18] R. Winkler and U. Zülicke, *Theory of electric, magnetic, and toroidal polarizations in crystalline solids with applications to hexagonal lonsdaleite and cubic diamond*, Phys. Rev. B **107**, 155201 (2023).

[19] B. A. Tavger and V. M. Zaitsev, *Magnetic symmetry of crystals*, Sov. Phys. JETP **3**, 430 (1956).

[20] B. A. Tavger, *The symmetry of ferromagnetics and antiferromagnetics*, Sov. Phys. Crystallogr. **3**, 341 (1958).

[21] Y. Le Corre, *Les groupes cristallographiques magnétiques et leurs propriétés*, J. Phys. Radium **19**, 750 (1958).

[22] Y. Kuramoto, *Electronic higher multipoles in solids*, Prog. Theor. Phys. Suppl. **176**, 77 (2008).

[23] M.-T. Suzuki, T. Koretsune, M. Ochi, and R. Arita, *Cluster multipole theory for anomalous Hall effect in antiferromagnets*, Phys. Rev. B **95**, 094406 (2017).

[24] H. Watanabe and Y. Yanase, *Group-theoretical classification of multipole order: Emergent responses and candidate materials*, Phys. Rev. B **98**, 245129 (2018).

[25] M. Yatsushiro, H. Kusunose, and S. Hayami, *Multipole classification in 122 magnetic point groups for unified understanding of multiferroic responses and transport phenomena*, Phys. Rev. B **104**, 054412 (2021).

[26] H. Kusunose, R. Oiwa, and S. Hayami, *Symmetry-adapted modeling for molecules and crystals*, Phys. Rev. B **107**, 195118 (2023).

[27] V. M. Dubovik, L. A. Tosunyan, and V. V. Tugushev, *Axial toroidal moments in electrodynamics and solid-state physics*, Sov. Phys. JETP **63**, 344 (1986).

[28] J. Hlinka, J. Privratska, P. Ondrejkovic, and V. Janovec, *Symmetry guide to ferroaxial transitions*, Phys. Rev. Lett. **116**, 177602 (2016).

[29] A. A. Gorbatsevich and Y. V. Kopaev, *Toroidal order in crystals*, Ferroelectrics **161**, 321 (1994).

[30] I. Fernandez-Corbaton, S. Nanz, and C. Rockstuhl, *On the dynamic toroidal multipoles from localized electric current distributions*, Sci. Rep. **7**, 7527 (2017).

[31] R. M. Martin, *Comment on calculations of electric polarization in crystals*, Phys. Rev. B **9**, 1998 (1974).

[32] R. D. King-Smith and D. Vanderbilt, *Theory of polarization of crystalline solids*, Phys. Rev. B **47**, 1651 (1993).

[33] R. Resta, *Macroscopic polarization in crystalline dielectrics: The geometric phase approach*, Rev. Mod. Phys. **66**, 899 (1994).

[34] R. Resta, *Electrical polarization and orbital magnetization: The modern theories*, J. Phys. Condens. Matter **22**, 123201 (2010).

[35] L. L. Hirst, *The microscopic magnetization: Concept and application*, Rev. Mod. Phys. **69**, 607 (1997).

[36] R. Winkler and U. Zülicke, *Gauge-invariant absolute quantification of electric and magnetic multipole densities in crystals*, arXiv:2509.17278.

[37] L. E. Reichl, *A Modern Course in Statistical Physics*, 2nd ed. (Wiley, New York, 1998).

[38] L. D. Landau and E. M. Lifshitz, *Statistical Physics, Part 1*, 3rd ed., Course of Theoretical Physics Vol. 5 (Pergamon, Oxford, 1980).

[39] N. A. Spaldin, M. Fechner, E. Bousquet, A. Balatsky, and L. Nordström, *Monopole-based formalism for the diagonal magnetoelectric response*, Phys. Rev. B **88**, 094429 (2013).

[40] M.-T. Suzuki, H. Ikeda, and P. M. Oppeneer, *First-principles theory of magnetic multipoles in condensed matter systems*, J. Phys. Soc. Jpn. **87**, 041008 (2018).

[41] T. Hitomi and Y. Yanase, *Electric octupole order in bilayer ruthenate* $Sr_3Ru_2O_7$, J. Phys. Soc. Jpn. **83**, 114704 (2014).

[42] T. Hitomi and Y. Yanase, *Electric octupole order in bilayer Rashba system*, J. Phys. Soc. Jpn. **85**, 124702 (2016).

[43] K. Mislow, *Molecular chirality, in Topics in Stereochemistry*, edited by S. E. Denmark (Wiley, New York, 1999), Vol. 22, Chap. 1, pp. 1–82.

[44] H. D. Flack, *Chiral and achiral crystal structures*, Helv. Chim. Acta **86**, 905 (2003).

[45] L. D. Barron, *Molecular Light Scattering and Optical Activity*, 2nd ed. (Cambridge University Press, Cambridge, England, 2004).

[46] G. H. Wagnière, *On Chirality and the Universal Asymmetry* (Helvetica Chimica Acta, Zürich, 2007).

[47] G. H. Fecher, J. Kübler, and C. Felser, *Chirality in the solid state: Chiral crystal structures in chiral and achiral space groups*, Materials **15**, 5812 (2022).

[48] J. Kishine, H. Kusunose, and H. M. Yamamoto, *On the definition of chirality and enantioselective fields*, Isr. J. Chem. **62**, e202200049 (2022).

[49] E. Bousquet, M. Fava, Z. Romestan, F. Gómez-Ortiz, E. E. McCabe, and A. H. Romero, *Structural chirality and related properties in periodic inorganic solids: Review and perspectives*, J. Phys. Condens. Matter **37**, 163004 (2025).

[50] C. P. Romao and D. M. Juraschek, *Chirality à la carte*, Science **387**, 361 (2025).

[51] L. D. Landau and E. M. Lifshitz, *Electrodynamics of Continuous Media*, 2nd ed. (Pergamon, Oxford, 1984).

[52] J. Brown, W. F., S. Shtrikman, and D. Treves, *Possibility of visual observation of antiferromagnetic domains*, J. Appl. Phys. **34**, 1233 (1963).

[53] H. Thomas, *Magnetische Strukturen*, Z. Angew. Phys. **18**, 404 (1965).

[54] H. Schmid, *On a magnetoelectric classification of materials*, Int. J. Magn. **4**, 337 (1973).

[55] W. Opechowski, *Magnetoelectric symmetry*, Int. J. Magn. **5**, 317 (1974).

[56] V. Kopský, *The structure of Heesch groups and its relation to material property tensors*, J. Magn. Magn. Mater. **3**, 201 (1976).

[57] V. Kopský, *A simplified calculation and tabulation of tensorial covariants for magnetic point groups belonging to the same Laue class*, Acta Crystallogr. Sect. A **35**, 95 (1979).

[58] V. Kopský, *Opechowski's magic relations*, Z. Kristallogr. **221**, 51 (2006).

[59] H. Grimmer, *General connections for the form of property tensors in the 122 Shubnikov point groups*, Acta Crystallogr. Sect. A **47**, 226 (1991).

[60] H. Grimmer, *The forms of tensors describing magnetic, and toroidal properties*, Ferroelectrics **161**, 181 (1994).

[61] D. B. Litvin, *Magnetic physical-property tensors*, Acta Crystallogr. Sect. A **50**, 406 (1994).

[62] H. Schmid, *Some symmetry aspects of ferroics and single phase multiferroics*, J. Phys. Condens. Matter **20**, 434201 (2008).

[63] M. Ikhlas, S. Dasgupta, F. Theuss, T. Higo, S. Kittaka, B. J. Ramshaw, O. Tchernyshyov, C. W. Hicks, and S. Nakatsuji, *Piezomagnetic switching of the anomalous Hall effect in an antiferromagnet at room temperature*, Nat. Phys. **18**, 1086 (2022).

[64] L. Ye, M. E. Sorensen, M. D. Bachmann, and I. R. Fisher, *Measurement of the magnetic octupole susceptibility of* PrV_2Al_{20}, Nat. Commun. **15**, 7005 (2024).

[65] L. D. Landau and E. M. Lifshitz, *Quantum Mechanics*, 3rd ed., Course of Theoretical Physics Vol. 3 (Pergamon, Oxford, 1977).

[66] G. Burns and A. M. Glazer, *Space Groups for Solid State Scientists*, 3rd ed. (Academic, Amsterdam, 2013).

[67] A. R. Edmonds, *Angular Momentum in Quantum Mechanics*, 2nd ed. (Princeton University Press, Princeton, NJ, 1960).

[68] W.-K. Tung, *Group Theory in Physics* (World Scientific, Singapore, 1985).

[69] Previous work does not offer a universally accepted notation for the four basic types of tensors. In Refs. [59,60], tensors with signatures $++$, $+-$, $-+$, and $--$ are denoted as i-tensor, s-tensor, t-tensor, and u-tensor, respectively, while Refs. [56–58] use the symbols 1_e^+, 1_m^+, 1_e^-, and 1_m^-. See also Table 4 in Ref. [62].

[70] The parity of the integer ℓ indicates, as in number theory, whether ℓ is even or odd, see, e.g., M. Hunacek, *Introduction to Number Theory* (CRC, Boca Raton, FL, 2023).

[71] J. D. Jackson, *Classical Electrodynamics*, 3rd ed. (Wiley, NewYork, 1999).

[72] R. E. Raab and O. L. de Lange, *Multipole Theory in Electromagnetism* (Clarendon, Oxford, 2005).

[73] V. M. Dubovik and V. V. Tugushev, *Toroid moments in electrodynamics and solid-state physics*, Phys. Rep. **187**, 145 (1990).

[74] S. Nanz, *Toroidal Multipole Moments in Classical Electrodynamics* (Springer, Wiesbaden, 2016).

[75] M. E. Rose, *Spherical tensors in physics*, Proc. Phys. Soc. London Sect. A **67**, 239 (1954).

[76] P. M. Morse and H. Feshbach, *Methods of Theoretical Physics*, Vol. 2 (McGraw-Hill, New York, 1953).

[77] F. E. Low, *Classical Field Theory* (Wiley, New York, 1997).

[78] V. M. Dubovik and A. A. Cheshkov, *Multipole expansion in classical and quantum field theory and radiation*, Sov. J. Part. Nucl. **5**, 791 (1974).

[79] If G contains none of the transformations i, θ, or $i\theta$ as individual elements, then $\tilde{G} = G$ and $C_\zeta \equiv C_1$. If G contains all three of these transformations as elements, then $C_\zeta \equiv C_{i\times\theta}$. The only remaining possibility is that G contains exactly one inversion symmetry γ as an individual group element, in which case $C_\zeta \equiv C_\gamma$.

[80] A. B. Hellenes, T. Jungwirth, R. Jaeschke-Ubiergo, A. Chakraborty, J. Sinova, and L. Šmejkal, *P-wave magnets*, arXiv:2309.01607.

[81] Y. Yu, M. B. Lyngby, T. Shishidou, M. Roig, A. Kreisel, M. Weinert, B. M. Andersen, and D. F. Agterberg, *Odd-parity magnetism driven by antiferromagnetic exchange*, Phys. Rev. Lett. **135**, 046701 (2025).

[82] S. Bhowal and N. A. Spaldin, *Ferroically ordered magnetic octupoles in d-wave altermagnets*, Phys. Rev. X **14**, 011019 (2024).

[83] B. A. Tavger, *Symmetry of piezomagnetism of antiferromagnetics*, Sov. Phys. Crystallogr. **3**, 344 (1958).

[84] H. Wang and X. Qian, *Electrically and magnetically switchable nonlinear photocurrent in PT-symmetric magnetic topological quantum materials*, npj Comput. Mater. **6**, 199 (2020).

[85] H. Watanabe and Y. Yanase, *Chiral photocurrent in parity-violating magnet and enhanced response in topological antiferromagnet*, Phys. Rev. X **11**, 011001 (2021).

[86] R. Fei, W. Song, L. Pusey-Nazzaro, and L. Yang, *PT-symmetry-enabled spin circular photogalvanic effect in antiferromagnetic insulators*, Phys. Rev. Lett. **127**, 207402 (2021).

[87] B. G. Wybourne, *Classical Groups for Physicists* (Wiley, New York, 1974).

[88] M.-T. Suzuki, T. Nomoto, R. Arita, Y. Yanagi, S. Hayami, and H. Kusunose, *Multipole expansion for magnetic structures: A generation scheme for a symmetry-adapted orthonormal basis set in the crystallographic point group*, Phys. Rev. B **99**, 174407 (2019).

[89] The electrotoroidal tensor T_1^{++} is an interesting exception among all spherical tensors. It cannot be expressed as a compound tensor combining one nontrivial and one or two trivial tensors. This tensor does not arise in Table V either. In addition, the tensor component T_{10}^{++} is not an invariant tensor for any continuous dihedral group $G_{d\infty}$; it is only invariant under the continuous cyclic group $G_{c\infty} \times C_{i\times\theta}$, so it cannot be distinguished from even-ℓ electric components T_{g0}^{++} (see Appendix B 2). Therefore T_1^{++} is not considered further in this work.

[90] R. Resta and D. Vanderbilt, *Theory of polarization: A modern approach*, in *Physics of Ferroelectrics*, edited by K. M. Rabe, C. H. Ahn, and J.-M. Triscone (Springer, Berlin, 2007), pp. 31–68.
[91] D. Vanderbilt, *Berry Phases in Electronic Structure Theory* (Cambridge University Press, Cambridge, England, 2018).
[92] R. Resta, *Why are insulators insulating and metals conducting?*, J. Phys. Condens. Matter **14**, R625 (2002).
[93] S. Ono, L. Trifunovic, and H. Watanabe, *Difficulties in operator-based formulation of the bulk quadrupole moment*, Phys. Rev. B **100**, 245133 (2019).
[94] A. Daido, A. Shitade, and Y. Yanase, *Thermodynamic approach to electric quadrupole moments*, Phys. Rev. B **102**, 235149 (2020).
[95] H.-W. Streitwolf, *Group Theory in Solid-State Physics* (Macdonald, London, 1971).
[96] R. E. Newnham, *Properties of Materials* (Oxford University Press, New York, 2005).
[97] S. Picozzi, *Spin–orbit coupling in quantum materials: Emergent phenomena, their modelling and examples from two-dimensional magnets*, Riv. Nuovo Cimento **47**, 609 (2024).
[98] C. Herring, *Effect of time-reversal symmetry on energy bands of crystals*, Phys. Rev. **52**, 361 (1937).
[99] C. Herring, *Accidental degeneracy in the energy bands of crystals*, Phys. Rev. **52**, 365 (1937).
[100] S. Hayami, M. Yatsushiro, Y. Yanagi, and H. Kusunose, *Classification of atomic-scale multipoles under crystallographic point groups and application to linear response tensors*, Phys. Rev. B **98**, 165110 (2018).
[101] For conceptual clarity, the current analysis is restricted to bands without orbital degeneracies near the Γ point $k = 0$ of the Brillouin zone. All arguments can be extended to bands with orbital degeneracies and other expansion points in the Brillouin zone [14].
[102] E. I. Rashba and V. I. Sheka, *Symmetry of energy bands in crystals of wurtzite type: II. symmetry of bands including spin-orbit interaction*, Fiz. Tverd. Tela: Collected Papers **2**, 162 (1959). For an English translation, see the supplement of G. Bihlmayer, O. Rader, and R. Winkler, *Focus on the Rashba effect*, New J. Phys. **17**, 050202 (2015).
[103] G. Dresselhaus, *Spin-orbit coupling effects in zinc blende structures*, Phys. Rev. **100**, 580 (1955).
[104] Y. Yanase, *Magneto-electric effect in three-dimensional coupled zigzag chains*, J. Phys. Soc. Jpn. **83**, 014703 (2014).
[105] S. Hayami, H. Kusunose, and Y. Motome, *Toroidal order in metals without local inversion symmetry*, Phys. Rev. B **90**, 024432 (2014).
[106] R. Winkler and U. Zülicke, *Collinear orbital antiferromagnetic order and magnetoelectricity in quasi-two-dimensional itinerant-electron paramagnets, ferromagnets, and antiferromagnets*, Phys. Rev. Res. **2**, 043060 (2020).
[107] G. Yin, J.-X. Yu, Y. Liu, R. K. Lake, J. Zang, and K. L. Wang, *Planar Hall effect in antiferromagnetic MnTe thin films*, Phys. Rev. Lett. **122**, 106602 (2019).
[108] I. Dzyaloshinsky, *A thermodynamic theory of, "weak" ferromagnetism of antiferromagnetics*, J. Phys. Chem. Solids **4**, 241 (1958).
[109] Different symmetry classifications identifying point and space group symmetries permitting weak ferromagnetism have been developed by Tavger [20] and Turov [110].
[110] E. A. Turov, *Conditions for the existence of weak ferromagnetism and the classification of weakly ferromagnetic structures*, Sov. Phys.–JETP **15**, 1098 (1962).
[111] N. Nagaosa, J. Sinova, S. Onoda, A. H. MacDonald, and N. P. Ong, *Anomalous Hall effect*, Rev. Mod. Phys. **82**, 1539 (2010).
[112] H. Chen, Q. Niu, and A. H. MacDonald, *Anomalous Hall effect arising from noncollinear antiferromagnetism*, Phys. Rev. Lett. **112**, 017205 (2014).
[113] R. D. Gonzalez Betancourt, J. Zubáč, R. Gonzalez-Hernandez, K. Geishendorf, Z. Šobáň, G. Springholz, K. Olejník, L. Šmejkal, J. Sinova, T. Jungwirth, S. T. B. Goennenwein, A. Thomas, H. Reichlová, J. Železný, and D. Kriegner, *Spontaneous anomalous Hall effect arising from an unconventional compensated magnetic phase in a semiconductor*, Phys. Rev. Lett. **130**, 036702 (2023).
[114] J. Kübler and C. Felser, *Non-collinear antiferromagnets and the anomalous Hall effect*, Europhys. Lett. **108**, 67001 (2014).
[115] S. Nakatsuji, N. Kiyohara, and T. Higo, *Large anomalous Hall effect in a non-collinear antiferromagnet at room temperature*, Nature (London) **527**, 212 (2015).
[116] S. Shtrikman and H. Thomas, *Remarks on linear magnetoresistance and magneto-heat-conductivity*, Solid State Commun. **3**, 147 (1965).
[117] H. Grimmer, *General relations for transport properties in magnetically ordered crystals*, Acta Crystallogr. Sect. A **49**, 763 (1993).
[118] H. Fujii, N. Shohata, T. Okamoto, and E. Tatsumoto, *Magnetic properties of rare earth gallium compounds RGa*, J. Phys. Soc. Jpn. **31**, 1592 (1971).
[119] B. Barbara, V. N. Nguyen, and E. Siaud, *Propriétés magnétiques des composés équiatomiques terres rares-gallium*, C. R. Acad. Sci. (France) **B274**, 1053 (1972).
[120] B. J. Campbell, H. T. Stokes, J. M. Perez-Mato, and J. Rodriguez-Carvajal, *A recapitulation of magnetic space groups and their UNI symbols*, Acta Crystallogr. Sect. B **80**, 401 (2024).
[121] V. Pomjakushin, *On the magnetic and crystal structures of NiO and MnO*, Acta Crystallogr. Sect. B **80**, 385 (2024).
[122] D. B. Litvin and W. Opechowski, *Spin groups*, Physica **76**, 538 (1974).
[123] R. M. White, *Quantum Theory of Magnetism*, 3rd ed. (Springer, Berlin, 2007).
[124] G. Bihlmayer, *Density functional theory of magnetism*, in *Handbook of Magnetism and Advanced Magnetic Materials*, Vol. I, edited by H. Kronmüller and S. Parkin (Wiley, Chichester, UK, 2007), pp. 1–26.
[125] D. Gosálbez-Martínez, I. Souza, and D. Vanderbilt, *Chiral degeneracies and Fermi-surface Chern numbers in bcc Fe*, Phys. Rev. B **92**, 085138 (2015).

[126] L.-D. Yuan, Z. Wang, J.-W. Luo, E. I. Rashba, and A. Zunger, *Giant momentum-dependent spin splitting in centrosymmetric low-Z antiferromagnets*, Phys. Rev. B **102**, 014422 (2020).
[127] R. Winkler and U. Zülicke, *Time inversion symmetry in the Dirac and Schrödinger-Pauli theories*, Phys. Lett. A **558**, 130873 (2025).
[128] S. Dong, H. Xiang, and E. Dagotto, *Magnetoelectricity in multiferroics: A theoretical perspective*, Natl. Sci. Rev. **6**, 629 (2019).
[129] M.-C. Chang and Q. Niu, *Berry curvature, orbital moment, and effective quantum theory of electrons in electromagnetic fields*, J. Phys. Condens. Matter **20**, 193202 (2008).
[130] S. Lowitzer, D. Ködderitzsch, and H. Ebert, *Coherent description of the intrinsic and extrinsic anomalous Hall effect in disordered alloys on an ab initio level*, Phys. Rev. Lett. **105**, 266604 (2010).
[131] D. Wagenknecht, L. Šmejkal, Z. Kašpar, J. Sinova, T. Jungwirth, J. Kudrnovský, K. Carva, and I. Turek, *Temperature-dependent resistivity and anomalous Hall effect in NiMnSb from first principles*, Phys. Rev. B **99**, 174433 (2019).
[132] See Ref. [46] for a general overview. The relation between modern uses for the term "handedness" and the precise meaning of "chirality" is discussed, e.g., in Ref. [47].
[133] The definition, basic structure, and general properties of magnetic-point-group classes are discussed in Appendix A 3. The application to continuous and discrete point groups is discussed in Appendix B.
[134] M. V. Hobden, *Optical activity in a non-enantiomorphous crystal silver gallium sulphide*, Nature (London) **216**, 678 (1967).
[135] H. Zocher and C. Török, *About space-time asymmetry in the realm of classical general and crystal physics*, Proc. Natl. Acad. Sci. U.S.A. **39**, 681 (1953).
[136] L. Barron, *True and false chirality and parity violation*, Chem. Phys. Lett. **123**, 423 (1986).
[137] L. D. Barron, *False chirality, absolute enantioselection and CP violation: Pierre Curie's legacy*, Magnetochemistry **6**, 5 (2020).
[138] The chiral charges $T_0^{ss'}$ are different from the chiral charges encountered in relativistic field theories based on Noether's theorem, i.e., based on a conservation law reflecting a continuous chiral symmetry [139]. The chiral charges $T_0^{ss'}$ reflect the discrete symmetries in a crystalline environment.
[139] M. E. Peskin and D. V. Schroeder, *An Introduction to Quantum Field Theory* (Addison-Wesley, Reading, MA, 1995).
[140] Systems considered to be chiral according to the definitions of Ref. [45] could be either electrochiral or multichiral. Both the parachiral and magnetochiral categories would conventionally be considered as achiral, and antimagnetochirality is equivalent to false chirality. Magnetic chirality as discussed, e.g., in Ref. [141] constitutes a subset of the electrochiral category.
[141] S.-W. Cheong and X. Xu, *Magnetic chirality*, npj Quantum Mater. **7**, 40 (2022).
[142] M. Fava, W. Lafargue-Dit-Hauret, A. H. Romero, and E. Bousquet, *Ferroelectricity and chirality in the* $Pb_5Ge_3O_{11}$ *crystal*, Phys. Rev. B **109**, 024113 (2024).
[143] T. Hayashida, K. Kimura, D. Urushihara, T. Asaka, and T. Kimura, *Observation of ferrochiral transition induced by an antiferroaxial ordering of antipolar structural units in* $Ba(TiO)Cu_4(PO_4)_4$, J. Am. Chem. Soc. **143**, 3638 (2021).
[144] S. Hayami and H. Kusunose, *Time-reversal switching responses in antiferromagnets*, Phys. Rev. B **108**, L140409 (2023).
[145] R. Hoyer, P. P. Stavropoulos, A. Razpopov, R. Valenti, L. Smejkal, and A. Mook, *Altermagnetic splitting of magnons in hematite (*α-Fe_2O_3*)*, Phys. Rev. B **112**, 064425 (2025).
[146] G. T. Rado and V. J. Folen, *Observation of the magnetically induced magnetoelectric effect and evidence for antiferromagnetic domains*, Phys. Rev. Lett. **7**, 310 (1961).
[147] E. Bousquet, E. Lelièvre-Berna, N. Qureshi, J.-R. Soh, N. A. Spaldin, A. Urru, X. H. Verbeek, and S. F. Weber, *On the sign of the linear magnetoelectric coefficient in* Cr_2O_3, J. Phys. Condens. Matter **36**, 155701 (2024).
[148] X. Xu, F.-T. Huang, A. S. Admasu, M. Kratochvílová, M.-W. Chu, J.-G. Park, and S.-W. Cheong, *Multiple ferroic orders and toroidal magnetoelectricity in the chiral magnet* $BaCoSiO_4$, Phys. Rev. B **105**, 184407 (2022).
[149] D. Szaller, S. Bordács, and I. Kézsmárki, *Symmetry conditions for nonreciprocal light propagation in magnetic crystals*, Phys. Rev. B **87**, 014421 (2013).
[150] G. Wagnière and A. Meier, *The influence of a static magnetic field on the absorption coefficient of a chiral molecule*, Chem. Phys. Lett. **93**, 78 (1982).
[151] L. Barron and J. Vrbancich, *Magneto-chiral birefringence and dichroism*, Mol. Phys. **51**, 715 (1984).
[152] G. L. J. A. Rikken and E. Raupach, *Observation of magneto-chiral dichroism*, Nature (London) **390**, 493 (1997).
[153] M. Atzori, G. L. J. A. Rikken, and C. Train, *Magneto-chiral dichroism: A playground for molecular chemists*, Chem. Eur. J. **26**, 9784 (2020).
[154] X. Xu, F.-T. Huang, and S.-W. Cheong, *Magnetic toroidicity*, J. Phys. Condens. Matter **36**, 203002 (2024).
[155] E. L. Ivchenko and G. E. Pikus, *New photogalvanic effect in gyrotropic crystals*, Pis'ma Zh. Eksp. Teor. Fiz. **27**, 640 (1978)[JETP Lett. **27**, 604 (1978)].
[156] T. Furukawa, Y. Watanabe, N. Ogasawara, K. Kobayashi, and T. Itou, *Current-induced magnetization caused by crystal chirality in nonmagnetic elemental tellurium*, Phys. Rev. Res. **3**, 023111 (2021).
[157] R. Winkler, *Spin-dependent transport of carriers in semiconductors*, in *Handbook of Magnetism and Advanced Magnetic Materials*, Vol. V, edited by H. Kronmüller and S. Parkin (Wiley, Chichester, UK, 2007), pp. 2830–2843.
[158] S.-W. Cheong, S. Lim, K. Du, and F.-T. Huang, *Permutable SOS (symmetry operational similarity)*, npj Quantum Mater. **6**, 58 (2021).
[159] T. Hayashida, K. Matsumoto, and T. Kimura, *Electric field-induced nonreciprocal directional dichroism in a time-reversal-odd antiferromagnet*, Adv. Mater. **37**, 2414876 (2025).
[160] T. Sato, N. Abe, S. Kimura, Y. Tokunaga, and T. H. Arima, *Magnetochiral dichroism in a collinear antiferromagnet*

with no magnetization, Phys. Rev. Lett. **124**, 217402 (2020).

[161] G. A. Smolenskiĭ, R. V. Pisarev, and I. G. Siniĭ, *Birefringence of light in magnetically ordered crystals*, Sov. Phys. Usp. **18**, 410 (1975).

[162] T. Hayashida, K. Arakawa, T. Oshima, K. Kimura, and T. Kimura, *Observation of antiferromagnetic domains in* Cr_2O_3 *using nonreciprocal optical effects*, Phys. Rev. Res. **4**, 043063 (2022).

[163] G. Chang, B. J. Wieder, F. Schindler, D. S. Sanchez, I. Belopolski, S.-M. Huang, B. Singh, D. Wu, T.-R. Chang, T. Neupert, S.-Y. Xu, H. Lin, and M. Z. Hasan, *Topological quantum properties of chiral crystals*, Nat. Mater. **17**, 978 (2018).

[164] D. Gosálbez-Martínez, A. Crepaldi, and O. V. Yazyev, *Diversity of radial spin textures in chiral materials*, Phys. Rev. B **108**, L201114 (2023).

[165] E. O. Kane, *Band structure of indium antimonide*, J. Phys. Chem. Solids **1**, 249 (1957).

[166] U. Rössler, *Nonparabolicity and warping in the conduction band of GaAs*, Solid State Commun. **49**, 943 (1984).

[167] Recent work has studied chirality-induced orbital-angular-momentum textures [168–170].

[168] Q. Yang, J. Xiao, I. Robredo, M. G. Vergniory, B. Yan, and C. Felser, *Monopole-like orbital-momentum locking and the induced orbital transport in topological chiral semimetals*, Proc. Natl. Acad. Sci. U.S.A. **120**, e2305541120 (2023).

[169] B. Kim, D. Shin, S. Namgung, N. Park, K.-W. Kim, and J. Kim, *Optoelectronic manifestation of orbital angular momentum driven by chiral hopping in helical Se chains*, ACS Nano **17**, 18873 (2023).

[170] S. S. Brinkman, X. L. Tan, B. Brekke, A. C. Mathisen, O. Finnseth, R. J. Schenk, K. Hagiwara, M.-J. Huang, J. Buck, M. Kalläne, M. Hoesch, K. Rossnagel, K.-H. Ou Yang, M.-T. Lin, G.-J. Shu, Y.-J. Chen, C. Tusche, and H. Bentmann, *Chirality-driven orbital angular momentum and circular dichroism in CoSi*, Phys. Rev. Lett. **132**, 196402 (2024).

[171] S. B. Lee, S. Trebst, Y. B. Kim, and A. Paramekanti, *Landau theory of multipolar orders in* $\mathrm{Pr}(Y)_2X_{20}$ *Kondo materials* ($Y = \mathrm{Ti, V, Rh, Ir}$; $X = \mathrm{Al, Zn}$), Phys. Rev. B **98**, 134447 (2018).

[172] A. S. Patri, A. Sakai, S. Lee, A. Paramekanti, S. Nakatsuji, and Y. B. Kim, *Unveiling hidden multipolar orders with magnetostriction*, Nat. Commun. **10**, 4092 (2019).

[173] P. A. McClarty and J. G. Rau, *Landau theory of altermagnetism*, Phys. Rev. Lett. **132**, 176702 (2024).

[174] M. Mostovoy, *Phenomenology of altermagnets*, Appl. Phys. Lett. **127**, 060501 (2025).

[175] V. Baltz, A. Manchon, M. Tsoi, T. Moriyama, T. Ono, and Y. Tserkovnyak, *Antiferromagnetic spintronics*, Rev. Mod. Phys. **90**, 015005 (2018).

[176] A. Dal Din, O. J. Amin, P. Wadley, and K. W. Edmonds, *Antiferromagnetic spintronics and beyond*, npj Spintronics **2**, 25 (2024).

[177] S. Hayami, R. Yambe, and H. Kusunose, *Analysis of photo-induced chirality and magnetic toroidal moment based on Floquet formalism*, J. Phys. Soc. Jpn. **93**, 043702 (2024).

[178] S. Hayami, *Conversion between dipoles with different spatial parities by circularly polarized light*, Mater. Today Quantum **5**, 100019 (2025).

[179] M. Yarmohammadi, U. Zülicke, J. Berakdar, J. Linder, and J. K. Freericks, *Anisotropic light-tailored RKKY interaction in two-dimensional d-wave altermagnets*, Phys. Rev. B **111**, 224412 (2025).

[180] R. R. Birss, *Symmetry and Magnetism* (North-Holland, Amsterdam, 1964).

[181] A. M. Zamorzaev, *Generalization of Fedorov groups*, Sov. Phys. Crystallogr. **2**, 10 (1957).

[182] H. Padmanabhan, J. M. Munro, I. Dabo, and V. Gopalan, *Antisymmetry: Fundamentals and applications*, Annu. Rev. Mater. Res. **50**, 255 (2020).

[183] The rows of Tables XI, XIII, and XIV, listing only one invariant tensor on the right, can be interpreted as sections of the character tables for the $\ell = 0$ IRs of the full rotation group $R_{i\times\theta}$ (Table XI) and the $m = 0$ IRs of $C_\infty \times C_{i\times\theta}$ (Table XIII) and the full axial rotation group $D_\infty \times C_{i\times\theta}$ (Table XIV), respectively. All of these IRs are one dimensional, and "•" ("∘") indicates that the respective character is $+1$ (-1). The invariant tensors on the right then represent basis functions for these IRs.

[184] B. A. Tavger, *Ultimate magnetic symmetry of physical systems*, Sov. Phys. Crystallogr. **5**, 646 (1961).

[185] J. Hlinka, *Eight types of symmetrically distinct vectorlike physical quantities*, Phys. Rev. Lett. **113**, 165502 (2014).

[186] D. B. Litvin, *Axial point groups: Rank 1, 2, 3 and 4 property tensor tables*, Acta Crystallogr. Sect. A **71**, 346 (2015).

[187] V. Janovec, *Axial crystals—macroscopic symmetry and tensor properties*, Phase Transitions **90**, 1 (2017).

[188] In Tables XII, XV, and XVIII, the main block of groups from a given class has the groups of type J, ii-I, i-II, and ii-II from this class at its four corners. See table captions for the discussion of how placement of magnetic groups within a class's main block illustrates SIS-TIS duality.

[189] V. Janovec, V. Dvořák, and J. Petzelt, *Symmetry classification and properties of equi-translation structural phase transitions*, Czech. J. Phys. **25**, 1362 (1975).

[190] E. Ascher and A. Janner, *Subgroups of black–white point groups*, Acta Crystallogr. **18**, 325 (1965).

[191] M. Damnjanović, *Subgroups of the magnetic axial point groups*, J. Phys. C **14**, 4185 (1981).

[192] M. Hermele, Matthew P. A. Fisher, and L. Balents, *Pyrochlore photons: The* $U(1)$ *spin liquid in a* $S = 1/2$ *three-dimensional frustrated magnet*, Phys. Rev. B **69**, 064404 (2004).

[193] C. Castelnovo, R. Moessner, and S. L. Sondhi, *Magnetic monopoles in spin ice*, Nature (London) **451**, 42 (2008).

[194] H. Burzlaff and H. Zimmermann, *Point-group symbols*, in *International Tables for Crystallography*, Vol. A, edited by H. Fuess, T. Hahn, H. Wondratschek, U. Müller, U. Shmueli, E. Prince, A. Authier, V. Kopský, D. B. Litvin, M. G. Rossmann, E. Arnold, S. Hall, B. McMahon, and T. Hahn (International Union of Crystallography, Chester, England, 2006) 1st ed., pp. 818–820.

[195] F. W. Hehl, Y. N. Obukhov, J.-P. Rivera, and H. Schmid, *Relativistic nature of a magnetoelectric modulus of* Cr_2O_3

crystals: A four-dimensional pseudoscalar and its measurement, Phys. Rev. A **77**, 022106 (2008).

[196] F. Calavalle, M. Suárez-Rodríguez, B. Martín-García, A. Johansson, D. C. Vaz, H. Yang, I. V. Maznichenko, S. Ostanin, A. Mateo-Alonso, A. Chuvilin, I. Mertig, M. Gobbi, F. Casanova, and L. E. Hueso, *Gate-tuneable and chirality-dependent charge-to-spin conversion in tellurium nanowires*, Nat. Mater. **21**, 526 (2022).

[197] P. Huang, Z. Xia, X. Gao, J. M. Rondinelli, X. Zhang, H. Zhang, K. R. Poeppelmeier, and A. Zunger, *Ferri-chiral compounds with potentially switchable Dresselhaus spin splitting*, Phys. Rev. B **102**, 235127 (2020).

[198] M. Sakano, M. Hirayama, T. Takahashi, S. Akebi, M. Nakayama, K. Kuroda, K. Taguchi, T. Yoshikawa, K. Miyamoto, T. Okuda, K. Ono, H. Kumigashira, T. Ideue, Y. Iwasa, N. Mitsuishi, K. Ishizaka, S. Shin, T. Miyake, S. Murakami, T. Sasagawa, and T. Kondo, *Radial spin texture in elemental tellurium with chiral crystal structure*, Phys. Rev. Lett. **124**, 136404 (2020).

[199] G. Gatti *et al.*, *Radial spin texture of the Weyl fermions in chiral tellurium*, Phys. Rev. Lett. **125**, 216402 (2020).

[200] S. V. Gallego, J. M. Perez-Mato, L. Elcoro, E. S. Tasci, R. M. Hanson, K. Momma, M. I. Aroyo, and G. Madariaga, *MAGNDATA: Towards a database of magnetic structures. I. The commensurate case*, J. Appl. Crystallogr. **49**, 1750 (2016).

[201] S. V. Gallego, J. M. Perez-Mato, L. Elcoro, E. S. Tasci, R. M. Hanson, M. I. Aroyo, and G. Madariaga, *MAGNDATA: Towards a database of magnetic structures. II. The incommensurate case*, J. Appl. Crystallogr. **49**, 1941 (2016).

[202] X.-J. Gao, Z.-T. Sun, R.-P. Yu, X.-Y. Guo, and K. T. Law, *Heesch Weyl fermions in inadmissible chiral antiferromagnets*, arXiv:2305.15876.

[203] A. Knoll and C. Timm, *Classification of Weyl points and nodal lines based on magnetic point groups for spin-*$1/2$ *quasiparticles*, Phys. Rev. B **105**, 115109 (2022).

[204] F. Foggetti, S.-W. Cheong, and S. Artyukhin, *Magnetic monopoles and toroidal moments in* $LuFeO_3$ *and related compounds*, Phys. Rev. B **100**, 180408(R) (2019).

[205] J. Ahn, S.-Y. Xu, and A. Vishwanath, *Theory of optical axion electrodynamics and application to the Kerr effect in topological antiferromagnets*, Nat. Commun. **13**, 7615 (2022).